20th Memorial Meeting of the Northern Section of the Japan Society for Aeronautical and Space Sciences
Sendai, Japan March 7-9, 2007

Scaling of Performance in Liquid Propellant Rocket Engine Combustors

~~Preliminary Draft~~

James R. Hulka
Jacobs Engineering, ESTS Group
Mail Stop ER32, NASA MSFC, Huntsville, AL, USA
James.R.Hulka@nasa.gov

Abstract

This paper discusses scaling of combustion and combustion performance in liquid propellant rocket engine combustion devices. In development of new combustors, comparisons are often made between predicted performance in a new combustor and measured performance in another combustor with different geometric and thermodynamic characteristics. Without careful interpretation of some key features, the comparison can be misinterpreted and erroneous information used in the design of the new device. This paper provides a review of this performance comparison, including a brief review of the initial liquid rocket scaling research conducted during the 1950s and 1960s, a review of the typical performance losses encountered and how they scale, a description of the typical scaling procedures used in development programs today, and finally a review of several historical development programs to see what insight they can bring to the questions at hand.

Introduction

Scaling of combustion devices for Liquid Propellant Rocket Engines (LPREs) has never been fully developed either analytically or experimentally, even though the first formal studies for rocket engines were conducted more than 50 years ago, and Damköhler's seminal papers were published nearly 70 years ago. Nevertheless, scaling remains a powerful potential tool for the development of new combustion devices, especially in the current era where significantly reduced financing is available for rocket engine development.

Scaling has been defined as "the ability to design new combustion devices with predictable performance on the basis of test experience with old devices."[1] Historically, this meant changing – usually increasing – the thrust level of an existing combustor to meet current needs. Usually, thrust was increased by increasing combustor size and mass flow rate, rather than pressure; often, nearly identical injection elements were packaged in a larger chamber.

Today, some type of scaling is used in every development program, essentially when information from one program is used to create a new design. A well-defined and defensible scaling methodology thus has obvious advantages for development programs of LPRE combustion devices. At the top level, a scaling methodology provides guidance, verification, and potential cost savings to the combustor design and development. The guidance allows for achievement of successful development of full-size designs more rapidly. Verification of key requirements earlier in the development process may be possible, as well as validation and improvement of reliability because of more thorough evaluation of margins. Development cost savings are possible due to the use of smaller and lower flow rate hardware, resulting in reduced costs for manufacturing development hardware, reduced iterations of full-size hardware, and reduced testing costs. The latter is possible since the smaller, lower flow rate test facilities consume less propellant and require fewer test personnel. One method of scaling, discussed in this paper, however, may require higher pressure test facilities, which would negate some of these cost savings.

With so many advantages, why haven't scaling relationships been well defined after such a long time? One reason is that the number of physical and chemical processes – literally dozens – and their complex inter-relationships in rocket engine combustion devices make clear and unambiguous relationships and interpretations difficult to obtain. As has been shown in many instances, maintaining full combustion similarity in rocket flow systems is practically impossible – there are too many conflicting requirements. This realization led to consideration of the notion of "partial modeling," or deliberately ignoring some of the similarity requirements depending upon the problem at hand. Also, these conflicting requirements created separate scaling concepts between steady and unsteady problems, so that the best scaled device to investigate performance and heat transfer was not necessarily the best device to investigate combustion stability.

Another reason for the lack of progress in scaling was the excessively compressed schedules to develop rocket engines in the 1950s and 1960s. The aerospace industry was in a great hurry to produce and use the rocket engines, and funding was widely available, so the development overwhelmingly proceeded with full-size devices at the full scale operating conditions. Design iterations, and even some of the basic research as well, were conducted with full-size hardware. At the end of

this period, and at great expense, rocket engine combustors were developed with acceptable performance and thermal and stability margins.

Follow-on research into scaling was also not conducted after this development period, due to a number of reasons: (1) high combustor efficiency was achieved, eliminating the necessity to develop performance scaling rules; (2) combustion instability persisted mostly independent of performance considerations; and (3) computer-intensive analyses became increasingly complex and inexpensive.[2]

Despite these advancements, there continues the desire to develop new hardware that exceeds the previously demonstrated performance, with added requirements to reduce weight and cost, which may reduce thermal, stability, and structural margins. These improvements are partly due to new materials, new ideas, and the slow march of incremental research that points out that the previous engines can be made higher performing, lower weight, and more reliable. Unfortunately, engine development today is occurring during an era of significantly reduced budgets. Consequently, the development of new or novel concepts, or upgrades to previous designs, is occurring with the same painful process as used previously, except without the financing. A well-defined methodology for scaling would be as valuable today as it might have been 50 years ago, for performance as well as combustion stability, heat transfer, and ignition.

After 50 years of advanced development in the United States, what can be said about the scaling of combustion devices for liquid propellant rocket engines and relationships to combustor performance, stability, compatibility, heat transfer, and ignition? Unfortunately, there is no "holy grail" of scaling yet defined, that will allow the development of large LPRE combustors to proceed directly from the information of small combustors. Yet there is still a path to determine the best method for this development.

The history of rocket engine research and development provides the design, fabrication, and test of thousands of different combustors. A compilation of the information from these devices can be considered a database for scaling. This database can be mined for information and cross references that can provide a significant step toward understanding important and useful scaling relationships. Each individual rocket engine company has kept track of some of its own data and information, but over time, with the turnaround of personnel, more information is left behind. It has become critical to capture the historical information and define scaling relationships with it. One empirical correlation discussed in this paper, the Hewitt Correlation, is exactly such a relationship. In addition to this hardware test database, another means is available today during this era of reduced budgets for research and development, with the use of Computational Fluid Dynamics (CFD) to investigate a large variety of influences to a far greater fidelity than previously possible.

This paper provides another link in a continuing effort to examine scaling on the basis of the historical data, as well as use that data to define appropriate research and development programs when the opportunity arises. For this occasion, the emphasis will be placed upon examining the scaling of steady combustion and combustor performance efficiency. The focus will be on how that information can be used in combustor development. Thus, a brief review of the previous scaling studies will be conducted, followed by an examination of a few examples from the database. This effort will lay the groundwork for future examinations of the scaling of transient rocket flows such as ignition, and unsteady rocket flows as are present during combustion instability.

Scaling of Combustion

Scaling of combustion devices for liquid propellant rocket engines was originally given substantial consideration starting in the 1950s in the United States, and is documented in a handful of well-referenced documents.[1-13] A review of these documents and a modern assessment of scaling was conducted in the 1990s and recently published,[14] while an even more recent review is also available.[15] Also, an examination of scaling from the specific point of view of combustion stability has also recently been provided.[16]

Scaling has been defined as "the ability to design new combustion devices with predictable performance on the basis of test experience with old devices."[1,14] An updated definition of scaling would include design not only from old devices, but also from specialized test hardware, and not only using test experience, but also analysis.[14] Some researchers have simply called this "modeling,"[11] but that term is better left today to purely analytical treatments. Specialized test hardware, which can be larger or smaller, single- or multi-element, reacting or nonreacting, at different pressure or temperature, or something unique, can improve the means to successfully design new, full-scale, hardware.[12-14] Some examples of scaling techniques recently published from Russia[14] emphasized making the model or subscale hardware much simpler than the actual object to isolate the phenomenon under examination, a technique from partial modeling.[11] Scaling methodologies are required to make use of test results of this specialized hardware for the design of the new hardware. Analysis can connect these test results to the new design, or even substitute for the testing itself. Thus, scaling techniques can be integrated

throughout the design and development process, rather than used just as a point of departure.

Exact Combustion Similarity for Steady Internal Aerothermochemistry

Exact combustion similarity between two combustion flows in chambers of different sizes is a very rigorous requirement, implying that all component processes of combustion, although occurring at different scales, occur in identical fashion.[4] Thus, the flow paths, flame patterns, locations and time histories of species generation and heat release, and contours of temperature, pressure, and velocity are geometrically similar, even though the actual scales may be different.[4]

A set of similarity parameters for steady internal aerothermochemistry in liquid propellant rocket combustion flows was obtained by Penner by writing the conservation equations for mass, momentum, and energy in nondimensional form, and identifying the nondimensional groups of parameters which multiply the dimensionless differential equations.[1,5] This complete set of such groups for exact combustion similarity for reacting multi-component gas mixtures neglecting radiant heat transfer and thermal diffusion effects, are:[5]

$$\text{Reynolds number} = Re = \frac{\rho v L}{\mu} \quad (1)$$

$$\text{Schmidt number} = Sc = \frac{\mu}{\rho D} \quad (2)$$

$$\text{Prandtl number} = Pr = \frac{c_p \mu}{k} \quad (3)$$

$$\text{Mach number} = M = \left(\frac{\rho v^2}{\gamma p} \right)^{1/2} \quad (4)$$

$$\text{Froude number} = Fr = \frac{v^2}{g_a L} \quad (5)$$

$$\Phi = \frac{1/2 v^2}{(c_p / \gamma) T} \quad (6)$$

$$\text{Specific Heat Ratio} = \gamma = \frac{c_p}{c_v} \quad (7)$$

$$\text{First Damköhler Group} = Da,i = \frac{L}{v \tau_i} \quad (8)$$

$$\text{Third Damköhler Group} = Da,iii = \frac{q' L}{v c_p T \tau_i} \quad (9)$$

The first seven groups are familiar from nonreacting flow processes, and can be maintained constant even without chemical reactions in the system. The Reynolds number (*Re*) is the ratio of inertial forces to viscous forces in the unit volume, the Schmidt number (*Sc*) the ratio of kinetic viscosity to molecular diffusivity, the Prandtl number (*Pr*) the ratio of momentum diffusivity to thermal diffusivity, the Mach number (*M*) the ratio of kinetic energy of the flow to internal energy (or linear velocity to sonic velocity), and the Froude number (*Fr*) the ratio of inertial forces to gravitational forces.

Chemical changes in the flow processes are introduced by the two Damköhler groups. *Da,i* is the ratio of the rate of convection time L/v to chemical time τ_i, or the inverse ratio of specie generation by chemical reaction and the rate of removal by convection. *Da,iii* is the ratio of the rate of heat addition per unit volume by chemical reaction, q'/τ_i, and the rate of removal of heat by convection of enthalpy, vc_pT/L.

Constancy of all nine dimensionless groups for all processes between different sized combustion chambers assures that the steady aerothermochemical processes will be similar, since the different combustion flows would then be described by identical nondimensional differential equations. Note that for fixed values of *Re* and *Pr*, the Nusselt heat transfer number is constant, so that the boundary conditions corresponding to heat transfer to chamber walls introduces no new similarity parameter.[5] It is also important to realize that many of the dimensionless numbers occur multiple times in the equations, because they appear in multiple processes. The *Re*, e.g., must be maintained for individual injection element flows as well as core flows and boundary layer flows in the combustion chamber. Also, note that this particular list of parameters does not necessarily apply to transient or unsteady processes.

Even with steady aerothermochemistry, the number of processes occurring in liquid rocket combustors is so large, scaling of these reacting flows with complete similarity is found to be practically impossible.[4,5] There are so many simultaneous constraints on the similarities between scales that it is simply impossible to satisfy them all at the same time. Many of the similarity parameters require opposable requirements. Even extensive simplifications of the number of processes and required similarities, as will be discussed below, do not allow for reasonable solutions. And even the list shown, in the end, may not include all the critical processes. It has been argued that additional parameters may be required for phenomena involving the liquid phase.[17]

Partial Modeling

Given these formidable initial obstacles, Penner[5] and Crocco[6] concluded that reasonable conjectures about scaling procedures would be possible only by classifying the physicochemical processes of the combustion into rate-controlling chemical reaction

steps, and including only the dominant processes, disregarding the others for engineering purposes. These tactics are defined as "partial modeling."[11]

By assuming homogeneous, low velocity flow systems without significant external forces, which are reasonable assumptions for the head end of a combustion chamber, Penner reduced the required set of similarity parameters for assuring similar steady combustion processes to five groups: *Re*, *Sc*, *Pr*, *Da,i*, and *Da,iii*.[5] These five groups are equivalent to Damköhler's original five criteria for assuring dynamic and reaction-kinetic similarity in low velocity flows without external forces and without heat loss to the chamber walls.[5]

For a given propellant system with fixed injector temperature, the important similarity groups for steady internal aerothermochemistry reduce to *Re* and *Da,i*,[8] while *M* may become important for high-velocity flow processes involving oscillations,[8] and, as will be shown, in combustion chambers with coarse element patterns.

For practical scaling laws, the critical variable is found to be the chemical conversion time τ_i. Based on the functional form assumed for τ_i, a variety of scaling rules for liquid rocket engine combustion chamber geometries can be devised.[1,5,6,8,9] Two of the early methods defined by Penner and Crocco will now be discussed. The comparison will be made between a "fullscale" combustor and a "subscale" combustor, where it is assumed the fullscale is the physically larger and has higher thrust.

The Penner-Tsien Scaling Rule

An example of the attempt to scale using the methods described by Penner[5-9] is now provided. Penner assumed that chamber pressure be maintained constant, so that τ_i increases with the square of the engine thrust or the square of the dimensions.[9] By assuming the two combustors use identical physicochemical properties (propellant chemistry, propellant inlet temperatures, flow mixture ratios, etc.), the *Sc* and *Pr* are maintained constant. Also, since q', c_p, and T likewise do not vary, then *Da,iii* is constant if *Da,i* is constant. Thus, the five groups are reduced to two, *Re* and *Da,i*. Even with such dramatic simplifications, the competition between *Re* and *Da,i* will demand perplexing requirements.

To develop his first important scaling rule, Penner makes the chamber pressure constant.[5-9] Thus, combining *Re* and *Da,i* results in

$$\left(\frac{\tau_{i,S}}{\tau_{i,F}}\right) = \left(\frac{L_S}{L_F}\right)^2 \qquad (10)$$

Equation (10) describes a situation such that, at constant chamber pressure and temperature and propellant properties, as the length scales are reduced, the chemical conversion times must be reduced as the *square* of the length scales. Thus, e.g., if the subscale is half the size of the fullscale, then the chemical conversion times in the subscale must be ¼ the fullscale. It is not obvious how this is required to happen.

Note that to maintain the *Re* constant at constant pressure, then

$$\left(\frac{v_S}{v_F}\right) = \left(\frac{L_F}{L_S}\right) \qquad (11)$$

and to maintain continuity through the injector elements,

$$\left(\frac{d_S}{d_F}\right)^2 = \left(\frac{L_S}{L_F}\right) \qquad (12)$$

Thus, the velocity increases as the length scales are reduced, while the injector dimensions scale proportionally to the length scales. In the example of the half-size subscale, the velocities in the subscale must be twice the fullscale. Thus, the flowrate through the subscale must be increased (by increasing the pressure drop across the injector) since, e.g., the half-size injector would normally flow only ¼ the flowrate of the fullscale. Thus, while these conditions force *Re* and *Da,i* to match, the *M* in the chamber is no longer constant (to increase the relative flowrate in the subscale at constant pressure).

This scaling relationship, called by Crocco the "Penner-Tsien Rule,"[9] essentially requires the subscale operate at the same pressure and temperature as the fullscale, but increase the injection velocities inversely proportional to the scale factor. Certainly the higher injection velocities will reduce the chemical time scales, but is it sufficient to change it by the square? Penner concluded additional control was required, such as from the addition of surfactants in the propellant composition to change the surface tension and hence the droplet size in the combustion sprays. This is a formidable requirement when little is really understood about the functional form of atomization and vaporization on the reaction rate.

The Crocco Scaling Rule

Crocco used a different approach than Penner, but in his "second rule" similarly encountered the competition between *Re* and *Da,i*.[9] Crocco assumed τ_i was inversely proportional to some power of chamber pressure,

generating a scaling rule that preserves combustion similarity and *Re*, but not *M*, causing dimensions and thrust to scale with chamber pressure as a function of that power.[6] The significant differences from the Penner-Tsien rule were the decision not to maintain constant pressure, and assuming that $\tau \sim 1/p^m$, or the chemical times inversely proportional to pressure to some power. These considerations result in

$$\left(\frac{\tau_{i,S}}{\tau_{i,F}}\right) = \left(\frac{L_S}{L_F}\right)^{2m/(m+1)} \quad (13)$$

and

$$\left(\frac{v_S}{v_F}\right) = \left(\frac{L_S}{L_F}\right)^{(1-m)/(1+m)} \quad (14)$$

and

$$\left(\frac{d_S}{d_F}\right) = \left(\frac{L_S}{L_F}\right)^{m/(m+1)} \quad (15)$$

and

$$\left(\frac{p_S}{p_F}\right) = \left(\frac{L_F}{L_S}\right)^{2/(m+1)} \quad (16)$$

Thus, e.g., if m=1 (i.e., $\tau \sim 1/p$), then

$$\left(\frac{\tau_{i,S}}{\tau_{i,F}}\right) = \left(\frac{L_S}{L_F}\right) \quad \text{and} \quad \left(\frac{v_S}{v_F}\right) = 1 \quad \text{and}$$

$$\left(\frac{d_S}{d_F}\right) = \left(\frac{L_S}{L_F}\right)^{1/2} \quad \text{and} \quad \left(\frac{p_S}{p_F}\right) = \left(\frac{L_S}{L_F}\right)$$

These equations describe a situation such that, at constant chamber temperature and propellant properties, as the length scales are reduced, the chemical conversion times must be reduced in proportion, while the velocities are equal and, most importantly, the pressures are increased. The injector elements are distorted by the square root of the scale. Thus, e.g., if the subscale is half the size of the fullscale, then the injector element dimensions are reduced by the square root of 2 and the chemical conversion times in the subscale must be half the fullscale. The pressures, on the other hand, are doubled.

Conclusions of 1950s Scaling Studies

The paths defined by both Penner and Crocco lead to challenging design requirements, and, frankly, very uncertain practices and grave and non-intuitive distortions between the fullscale and subscale hardware. The challenge is undoubtedly to understand how to model the chemical conversion time, τ_i, or even to determine the rate-controlling steps, which will require a thorough examination of the physical and chemical processes of combustion in LPRE combustors. Certainly such misgivings were another reason preventing the use of these scaling techniques during the formative years of the late 1950s through the 1960s, when the vast majority of research and development of liquid propellant rocket engines in the United States was conducted. Only time will tell whether these techniques were practiced elsewhere, such as in the former Soviet Union.

LPRE combustor development itself to date has provided no conclusions to these assumptions. As previously mentioned, early development of LPRE combustors was well funded, rapid, and intensely empirical, so stable and efficient designs were created in a relatively short time and at great expense, using full-scale hardware almost exclusively. Even later, less well-funded engine development programs – to regulate costly test programs – had little incentive to change these developed and successful designs, even though applications were often considerably different. It is the current generation which may use this database and analytical tools to investigate the scaling relationships.

Scaling of Performance

Relating combustion performance between different sizes of combustion devices is probably the least complex problem among all scaling processes. While this scaling may be straightforward, that does not mean it is simple, especially in an era today when performance is often required to be higher than previously demonstrated.

Performance Subelements

First, the various subelements that comprise LPRE combustor performance will be identified. These various subelements have been previously defined in a number of widely available documents.[18-20] For this discussion, the focus is on the combustor performance upstream of the throat – i.e., the energy release efficiency, which is still poorly predicted. Performance losses downstream of the throat (in the nozzle) are fairly well characterized by analytical means.[19]

Combustion performance losses in LPRE combustion devices – i.e., in the combustion chamber – can be broken down into five basic categories:

1. Collective (multi-element) inefficiency of all core elements
2. Collective (multi-element) inefficiency of all barrier elements
3. Surface boundary losses

4. Unintentional maldistribution of mass and velocity across the injector face
5. Intentional maldistribution of mass and velocity across the injector face.

The collective inefficiencies of the core and barrier can be further broken down into the following parts:

a) Single element mixing inefficiency for each element type
b) Single element vaporization inefficiency for each element type
c) Inter-element mixing inefficiency (or the multi-element mixing inefficiency, which is the sum of single element mixing inefficiencies modified by element interactions)
d) Inter-element vaporization inefficiency (or the multi-element vaporization inefficiency, which is the sum of single element vaporization inefficiencies modified by element interactions)
e) Losses due to two-dimensional effects of the flowstream
f) Losses due to reaction kinetics
g) Losses due to the radiation energy from various combustion species

The surface boundary losses, which can be included in the collective efficiency of the barrier, or, more handily, kept separately, include the following:

a) Heat energy losses from the fluids to the injector and chamber walls
b) Boundary layer losses (effect of wall boundaries on the flow streams)

Heat exchange between the products in the combustor and the fluids in the injector is usually not modeled, because this process is internal within the control volume of the injector inlet and the combustion chamber exit. However, heat exchange between the products in the combustor and the fluids in the coolant jacket of the combustion chamber may or may not be included, depending upon the definition of the control volume.

Unintentional maldistribution losses are due to:

a) Non-uniform mass, velocity, and pressure distributions at the injector inlets
b) Non-uniform mass, velocity, and pressure distributions resulting from the injector manifolding
c) Manufacturing tolerance variations on injector metering features

Intentional maldistributions losses are due to:

a) Fuel film coolant (FFC) injected into the chamber periphery
b) Deliberate mass flow rate bias of various elements across the injector face (mixture ratio bias)
c) Local element mass flow bias (e.g., off-set, angled or scarfed coaxial post)
d) Deliberate burning rate variations across the injector face, due to different elements used in the pattern

All combustors include some form of almost all of the first four categories of losses. The fifth category can be controlled to a large extent. The JANNAF rigorous procedure suggests that, using the prescribed methodology, performance can be calculated *a priori* within 1 %.[18] Injector designers today know that many applications require performance efficiencies in excess of 99%, putting the JANNAF predictability in question as well as the capability to measure as accurately.

Influence of the Combustion Chamber Geometry

Certain aspects of the combustion chamber geometry influence the performance comparison between scales. For example, one chamber can be shorter than the other, or use a shorter cylindrical section, or have a different L^*. The use of a scaled combustion chamber is to allow the designer to predict the full-size thrust chamber (injector and chamber system) performance and its sensitivities. The two most important features of the combustion chamber are its length and its shape.

Chamber Length

The length of the combustion chamber, from the injector face to the geometric throat plane, affects the overall vaporization efficiency of liquid and two-phase propellants, and the overall mixing efficiency. For vaporization-limited combustion, increasing chamber length will increase the overall performance until sufficient length is available to complete vaporization of all propellants. For mixing-limited combustion, increasing chamber length can increase the overall performance but often at a much slower rate, depending upon the element design. Large (or "coarse") elements, or elements that have less initial interpropellant mixing (such as many impinging element patterns), show a mixing improvement with increased length. Small (or "fine") elements, or elements that have more initial interpropellant mixing (such as many coaxial element patterns), show little mixing improvement with increased length.

Chamber Contraction Ratio

The contraction ratio defines the mean value of M in the combustion chamber, and affects the mean level of mixing in the developing combustion flow field.

Chamber Barrel Length

The shape of the combustion chamber, and specifically the length of constant diameter sections before the start of convergence in the nozzle, affect the vaporization, mixing, and heat transfer profiles. Depending upon the element axial energy release rate, the chamber geometry at the head end of the combustion chamber can have a profound effect on overall performance (as well as heat transfer and combustion stability).

Chamber Characteristic Length

The L* is a relativistic parameter that relates back to the residence or "stay" time of propellants in the combustion chamber.[20] To achieve combustor performance in excess of 99%, other factors play a larger role.

Influence of the Injection Element

Undoubtedly, the injection element itself has the most influence on the characteristics of performance, heat transfer, combustion stability, and ignition.

One of the first and most obvious relationships between a fullsize combustor and a subscale test article is to decide what size of element to use. The Penner-Tsien rule described above used element dimensions proportional to the scale, shown in Eqn. (12), while Crocco's second rule had a distortion of the element geometry as described by Eqn. (15).

Another key feature to describe is whether there is any element-to-element interaction. Consider a multi-element injector with many hundreds of elements. Any multi-element interaction will be designated as X_{ia}, where, for example, the relationship between fullsize and subscale characteristic exhaust velocity performance is $\eta_{C^*,f} = X_{ia,ss}{}^*\eta_{C^*,s}$, or the relationship between fullsize and single element characteristic exhaust velocity performance is $\eta_{C^*,f} = X_{ia,se}{}^*\eta_{C^*,se}$. While coaxial elements have been described to have virtually no interaction[14] (i.e., X_{ia}=1), impinging element patterns not only have some level of interaction but often rely on it. It is certainly not clear that X_{ia} is a constant value between scales. Comparison between single element performance and multi-element performance, where other aspects (such as heat loss to the combustion chamber walls) have been removed, is the determination of X_{ia}.

Two Common Scaling Methods

There seem to be two methods in current practice used to model full-size combustors with small-sized hardware: 1) using identical injector elements, and 2) using photo-scaled injector elements.

1) Identical Injector Elements

The first method simply uses the identical injector element geometry in the small-size combustor as found in the full-size combustor, as depicted in Fig. 1. Thus, the energy release characteristics (subdivided generally into atomization, vaporization, mixing, and reaction) can be made identical, depending upon aspects of the combustion chamber geometry. Note that these characteristics are not *scaled* in the sense as described earlier. The *Re* of the injector features in the small-size chamber are exactly the same as the *Re* of the injector features in the full-size chamber.

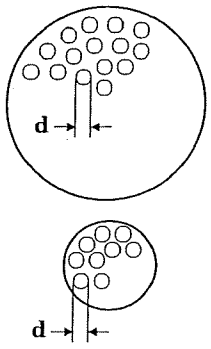

Figure 1. Scaling with constant injector element dimensions.

As alluded, the combustion chamber geometrical features can influence the performance (along with heat transfer and combustion stability) results in this small-size chamber. The typical chamber profile used in the small-size hardware is depicted in Fig. 2. This arrangement is driven usually by the requirement to maintain the same L' and the same contraction ratio as the full-size chamber. Keeping the L' constant primarily maintains similar first-order vaporization and mixing efficiencies, while keeping the contraction ratio constant maintains the same M at the head end of the chamber. Also of consideration is manufacturing a shorter and hence less expensive throat section for the subscale.

However, as Fig. 2 displays, there is a difference in the convergence profile from the near-head end region to the near-throat region, resulting in a different M profile. If this occurs in the region where the energy release rate is still changing, then the performance, even with the same injector elements, can be quite different. The influence is most profound with coarse elements. An example of the potential differences between two typical chambers is shown in Fig. 3.

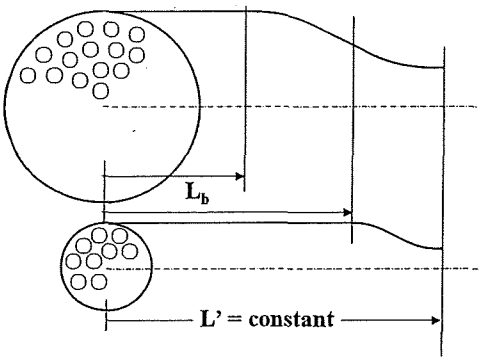

Figure 2. Comparison of typical combustion chambers used in scaling with constant element dimensions. L_b is not constant.

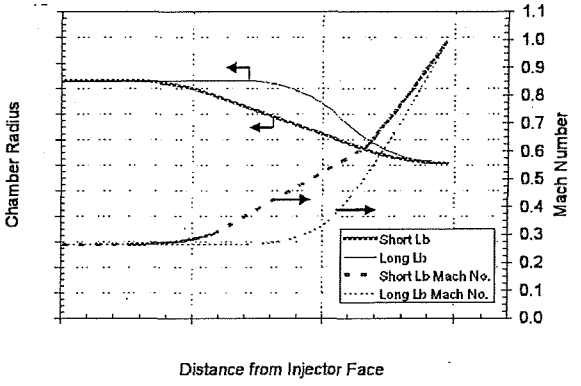

Figure 3. Typical change of M with varying L_b.

One way to correct this difference is match the convergence profile (A_{ch}/A^*) over the whole length of the combustion chamber, as shown in Fig. 4. This correction will result in chambers with different convergence angles. Note that even single element injectors can be installed in combustion chambers with constant M profiles. This method is not typically used because of the increased manufacturing costs of the nozzle section. Ross did not recommend this method as a general scaling rule because of the potential for excessive convergence angles and hence lower throat C_d.[10] In general, however, this is not likely to be a problem unless the chamber diameter difference is very large, in excess of 5 times.

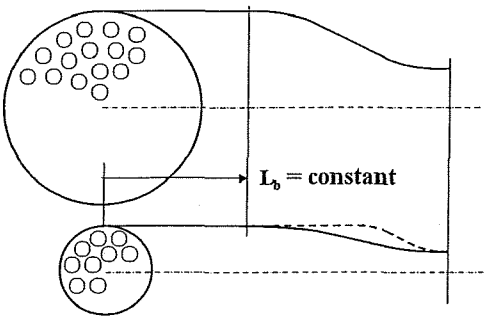

Figure 4. Subscale chamber with constant L_b and M.

2) Photo-scaled Injector Elements

The second method uses a *photo-scaled* injector in the small-size combustion chamber, meaning that all injector dimensions are changed in proportion to the combustion chamber length scales, as depicted in Fig. 5. This method is not similar to either of the two scaling laws presented earlier. While the injector dimensions scale as per Eqn. (12), to maintain constant chamber pressure the injection velocities must be made constant between scales, which is different than prescribed by Eqn. (11). If the injection velocities in the small-size combustor are increased, by increasing the mass flow rate through the injector, then the chamber pressure will increase because the chamber throat diameter has already been fixed. Thus, *Re* in the injection elements are not constant between the scales, and *Re* in the combustion chamber are not constant.

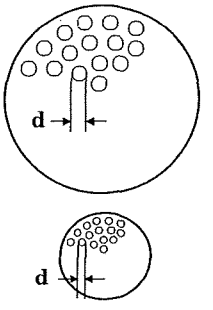

Figure 5. Scaling with photoscaled injector element dimensions.

This method is suggested from a compilation of empirical combustion stability data originally compiled by Hewitt, and first published openly in [21] (and since discussed in many forms, including most recently [22]). A typical plot of the Hewitt Correlation is shown in Fig. 6.[21] The Y-axis is the chamber diameter, and the X-axis is the ratio of the injector element diameter over the injector element velocity of the least volatile propellant. While this correlation was developed for combustion stability, it does also separate performance effects, as

shown, with higher performance in the upper left and lower performance in the lower right.

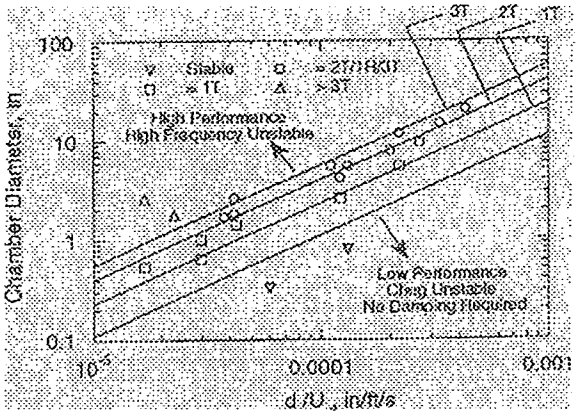

Figure 6. Hewitt Correlation of chamber diameter versus injector characteristic d/V.[21]

For combustion stability, Fig. 6 suggests that changing the d/V characteristic in relation to the combustion chamber diameter maintains a constant combustion stability margin. Thus, this rule is essentially

$$\left(\frac{d_S}{d_F}\right)\left(\frac{v_F}{v_S}\right)=\left(\frac{D_{c,S}}{D_{c,F}}\right) \qquad (17)$$

Thus, if the small-size chamber diameter is made ½ of the full-size chamber diameter, i.e., $D_{c,S}$ = ½ $D_{c,F}$, then either the injector orifice diameter is to be halved or the injection velocity doubled, to maintain similar stability characteristics. A proportional reduction in the element dimensions with the chamber diameter reduction while maintaining constant injection velocity is the photoscaled combustor at constant chamber pressure just described. This results in an injector design that is *photographically reduced* in relation to the chamber diameter, as depicted in Fig. 5.

What remain to be determined are the suitable chamber length dimensions. Should the chamber lengths (barrel and nozzle) be photographically reduced as well, or is there some other relation? This is not obvious, since the injector and chamber *Re* are not the same between scales.

For performance, clearly the photographically reduced smaller element will require less L' (and less L*) than the larger element. Without changing the injection velocities or the chamber velocities (essentially keeping chamber pressure constant), the contraction ratios will be the same, and at least the head end *M* will be the same. Both injection and chamber characteristic *Re* will be reduced from the larger chamber by the scale ratio, which means that atomization, vaporization, mixing, and probably reaction characteristics (i.e., the composite energy release rate) will be *relatively* worse in the smaller combustor (i.e., take longer) than had the injection and combustion *Re* been matched with the smaller injector diameters. Thus, it is equally clear that the smaller element will require more L' (and more L*) than the photographically reduced chamber parameters. The distinction, illustrated in Fig. 7, is not yet defined and requires further elaboration.

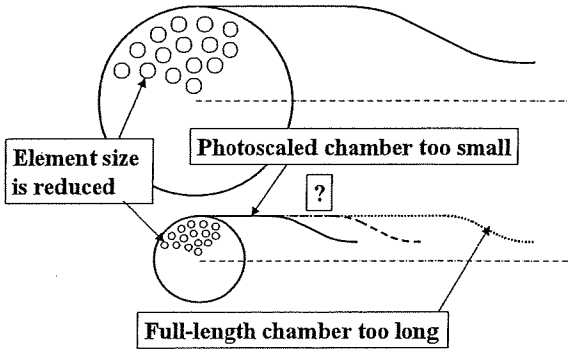

Figure 7. Photo-scaling the Combustion Chamber with a Photo-scaled Injector

Use of Non-Similar Scales in the Two Common Methods

Both the identical element and photoscaled element scaling method use elements that are not properly scaled to the combustion chamber per the methods described by Penner or Crocco. For combustion and performance, the identical element method is preferable because the injector parameters (defined by *Re*, etc.) practically match the fullscale, and with proper geometry, the *M* can match as well. As will be shown, this method has been preferred in development programs to date.

However, the photoscaled element scaling method offers the advantage of additional information from the scaled combustor test, primarily for combustion stability. Can combustion and performance information be meaningful from this test as well ?

The answer is shown by consideration of the regimes in which the scaling is taking place. While the element *Re* (and Weber Number *We*) are decreasing as injector diameter *d* is decreasing, perhaps the energy release processes actually do not change dramatically over the scaling range to make substantial differences. Investigations into the effect of scaling on the individual LPRE combustor processes of injection, atomization, vaporization, mixing, and reaction are required. A significant, research-oriented evaluation of scaling of LPRE combustion devices will eventually require evaluation of all these individual processes as well as their interactions. Some of these investigations are in

progress.[23] For example, it is well known that liquid jets in LPRE combustors operate in turbulent regimes many orders of magnitude above transitional or laminar regimes, and atomization occurs in the fully atomized regime many orders of magnitude above poorer atomization regimes.[23] One study of scaling of the primary atomization of LRPE liquid coaxial jets, reproduced in Fig. 8, shows just how far the separation between normal operation, or even dramatically scaled operation, and changes to the regime of primary atomization lies. The point is clear that the form of primary atomization for these dramatically scaled elements will change little, if at all, from their nominal operating points.

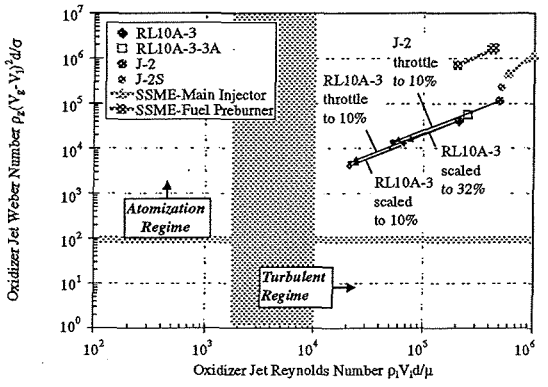

Figure 8. Comparison of jet *Re* and aerodynamic jet *We* and typical O2/H2 LPRE coaxial injector elements.[23]

Obviously this photoscaling has limitations – the dimensions can only be reduced so far before characteristics do change dramatically. Some examples are evident from development of microthrusters.[24,25] However, the operable range of the Hewitt Correlation[21,22] shows that the useful range for photoscaling is quite practical.

Historical Case Studies

It is now informative to revisit some of the historical development programs where notions of scaled hardware were used, and evaluate the results from the performance perspective. Note that for some of these programs, scaling of performance was only one of many considerations; often, efforts to derive information about combustion stability and heat transfer were as important if not more significant.

M-1

Probably the first recognition of the importance of using scaled hardware during development was with the M-1 engine, the largest liquid oxygen/hydrogen engine conceived in the United States. This 6670-kN (1,500 Klbf) thrust engine was an upper stage concept considered for Apollo and other missions, but was terminated in advanced component development.[26] While the injector was uncommonly large (42" in diameter), and similar in size to the F-1 engine injector, the less frantic schedule allowed a subscale methodology to be included during development that the F-1 program did not attempt.[27] The use of small-size hardware provided optimization of the performance and some of the combustion stability characteristics. Characteristics of the fullscale combustor that were matched in the subscale combustor were element geometries, element-to-element spacing, chamber length (L'), chamber contraction ratio, and chamber pressure.[27,28] The baseline element type was shear coaxial.

The M-1 is an interesting case study because of the gigantic size difference between the fullscale and subscale hardware. The full-size M-1 injector is shown in Figs. 9 and 10. The small-size subscale hardware is shown in Figs. 11 and 12.[28] A comparison of the combustor hardware to scale is shown in Fig. 13. Note that the subscale injector size approximates one of the fullscale injector baffle pockets, a relationship that has implications to combustion stability scaling.

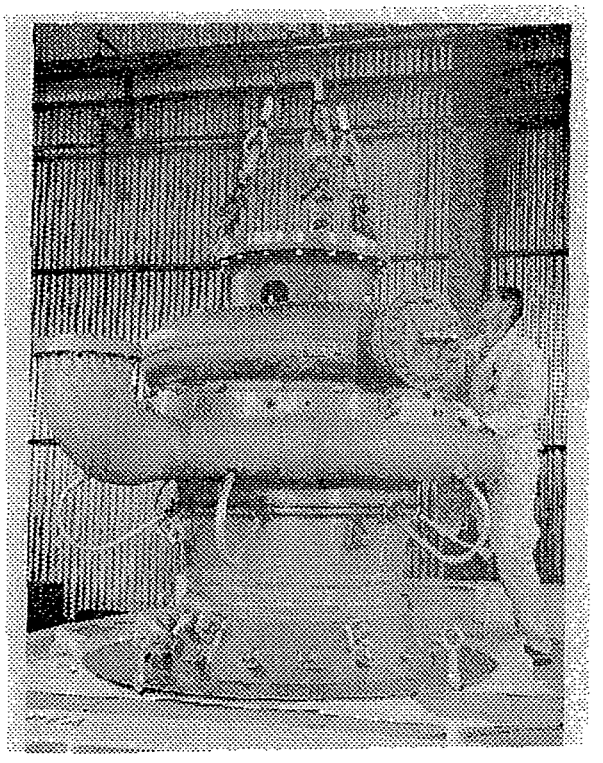

Figure 9. Fullscale M-1 Combustion Chamber.[26]

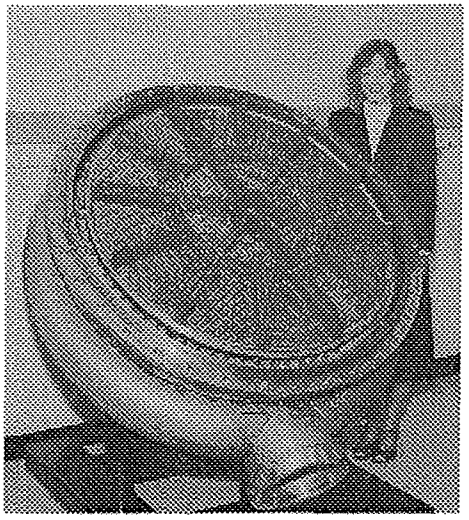

Figure 10. Fullscale M-1 Injector

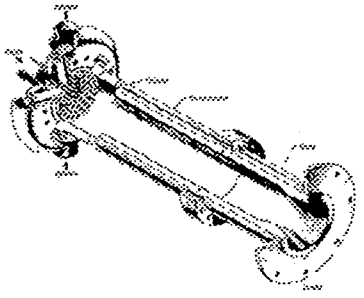

Figure 11. Subscale M-1 Combustion Chamber.[28]

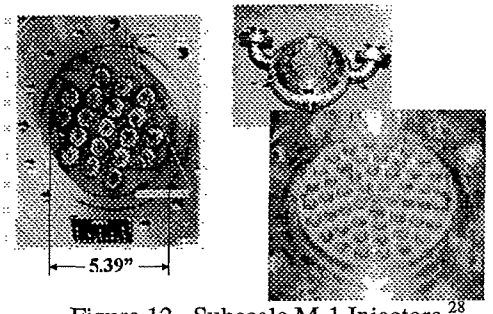

Figure 12. Subscale M-1 Injectors.[28]

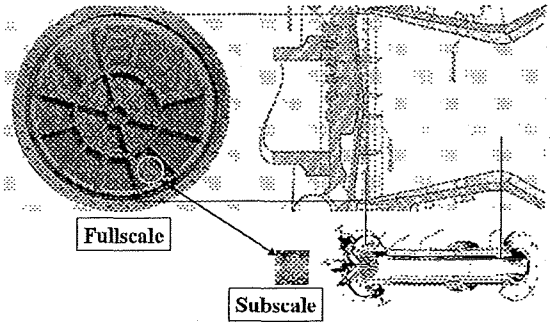

Figure 13. "To-scale" size comparison of M-1 fullscale and subscale combustors.[26,28]

A comparison of the measured η_{C^*} of the subscale to the fullscale is shown in Fig. 14.[27] At the design mixture ratio of 5.5, 99.3% efficiency was measured in the subscale while 96.0% was measured in the fullscale. To what do we subscribe the rather large difference in performance between these combustors ?

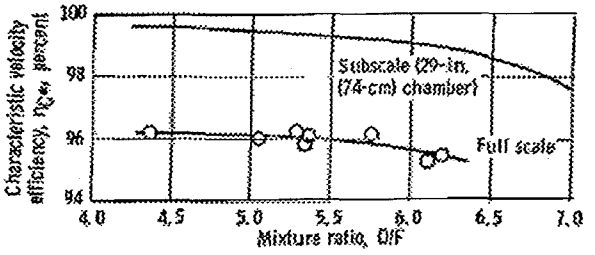

Figure 14. η_{C^*} performance comparison of M-1 fullscale and subscale combustors.[27]

The first difference is the obviously large differences in intentional maldistributions necessary to cool the walls and baffle surfaces. A simple streamtube mixing analysis as described in [29] suggests the difference in intentional maldistribution of the fullscale explains about 1.7% of the 3.3% difference. Another difference is that the elements adjacent to the baffles, which constituted 23% of the total number of elements, were subjected to a mechanical distortion of the round oxidizer exit orifice, in an effort to further protect the baffles from thermal distress. An estimate of the loss due to this change explains about another 0.6% of the 3.3% difference. Since both injectors used Rigimesh, a porous sintered metal, as the faceplate material, there were no real differences in loss due to face cooling. Finally, note that the subscale combustor used a straight barrel, while the fullscale barrel used a conical chamber. The axial combustion profile is thus subjected to different Mach number profiles as well as different L*. A calculation of this difference using [29] explains about 0.3% of the variation.

The summation of the explained differences leaves about 0.7% of the variation unexplained, which is fairly close to the expected measurement error (0.5%). However, one final difference may be attributable to unintentional maldistributions, which can be quite large in large hardware. The M-1 is one of the largest diameter injectors (42") ever tested, and supplying mass flow uniformly to every element across the injector face was certainly difficult. The liquid oxygen was supplied from a single radial inlet, whose point-nonuniformity was alleviated by a constant-velocity torus in the circumferential distribution. The cold gaseous hydrogen was supplied from an annular manifold at the chamber periphery, from where it turned 90-degrees and flowed radially through the forest of oxidizer posts before turning 90-degrees again and exit the face. CFD

is capable today of making reliable predictions of these losses.

Space Shuttle Orbital Maneuvering Engine

The Space Shuttle Orbital Maneuvering Engine (OME), originally developed in the early to mid-1970s, continues to fly today on the U.S. Space Shuttle.[30] This 26.7 kN (6 Klbf) thrust engine uses nitrogen tetroxide and monomethylhydrazine (N_2O_4/MMH) propellants at a mixture ratio of 1.65 and chamber pressure of 125 psia, in a chamber diameter of 8.11".[30,31] Hardware is shown in Fig. 15.[30]

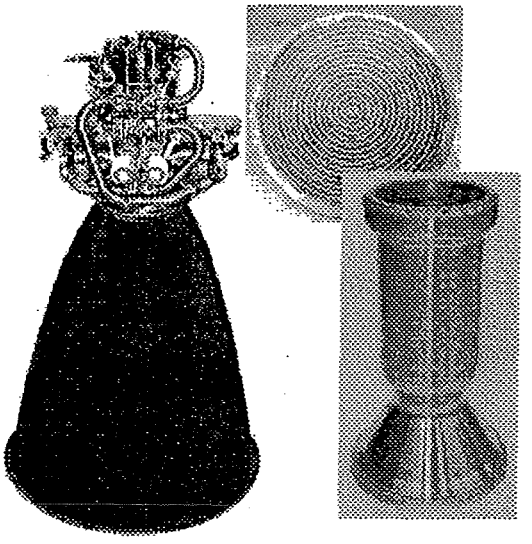

Figure 15. OME engine, injector, and combustion chamber hardware.[30]

Critical metering and injection features of the injector was fabricated by platelet technology, a manufacturing process that bonds thin metal sheets etched with desired features into a monolithic structure.[31] The element used for the final design was a transverse like-on-like doublet, a unique modification of the typical like-on-like doublet from the use of platelet technology.[30-34] Other elements investigated in development included unlike-doublets, splash plates, and other platelet-modified like-on-like doublets.[32,33]

Subscale hardware was used extensively in the development program. Subscale sizes included 600 lbf (2.7" Dch) and 1000 lbf thrust (3.5" Dch, 5" L') combustors.[14,32,33] A comparison of subscale and fullscale hardware for a development unlike-doublet element is shown in Fig. 16.[33] While the use of this subscale hardware was informative for the combustion stability verification,[14,34] we will review the performance comparisons.

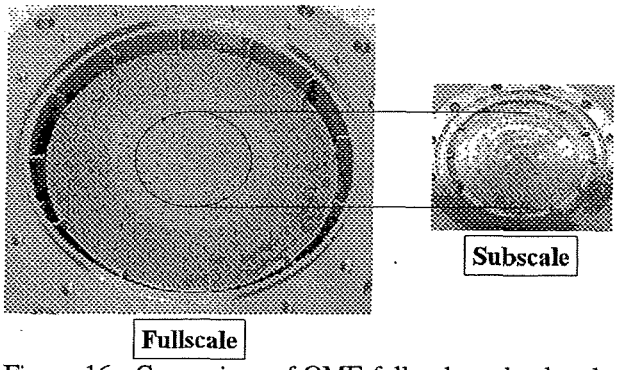

Figure 16. Comparison of OME fullscale and subscale injector hardware.[33]

600-lbf thrust injector Isp-based performance for a variety of elements is shown in Fig. 17.[33] Included in this figure are data from the single element testing, using an L'=4".[33] As discussed previously, the difference between single element and multi-element performance can be an indication of the interelement interaction, X_{ia}. However, in two cases as illustrated in Fig. 17, the single element performance is higher than the multi-element performance, indicating that X_{ia} can be less than one. However, the mixing continues to improve with these elements because for all cases the performance increases with increasing L'.

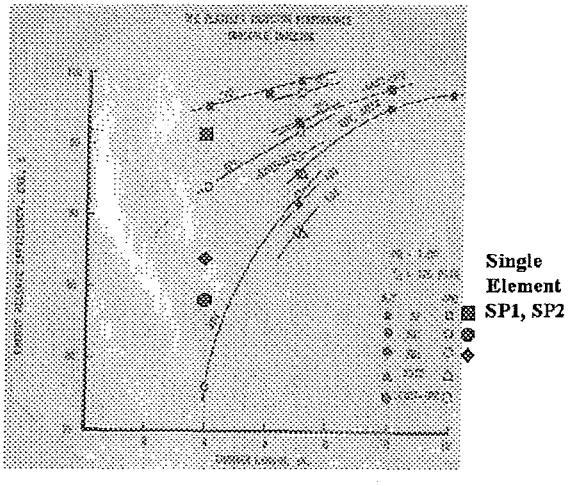

Figure 17. Comparison of OME multi-element and single element performance.[33]

Based on the delivered Isp of the flight engine, the ERE of the flight combustor was 98%.[30,31] There were no barrier-cooling schemes in the final configuration,[32] so there were no intentional maldistributions. Performance in the subscale hardware was within 0.5% of this value, within the value of experimental error.[32,33]

NASA LeRC Thrust/Element Tests

While not a scaling study per se, where various elements are tested in combustion chambers of different dimensions, the work at the NASA Lewis Research Center (LeRC) in the 1960s is an informative study of scaling the element size.[35] The combustor is shown in Fig. 18. Chamber diameter was 27.4 cm (10.78 in.). Propellants were liquid oxygen and cold gaseous hydrogen, with chamber pressure of 2.064 MN/m^2 (300 psia).[35] Injector elements of similar geometry but widely varying thrust (or flowrate)-per-element characteristics were tested in this chamber. Figure 19 shows the injector face for the smallest and largest element tested.

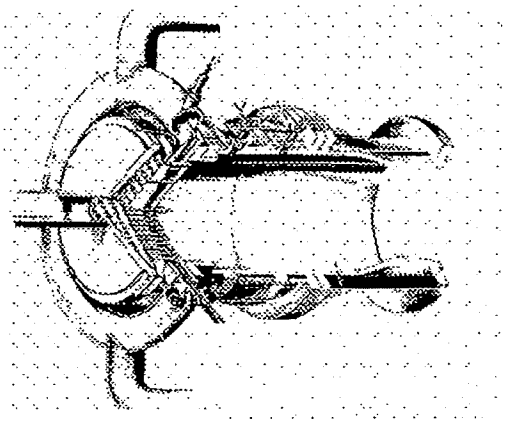

Figure 18. 20 Klbf thrust chamber for NASA LeRC injector element comparisons.[35]

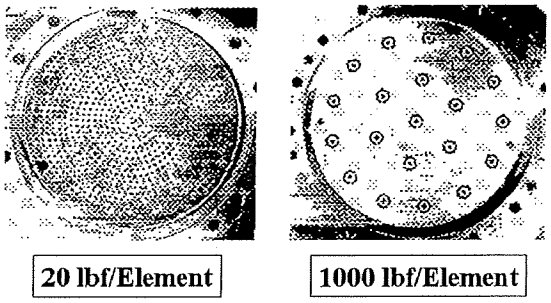

Figure 19. Injector element patterns for NASA LeRC element scaling testing.[35]

Results of this study are shown in Figs. 20 and 21.[35] As expected, the performance efficiency increases with decreasing element size. At fixed L' of 30.5 cm (12 in.), 20 lbf elements obtained the highest performance. 50, 100, and 200 lbf elements were grouped together at slightly lower performance. 572 and 1000 lbf elements suffered a dramatic reduction in performance.

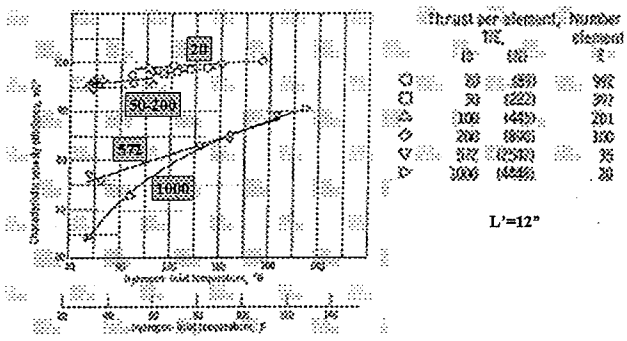

Figure 20. η_{C^*} performance comparison of NASA LeRC testing with varying thrust/element.[35]

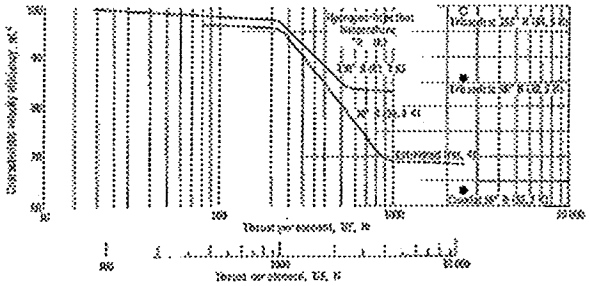

Figure 21. η_{C^*} performance comparison of NASA LeRC testing with varying thrust/element.[35]

It is important to realize this performance loss of the coarse elements turns out to be vaporization-limited. If the coarse elements are tested in a longer combustion chamber, the performance is dramatically increased, as shown in Fig. 22. Also included on Fig. 22 are data from the subscale M-1 testing, which used a similar coaxial injection element but a rather large thrust/element of 1267 lbf, which in a longer L' chamber achieved performance as high as the 100 lbf element. These results provide a demonstration of the coupled scaling between element and combustion chamber dimensions.

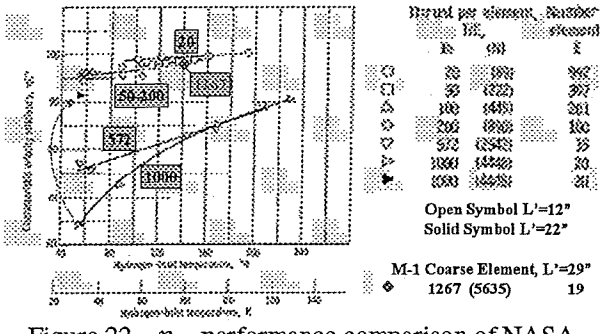

Figure 22. η_{C^*} performance comparison of NASA LeRC and M-1 subscale testing with variations in L'.[28,35]

Summary

Developing full-scale liquid rocket thrust chambers, especially booster engines, is still an expensive and time-consuming process because most of the development testing occurs with full-size hardware rather than something smaller. Full-scale hardware is used because no well-defined development methodology for using smaller size hardware is generally accepted throughout the rocket engine community. Unfortunately, a "holy grail" of scaling has never been invented which can provide in one examination verification of all the important processes for a LPRE combustor – performance, heat transfer, compatibility, combustion stability, and ignition.

Certainly one reason for this lack of invention is that scaling of the combustion flow in a LPRE with full similarity of the internal aerothermochemistry is not practical, even for steady conditions. There are simply too many conflicting requirements. Even partial similarity was found to be difficult; Penner and Crocco in the late 1950s developed two scaling rules, discussed herein, where some distortion of the injector or chamber geometry was required, and where uncharacteristic manipulation of the chemical conversion times was required.

However, combustor development since that time has made use of scaled hardware, even when it violated similarity relationships. One relationship – the use of constant element dimensions in combustion chambers of difference diameters and lengths – has been used in a number of programs and shown to succeed in validating the performance of the larger combustor, when proper features of the chamber are included. Another relationship – the use of photo-scaled element dimensions in combustion chambers of difference diameters and lengths, based on the Hewitt Correlation – has been shown to predict combustion stability characteristics but is not yet shown to validate performance.

A Note for the Future

Certainly one of the most significant differences between the current era and the past is analysis capability, represented by the increasing use of CFD methods, especially for combustion and particle-laden flows. While the use of CFD as a design tool for rocket engine combustor development generally lags behind the rest of the combustion industry (in no small part due to the significant increase in mass flux and energy density of the problem), the last 10 years has seen a dramatic increase in the use of CFD in this field. CFD, used in carefully crafted "numerical experiments," can advance the development of the scaling methodology as much as the investigation of the historical database, or the conduct of hardware-oriented experiments. These avenues are currently being explored at the NASA MSFC, and future publications showing the results of such "numerical experiments" in relation to aspects of scaling are planned.

Nomenclature

A = area, m^2
A^* = throat area, m^2
c = velocity of sound, m/sec
C_d = discharge coefficient
c_p = specific heat at constant pressure, kJ/kg-K
c_v = specific heat at constant volume, kJ/kg-K
c^* = characteristic exhaust velocity, m/sec
Da,i = First Damköhler Group
Da,iii = Third Damköhler Group
D = diffusion coefficient, m^2/sec
D_{ch} = thrust chamber internal diameter, m
d = diameter, m
f = frequency, Hz
Fr = Froude number
g_a = gravitational acceleration, m/sec^2
h = enthalpy per unit mass, kJ/kg
h_g = hot gas heat transfer coefficient, kW/m^2-K
I_{sp} = specific impulse, N-sec/m
k = thermal conductivity, J/m^2-sec-K
L = length, m
L_b = chamber cylindrical length, m
L' = geometrical chamber length (injector face to geometric throat), m
L^* = characteristic chamber length (V_c/A^*), m
$\dot{m}$ = mass flow rate, kg/sec
M = Mach number
N = number of injection elements
p = pressure, N/m^2
P_c = thrust chamber pressure, N/m^2
Pr = Prandtl Number
q = volume flow rate, m^3/sec
q' = heat addition per unit volume, kW/m^3
Q = heat load, kW
Q/A = heat flux, kW/m^2
r = oxidizer-to-fuel mixture ratio
Re = Reynolds number
Sc = Schmidt number
t = thickness, m
T = temperature, K
T_{aw} = adiabatic wall temperature, K
T_{wh} = hot gas wall temperature, K
T_c = combustion chamber gas temperature, K
V_c = chamber volume, m^3
v = velocity, m/sec
We = Weber number
X_{ia} = multielement interaction index

α = reciprocal of the equivalence ratio

γ = specific heat ratio
Δ = finite difference
ζ = mass fraction
η_{c*} = characteristic velocity efficiency
μ = absolute viscosity, kg/m-sec
ν = kinematic viscosity, m^2/sec
ρ = density, kg/m^3
τ = characteristic delay time, sec; sensitive timelag, sec
τ_i = characteristic conversion time of chemical species *i*, sec
τ_r = relaxation time, sec
ϕ = equivalence ratio

Acknowledgments

The author would like to thank the Japan Society of Aeronautical and Space Sciences for the invitation and opportunity to deliver this lecture, and Dr. Takuo Onodera of the Japan Aerospace Exploration Agency for organizing and funding my participation. The author would also like to thank the NASA MSFC for travel support. Thanks finally to Ross Hewitt of Aerojet for continued inspiration to investigate these topics.

References

1) Penner, S.S., *Chemical Problems in Jet Propulsion*, Pergamon Press, London, 1957, pp. 345-347, 376-388.
2) Harrje, D.T., and Reardon, F.H., (eds.), *Liquid Propellant Rocket Combustion Instability*, NASA SP-194, 1972, pp. 221-226.
3) Weller, A.E., "Similarities in Combustion, A Review," *Selected Combustion Problems, II*, AGARD Combustion Colloquium, 1956, pp. 371-383.
4) Stewart, D.G., "Scaling of Gas Turbine Combustion Systems," *Selected Combustion Problems, II*, AGARD Combustion Colloquium, 1956, pp. 384-413.
5) Penner, S.S., "Similarity Analysis for Chemical Reactors and the Scaling of Liquid Fuel Rocket Engines," *Combustion Research and Reviews*, AGARD, 1955, pp. 140-162.
6) Crocco, L., "Considerations on the Problem of Scaling Rocket Engines" *Selected Combustion Problems, II*, AGARD Combustion Colloquium, 1956, pp. 457-468.
7) Penner, S.S., and Datner, P.P., "Combustion Problems in Liquid-Fuel Rocket Engines," *Proceeding of the Fifth Symposium on Combustion*, Sept. 1954, pp. 11-28.
8) Penner, S.S., and Fuhs, A.E., "On Generalized Scaling Procedures for Liquid-Fuel Rocket Engines," *Combustion and Flame*, Vol. 1, 1957, pp. 229-240.
9) Penner, S.S., "On the Development of Rational Scaling Procedures for Liquid-Fuel Rocket Engines," *Jet Propulsion*, Sept. 1957, pp. 156-161.
10) Ross, C.C., "Scaling of Liquid Fuel Rocket Combustion Chambers" *Selected Combustion Problems, II*, AGARD Combustion Colloquium, 1956, pp. 444-456.
11) Spaulding, D.B., "The Art of Partial Modeling," *9th International Symposium on Combustion*, The Combustion Institute, 1963, pp. 833-843.
12) Lawhead, R.B., and Combs, L.P., "Modeling Techniques for Liquid Propellant Rocket Combustion Processes," *9th International Symposium on Combustion*, The Combustion Institute, 1963, pp. 973-981.
13) Beer, J.M., and Chigier, N.M., *Combustion Aerodynamics*, Chapter 7, "Modeling of Combustion Systems," pub. John Wiley & Sons, New York, 1972, pp. 196-211.
14) Dexter, C.E., Fisher, M.F., Hulka, J.R., Denisov, K.P., Shibanov, A.A., and Agarkov, A.F., "Scaling Techniques for Design, Development and Test," *Liquid Rocket Thrust Chambers: Aspects of Modeling, Analysis, and Design*, edited by V. Yang, M. Habiballah, J. Hulka, and M. Popp, Progress in Astronautics and Aeronautics, Vol. 200, AIAA, Washington, DC, 2004, pp. 553-600.
15) Anderson, W.E., Sisco, J.C, Long, M.R., and Sung, I.-K., "Scaling Test Methods for Combustion Devices," *Fifth International Symposium on Liquid Space Propulsion (CD-ROM)*, Chattanooga, TN, USA, 28-30 October, 2003.
16) Fisher, S.C., Dodd. F.E., and Jensen, R.J., "Scaling Techniques for Liquid Rocket Combustion Stability Testing," *Liquid Rocket Engine Combustion Instability*, edited by V. Yang, and W. Anderson, Progress in Astronautics and Aeronautics, Vol. 169, AIAA, Washington, DC, 1995, pp. 545-564.
17) Delabroy, O., Lacas, F., Labegorre, B., and Samaneigo, J.-M., "Paramètres de Similitude Pour la Combustion Diphasique," *Rev. Gén. Therm*, 37, 1998, pp. 934-953. (in French).
18) "JANNAF Rocket Engine Performance Prediction and Evaluation Manual," CPIA Publication 246, April 1975.
19) Coats, D.E., "Assessment of Thrust Chamber Performance," *Liquid Rocket Thrust Chambers: Aspects of Modeling, Analysis, and Design*, edited by V. Yang, M. Habiballah, J. Hulka, and M. Popp, Progress in Astronautics and Aeronautics, Vol. 200, AIAA, Washington, DC, 2004, pp. 601-620.
20) Huzel, D.K., and Huang, D.H., "Modern Engineering for Design of Liquid-Propellant Rocket Engines," Progress in Astronautics and Aeronautics, Vol. 147, AIAA, Washington, DC, 1992.

21) Anderson, W.E., Ryan III, H.M., Santoro, R.J., and Hewitt, R.A., "Combustion Instability Mechanisms in Liquid Rocket Engines Using Impinging Jet Injectors," AIAA Paper No. 95-2357, July 1995.
22) Hewitt, R.A., "Combustion Instability in Liquid Rockets (with a d/V Correlation Perspective)," invited lecture delivered at the 31st AIAA/ASME/SAE/ASEE Joint Propulsion Conference, July 10, 2006.
23) Kenny, R.J., Moser, M.D., Hulka, J., and Jones, G., "Cold Flow Testing For Liquid Propellant Rocket Injector Scaling and Throttling," AIAA Paper No. 2006-4705, July 2006.
24) Mueller, J., "Thruster Options for Microspacecraft: A Review and Evaluation of Existing Hardware and Emerging Technologies," AIAA Paper No. 97-3058, July 1997.
25) Bruno, C., "Chemical Microthrusters: Effects of Scaling on Combustion," AIAA Paper No. 2001-3711, July 2001.
26) Barsotti, R.J., Datsko, S.C., Louison, R., Kovach, R.J., Miller, D.J., and Pullman, W.P., "Development of Liquid Oxygen/Liquid Hydrogen Thrust Chamber for the M-1 Engine, Technology Report," Aerojet General Corp., NASA CR 54813, AGC 9400-5, May 15, 1968.
27) Dankhoff, W.F., Johnson, I.A., Conrad, E.W., and Tomazic, W.A., "M-1 Injector Development – Philosophy and Implementation," NASA Lewis Research Center, TN D-4730, Aug. 1968.
28) Scott, H.E., Bloomer, H.E., and Mansour, A.H., "M-1 Engine Subscale Injector Tests," NASA Lewis Research Center, TN D-4053, July 1967.
29) Muss, J.A., Nguyen, T.V., and Johnson, C.W., "User's Manual for Rocket Combustor Interactive Design (ROCCID) and Analysis Computer Program, Volume I," NASA CR-187109, May 1991.
30) Neill, T., "Flight and Development History of the Highly Reliable Space Shuttle Orbital Maneuvering Engine," AIAA Presentation, 42nd AIAA/ASME/SAE/ASEE Joint Propulsion Conference, Sacramento, CA, July 12, 2006.
31) David, D., "Space Shuttle Orbit Maneuvering Subsystem (OMS) Rocket Engine Development Status Update – July 1977," AIAA Paper No. 77-811, July 1977.
32) Kahl, R.C., LaBotz, R.J., and Bassham, L.B., "Platelet Injectors for Space Shuttle Orbit Maneuvering Engine," AIAA Paper No. 74-1108, October 1974.
33) "Space Shuttle Orbit Maneuvering Engine Platelet Injector Program," NASA CR-151442, Aerojet Liquid Rocket No. Final Report 13133-F-1, Dec. 1975.
34) Hurlbert, E.A., Sun, J.L., and Zhang, B., "Instability Phenomena in Earth Storable Bipropellant Engines," *Liquid Rocket Engine Combustion Instability*, edited by V. Yang, and W. Anderson, Progress in Astronautics and Aeronautics, Vol. 169, AIAA, Washington, DC, 1995, pp. 113-142.
35) Salmi, R.J., Wanhainen, J.P., and Hannum, N.P., "Effect of Thrust Per Element on Combustion Stability Characteristics of Hydrogen-Oxygen Rocket Engines," NASA Lewis Research Center, TN D-4851, Oct. 1968.

Marshall Space Flight Center

Scaling of Performance in Liquid Propellant Rocket Engine Combustors

March 7, 2007

James Hulka
Jacobs Engineering, ESTS Group
NASA MSFC, Huntsville, AL USA

JE JACOBS ESTS Group

Objectives

- Re-introduce to you the concept of scaling
- Describe the scaling research conducted in the 1950s and early 1960s, and present some of their conclusions
- Narrow the focus to scaling for performance of combustion devices for liquid propellant rocket engines
- Present some results of subscale to fullscale performance from historical programs

What is Scaling ?

- "The ability to develop new combustion devices with predictable performance on the basis of test experience with old devices."

- Can be used to develop combustion devices of any thrust size from any thrust size
  - Applied mostly to *increase* thrust

- Objective is to use scaling as a *development tool*
  - Move injector design from an "art" to a "science"

Why is Scaling Important ?

- Provides guidance and validation to the combustor design and development
  - Develop full-size designs that are closer to success more quickly
  - Validate key requirements earlier in the development process
- May allow use of smaller and lower flow rate hardware during development
  - Reduce costs for manufacturing development hardware
  - Reduce iterations of full-size hardware
  - Reduce development testing costs
    - (-) Smaller, lower flow rate test facilities
    - (-) Less propellant consumption, fewer test personnel
    - (+ ?) Higher pressure test facilities
  - Increase reliability with more thorough evaluation of margins

Is There a Scaling "Holy Grail"?

- Is there a development scaling methodology for combustion devices that offers:
  1. Reduced size and lower flow rate than original
  2. Lower pressure than original
  3. Easily and inexpensively producible
  4. Complete validation for performance, combustion stability, heat transfer, and ignition

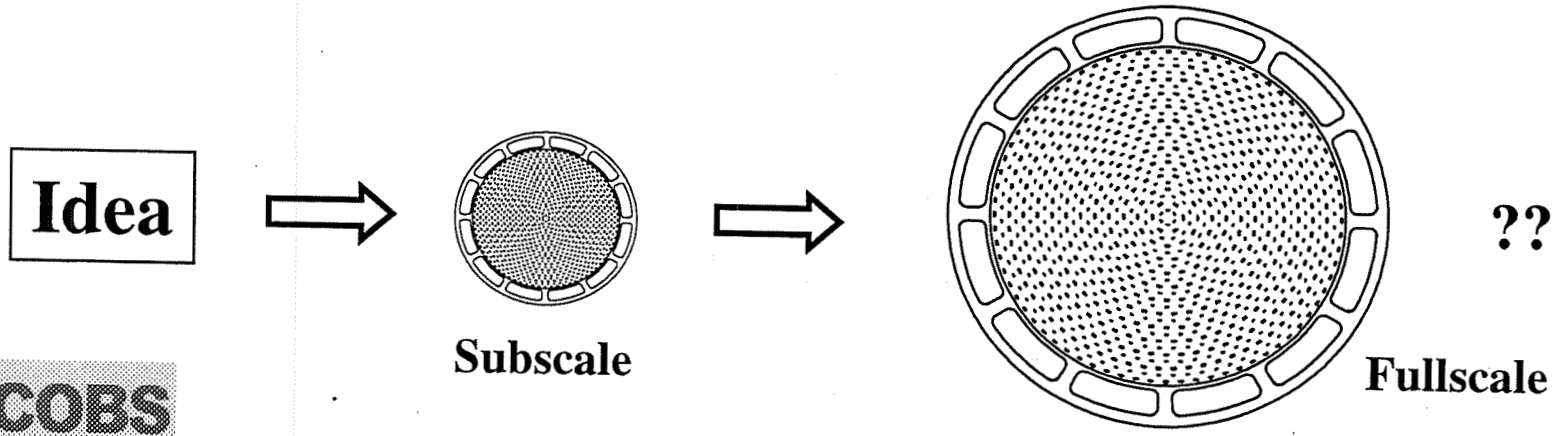

Scaling H-1 to F-1

$\eta_{C*} = 97.3\%$

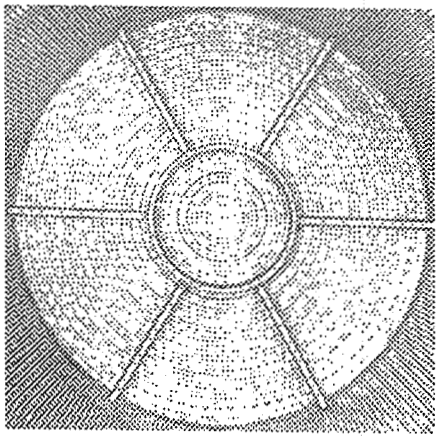

← 20.9" →

$\eta_{C*} = 93.8\%$

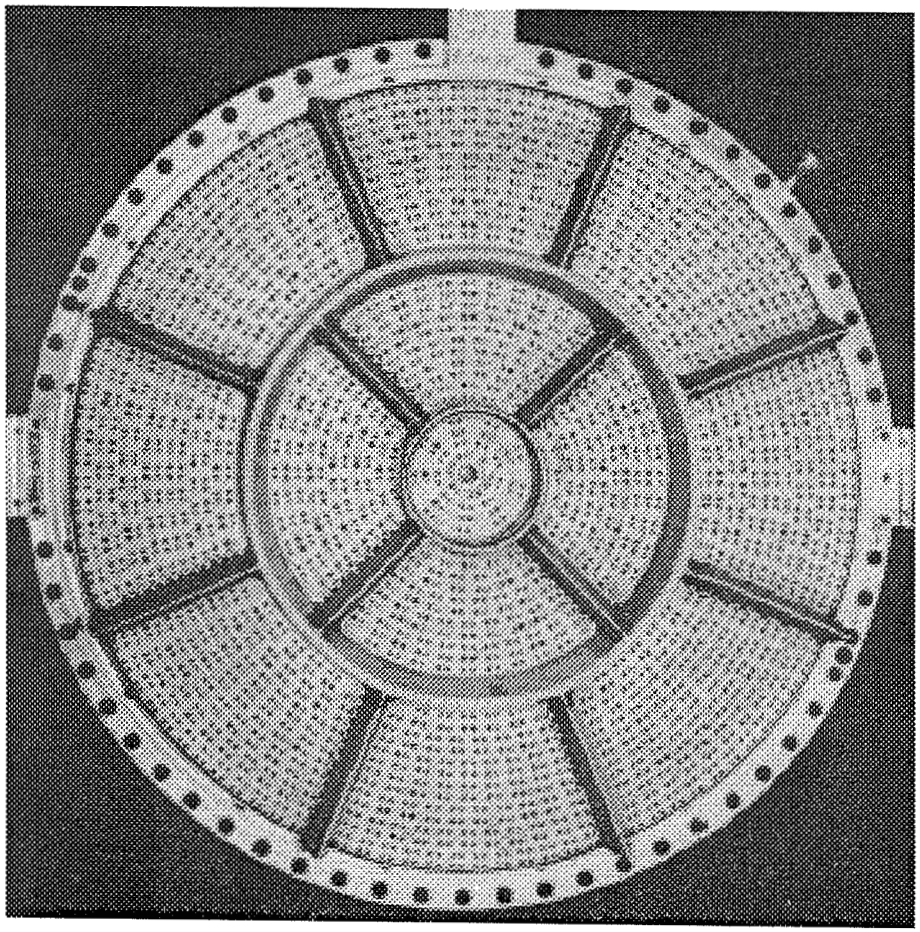

← 39.2" →

Scaling H-1 to F-1 – Why didn't it work ?

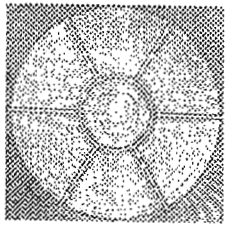

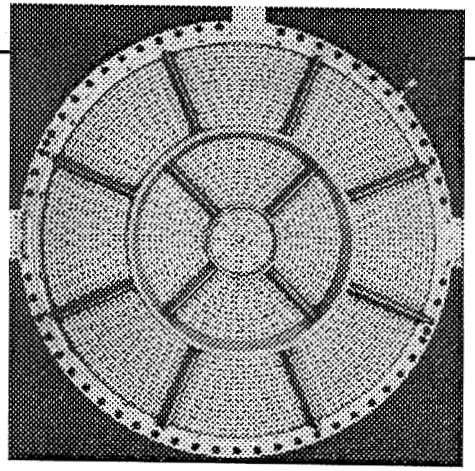

• ηC* = 97.3% ⟷	• ηC* = 93.8%
• Dch = 20.9" ⟷	• Dch = 39.2"
• L' = 31.2"	• L' = 40.0"
• L* = 48"	• L* = 48"
• Pc = 705 psia	• Pc = 1128 psia
• Fsl = 205 Klbf ⟷	• Fsl = 1522 Klbf
• 365 ox, 612 fuel	• 714 ox, 702 fuel
• F/E = 560 lbf ⟷	• F/E = 2142 lbf

JE JACOBS ESTS Group

Exact Combustion Similarity

- All processes occur in identical fashion, even though they occur with different scales
  - Flow paths
  - Flame patterns
  - Locations and time histories of specie generation
  - Locations and time histories of heat release
  - Contours of temperature, pressure, and velocity
- Focus on steady internal aerothermochemistry
- Note that unsteady flows are not expected to have the same scaling rules

Similarity Parameters from Mass, Momentum, and Energy Equations for Exact Combustion Similarity

Reynolds No. = $Re = \dfrac{\rho v L}{\mu}$

Schmidt No. = $Sc = \dfrac{\mu}{\rho D}$

Prandtl No. = $Pr = \dfrac{c_p \mu}{k}$

Mach No. = $M = \left(\dfrac{\rho v^2}{\gamma p} \right)^{1/2}$

Froude No. = $Fr = \dfrac{v^2}{g_a L}$

$$\Phi = \frac{1/2 v^2}{(c_p/\gamma)T}$$

Specific Heat Ratio = $\gamma = \dfrac{c_p}{c_v}$

First Damköhler Group = $Da,i = \dfrac{L}{v\tau_i}$

Third Damköhler Group = $Da,iii = \dfrac{q' L}{v c_p T \tau_i}$

Defined by Penner, 1955

Seven Similarity Parameters for Non-Reacting Flow Processes

Non-Reacting Flows

Reynolds No. = $Re = \frac{\rho v L}{\mu}$

Schmidt No. = $Sc = \frac{\mu}{\rho D}$

Prandtl No. = $Pr = \frac{c_p \mu}{k}$

Mach No. = $M = \left(\frac{\rho v^2}{\gamma p} \right)^{1/2}$

Froude No. = $Fr = \frac{v^2}{g_a L}$

$$\Phi = \frac{1/2 v^2}{(c_p / \gamma) T}$$

Specific Heat Ratio = $\gamma = \frac{c_p}{c_v}$

First Damköhler Group = $Da,i = \frac{L}{v \tau_i}$

Third Damköhler Group = $Da,iii = \frac{q' L}{v c_p T \tau_i}$

Two Similarity Parameters for Reacting Flow Processes

Reynolds No. = $Re = \dfrac{\rho v L}{\mu}$

Schmidt No. = $Sc = \dfrac{\mu}{\rho D}$

Prandtl No. = $Pr = \dfrac{c_p \mu}{k}$

Mach No. = $M = \left(\dfrac{\rho v^2}{\gamma p} \right)^{1/2}$

Froude No. = $Fr = \dfrac{v^2}{g_a L}$

$$\Phi = \frac{1/2 v^2}{(c_p/\gamma)T}$$

Specific Heat Ratio = $\gamma = \dfrac{c_p}{c_v}$

First Damköhler Group = $Da,i = \dfrac{L}{v \tau_i}$

Third Damköhler Group = $Da,iii = \dfrac{q' L}{v c_p T \tau_i}$

Reacting Flows

Reduced Set from Penner

$$\text{Reynolds No.} = Re = \frac{\rho v L}{\mu}$$

$$\text{Schmidt No.} = Sc = \frac{\mu}{\rho D}$$

$$\text{Prandtl No.} = Pr = \frac{c_p \mu}{k}$$

- Homogeneous Flow
- Low Velocity
- No Significant External Forces

$$\text{First Damköhler Group} = Da,i = \frac{L}{v \tau_i}$$

$$\text{Third Damköhler Group} = Da,iii = \frac{q' L}{v c_p T \tau_i}$$

Marshall Space Flight Center

Constant properties will result in competition between *Re* and *Da,i*

Reynolds No. = $Re = \frac{\rho v L}{\mu}$

- ρ, μ, D, c_p, k = constant

Schmidt No. = $Sc = \frac{\mu}{\rho D}$

Prandtl No. = $Pr = \frac{c_p \mu}{k}$

First Damköhler Group = $Da,i = \frac{L}{v \tau_i}$

Third Damköhler Group = $Da,iii = \frac{q' L}{v c_p T \tau_i} = Da,i * \frac{q'}{c_p T}$

JACOBS ESTS Group

Heat Transfer to the Chamber Walls

- *Re* and *Pr* are fixed

Reynolds No. = $Re = \frac{\rho v L}{\mu}$ Prandtl No. = $Pr = \frac{c_p \mu}{k}$

- Therefore Nusselt number *Nu* is fixed

Nusselt No. = $Nu \sim$ Constant * $Re^x Pr^y$

- Therefore, heat transfer characteristics are scaled properly since *Re* and *Pr* are scaled properly

Scaling Between Large & Small → Penner-Tsien Rule & Constant Pressure

- Properties = Constant (μ, ρ, D, c_p, k)

$$Sc = \frac{\mu}{\rho D} = \text{Constant} \qquad Pr = \frac{c_p \mu}{k} = \text{Constant}$$

- $Re = \dfrac{\rho v L}{\mu} = \text{Constant}$

$$vL\Big|_{\text{subscale}} = vL\Big|_{\text{fullscale}} \rightarrow \left(\frac{v_S}{v_F}\right)\left(\frac{L_S}{L_F}\right) = 1$$

- $Da,i = \text{Constant}$

$$\frac{L}{v\tau_i}\Bigg|_{\text{subscale}} = \frac{L}{v\tau_i}\Bigg|_{\text{fullscale}} \rightarrow \boxed{\left(\frac{\tau_{i,S}}{\tau_{i,F}}\right) = \left(\frac{L_S}{L_F}\right)^2}$$

The Meaning of $\left(\frac{\tau_{i,S}}{\tau_{i,F}}\right) = \left(\frac{L_S}{L_F}\right)^2$

- At constant chamber pressure and temperature, as the length scales are reduced, the chemical conversion times must be reduced as the *square* of the length scales
  - For example, as $L_S = ½\, L_F$ (half geometric scale)

    then $\tau_{i,S} = ¼\, \tau_{i,F}$ (chemical times quartered)
- Note that because of *Re*=constant, then

  as $L_S = ½\, L_F$ (half geometric scale)

  then $v_S = 2\, v_F$ (velocities doubled)
- Does this happen naturally, or must it be forced ?
  - Penner concluded this control is obtained by control of droplet size

The Meaning of $\left(\frac{\tau_{i,S}}{\tau_{i,F}}\right) = \left(\frac{L_S}{L_F}\right)^2$

- Note that injector orifice diameter = scale ratio
- Thus if $L_S = ½\, L_F$, then $d_S = ½\, d_F$ and $A_S = ¼\, A_F$, $v_S = 2\, v_F$
  - Element flow continuity $m_S = (\rho_F)(¼\, A_F)(2\, v_F) = ½\, m_F$
    - Note that with geometric half-size element, $m_S = ¼\, m_F$
  - Element pressure drop $\Delta P_S \sim \rho_S v_S^2 \sim \rho_F 4 v_F^2 \sim 4\, \Delta P_F$
- Therefore, through a half-sized element, have to *increase* the flowrate to achieve 4 times ΔP
  - High velocity sprays with enhanced atomization
  - Note that *Re* are still matched
  - How are flow rates doubled but chamber pressures constant ?
    - *M*. not constant – change chamber contraction ratio
- But is $\tau_{i,S} = ¼\ \tau_{i,F}$ as required ? Not clear…

Penner's Conclusions

- Penner concluded control of chemical conversion rate is obtained by artificial modification of droplet size
  - Variation of surface tension by, e.g., surface active agents
- Successful scaling probably accomplished only for bipropellants with greatly different volatilities
- Engine development involves testing small scale injectors with high injection velocities and fine sprays for the less volatile propellant
  - Injector dimensions scale same as chamber dimensions

Scaling Between Large & Small → Crocco & Pressure Dependence $\tau \sim p^{-m}$

- $Re = \dfrac{\rho v L}{\mu}$ = Constant, and $\rho \sim p$

$$pvL\Big|_{\text{subscale}} = pvL\Big|_{\text{fullscale}} \rightarrow \left(\frac{p_S}{p_F}\right)\left(\frac{v_S}{v_F}\right)\left(\frac{L_S}{L_F}\right) = 1$$

- Da,i = Constant

$$\frac{L}{v\tau_i}\Big|_{\text{subscale}} = \frac{L}{v\tau_i}\Big|_{\text{fullscale}} \rightarrow \boxed{\left(\frac{\tau_{i,S}}{\tau_{i,F}}\right) = \left(\frac{L_S}{L_F}\right)^{2m/(m+1)}}$$

- Note that $\left(\dfrac{v_S}{v_F}\right) = \left(\dfrac{L_S}{L_F}\right)^{(1-m)/(1+m)}$ and $\left(\dfrac{d_S}{d_F}\right) = \left(\dfrac{L_S}{L_F}\right)^{m/(m+1)}$

The Meaning of $\left(\frac{\tau_{i,S}}{\tau_{i,F}}\right) = \left(\frac{L_S}{L_F}\right)^{2m/(m+1)}$

- For m = 1 (i.e., $\tau \sim 1/p$, from Crocco)

$$\left(\frac{\tau_{i,S}}{\tau_{i,F}}\right) = \left(\frac{L_S}{L_F}\right)$$

  - As the length scales are reduced, the chemical conversion times must be reduced proportionally
  - For example, as $L_S = \frac{1}{2} L_F$ (half geometric scale)

    then $\tau_{i,S} = \frac{1}{2} \tau_{i,F}$
  - However, the chamber pressure is <u>increased</u>, in this case, since $(p_S / p_F)^m = (\tau_{i,F} / \tau_{i,S})$,

    or $p_S = 2\, p_F$
  - Also, $v_S = v_F$, or M = constant

The Meaning of $\left(\frac{\tau_{i,S}}{\tau_{i,F}}\right) = \left(\frac{L_S}{L_F}\right)^{2m/(m+1)}$

- Continuing for m=1 and $L_S = ½\, L_F$,
  - then $d_S = \sqrt{½}\, d_F$ and $A_S = ½\, A_F$, $v_S = v_F$
  - Element flow continuity $m_S = (\rho_F)(½\, A_F)(v_F) = ½\, m_F$
    - Note that through half-size element, $m_S = ¼\, m_F$ normally
  - Element pressure drop $\Delta P_S \sim \rho_S v_S^2 \sim \rho_F v_F^2 \sim \Delta P_F$
- Therefore, element flowrate is doubled but element area is doubled so pressure drop is constant
  - Equal velocity sprays
  - Note that *Re* are still matched
- Also, is $\tau_{i,S} = ½\ \tau_{i,F}$ as required ?

Crocco's Conclusions

- Control of chemical conversion rate is obtained by control of pressure
- Engine development involves testing small scale injectors with high pressures
  - Injector dimensions are *not* scaled the same as chamber dimensions

Conclusions From Early Scaling Studies

- Similarity of some of the parameters resulted in difficult design situations
  - Penner-Tsien: small injectors with increased pressure drops in chambers with distorted contraction ratios, uncertain requirements for τ
  - Crocco: small injectors at higher chamber pressures with distorted injector dimensions, uncertain requirements for τ

Marshall Space Flight Center

Five Sub-Elements of Combustor Performance

1. Collective (multi-element) inefficiency of all core elements
2. Collective (multi-element) inefficiency of all barrier elements
3. Boundary losses
4. Unintentional maldistribution of mass and velocity across the injector face
5. Intentional maldistribution of mass and velocity across the injector face.

Marshall Space Flight Center

Collective Efficiencies of Core and Barrier are Comprised of Many Parts

1. Single element mixing inefficiency for each element type
2. Single element vaporization inefficiency for each element type
3. Inter-element mixing inefficiency (or the multi-element mixing inefficiency, which is the sum of single element mixing inefficiencies modified by element interactions)
4. Inter-element vaporization inefficiency (or the multi-element vaporization inefficiency, which is the sum of single element vaporization inefficiencies modified by element interactions)
5. Losses due to two-dimensional effects of the flowstream
6. Losses due to reaction kinetics
7. Losses due to the radiation energy from various combustion species

Boundary Losses

- The boundary losses, which can be included in the collective efficiency of the barrier, or, more handily, kept separately, include the following:
  - Heat energy losses from the fluids to the injector and chamber walls
  - Boundary layer losses (effect of wall boundaries on the flow streams)

Maldistribution Losses

- Unintentional
  - Non-uniform mass, velocity, and pressure distributions at the injector inlets
  - Non-uniform mass, velocity, and pressure distributions from the injector manifolding
  - Manufacturing tolerance variations on injector metering features
- Intentional
  - Fuel film coolant (FFC) injected into the chamber periphery
  - Deliberate mass flow rate bias of various elements across the injector face (mixture ratio bias)
  - Local element mass flow bias (e.g., off-set, angled or scarfed coaxial posts)
  - Deliberate burning rate variations across the injector face, due to different elements used in the pattern

Scaling the Combustion Chamber

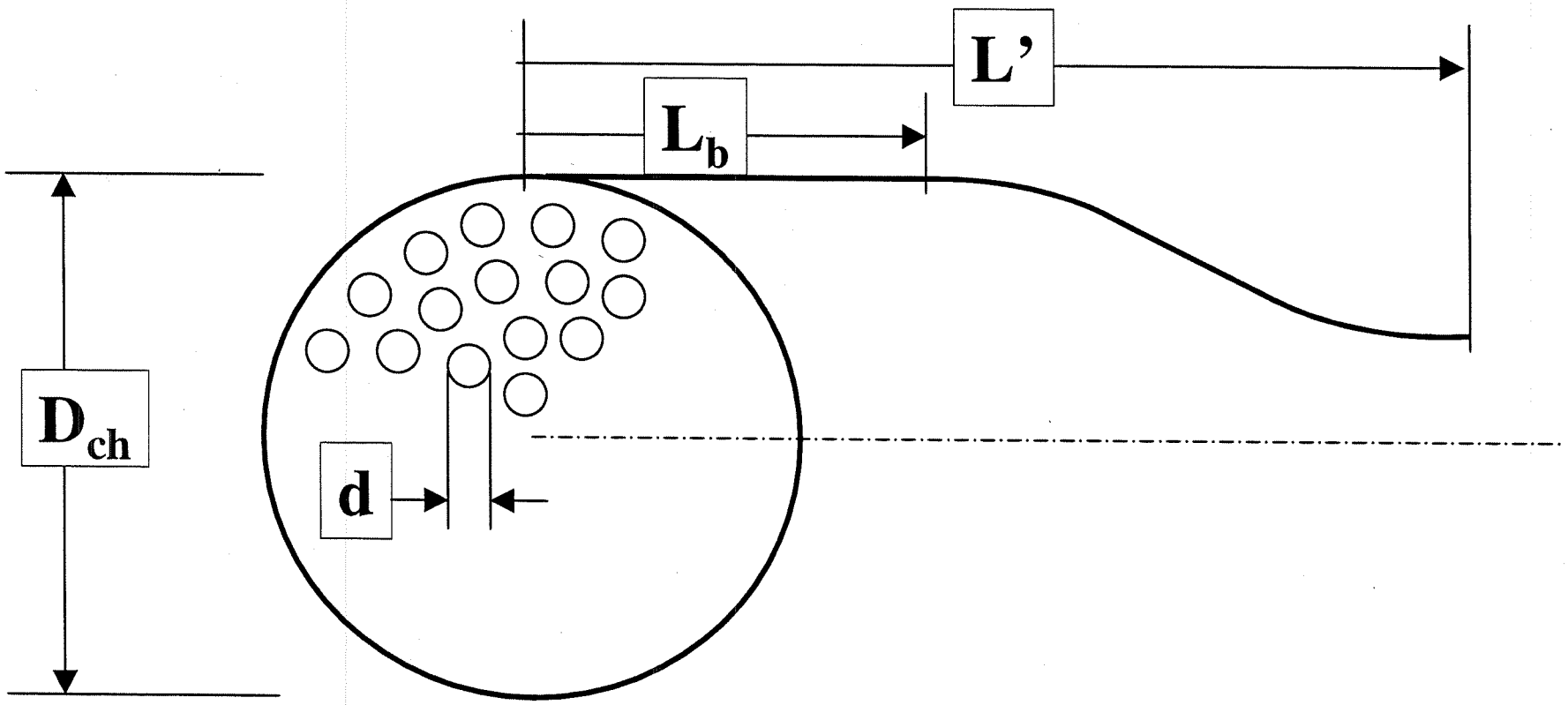

Typical Subscale Chamber Configurations

3-D Chamber

- Subscale Chamber
- Full Scale Injection Elements
- Subscale Transverse Mode for Full Scale Transverse Mode

2D Chamber

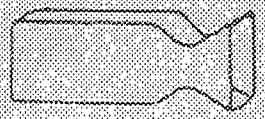

- Chamber Width Mode to Simulate Full Scale Mode
- Full Scale Injection Elements
- Variable Width and No. of Elements to Simulate Different Full Scale Modes

3-D Chamber

- Subscale Chamber
- Subscale Injection Elements
- Subscale Transverse Mode for Full Scale Transverse

Transverse Excitation Chamber

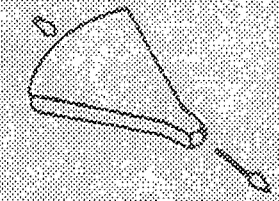

- Pie Shape of Full Scale Chamber Diameter
- Full Scale Injection Elements
- Throat at Centerline
- Two Dimensional
- Radial Flow

Longitudinal Chamber

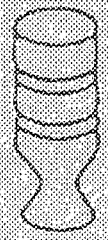

- Subscale Chamber
- Full Scale Injection Elements
- Subscale Longitudinal Mode for Full Scale Transverse Mode

Wedge Chamber

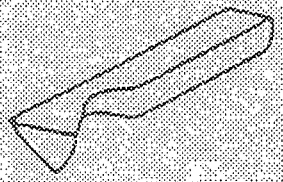

- A Segment of Full Scale Chamber
- Full Scale Injector

Scaling with Constant Element Dimensions

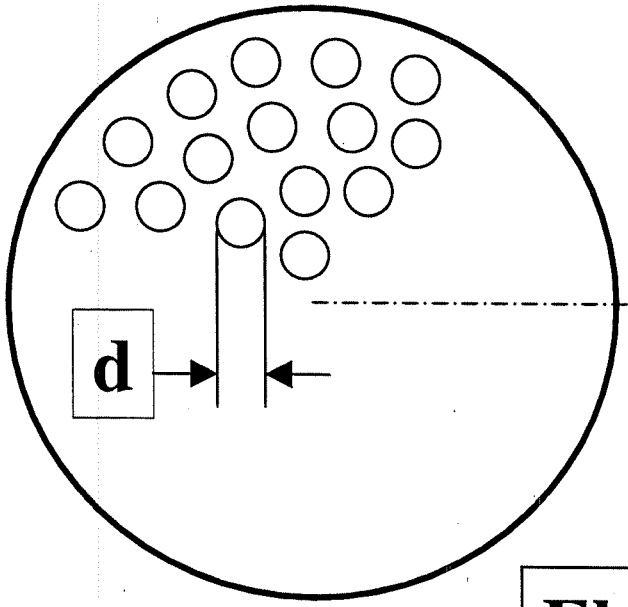

Element size d is the same

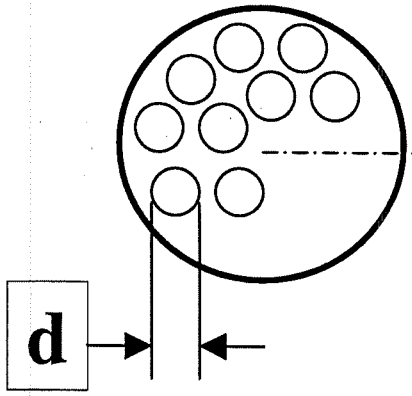

Scaling with Constant Element Dimensions – Typical Chamber Configurations Used Today

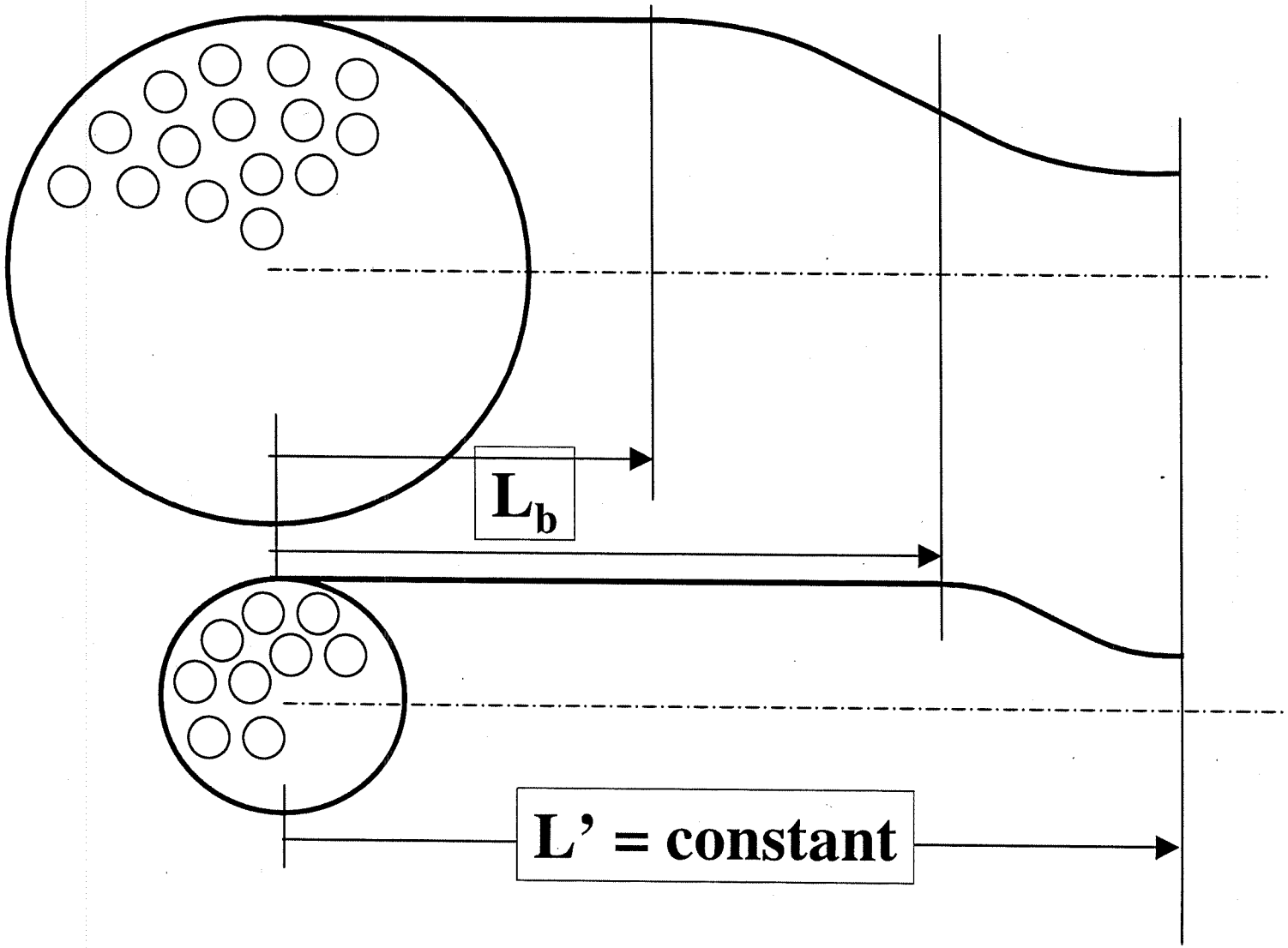

Scaling with Constant Element Dimensions – Maintain Constant Mach No.

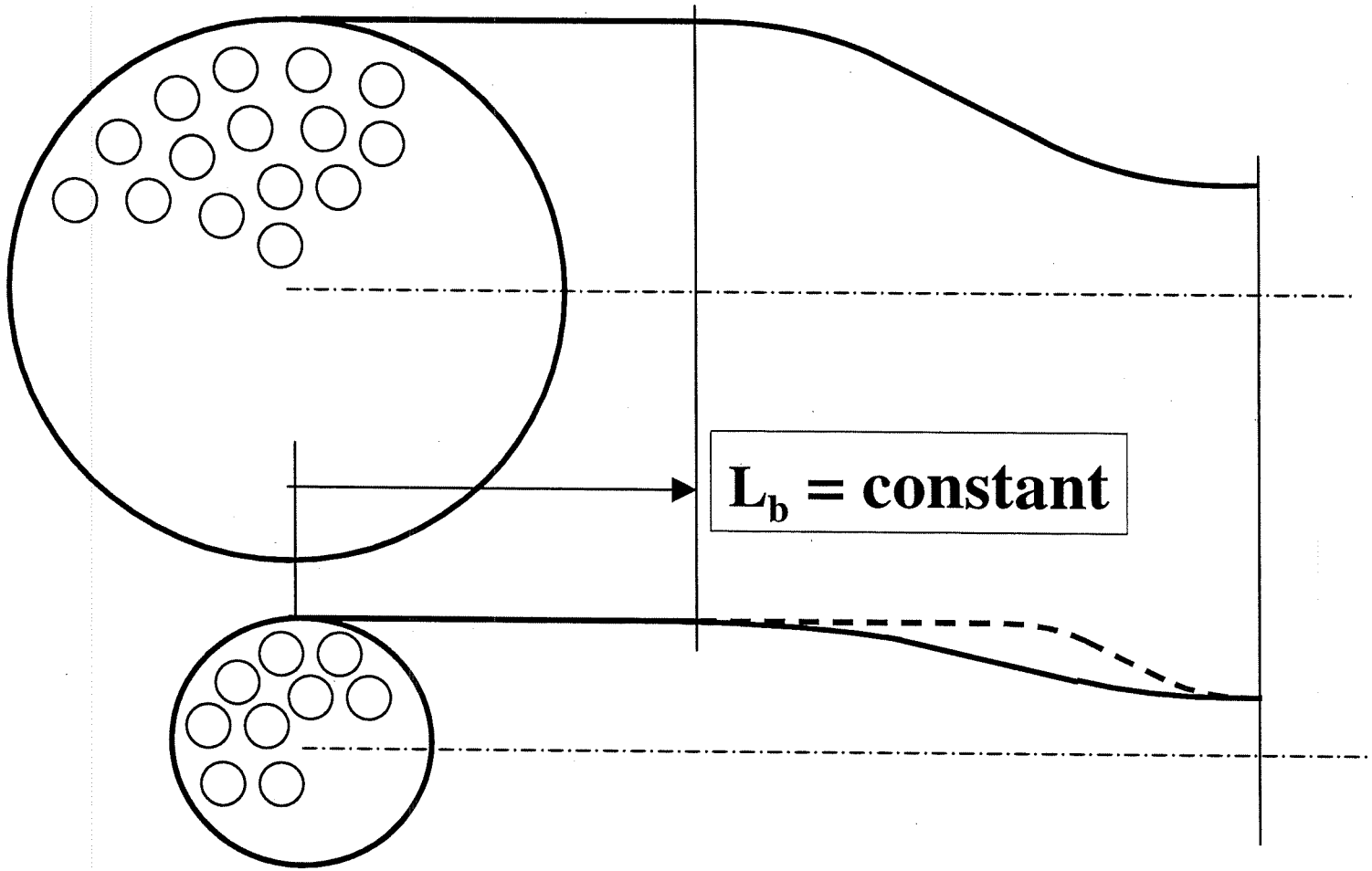

Marshall Space Flight Center

Mach No. Differences in Short and Long Barrel Chambers

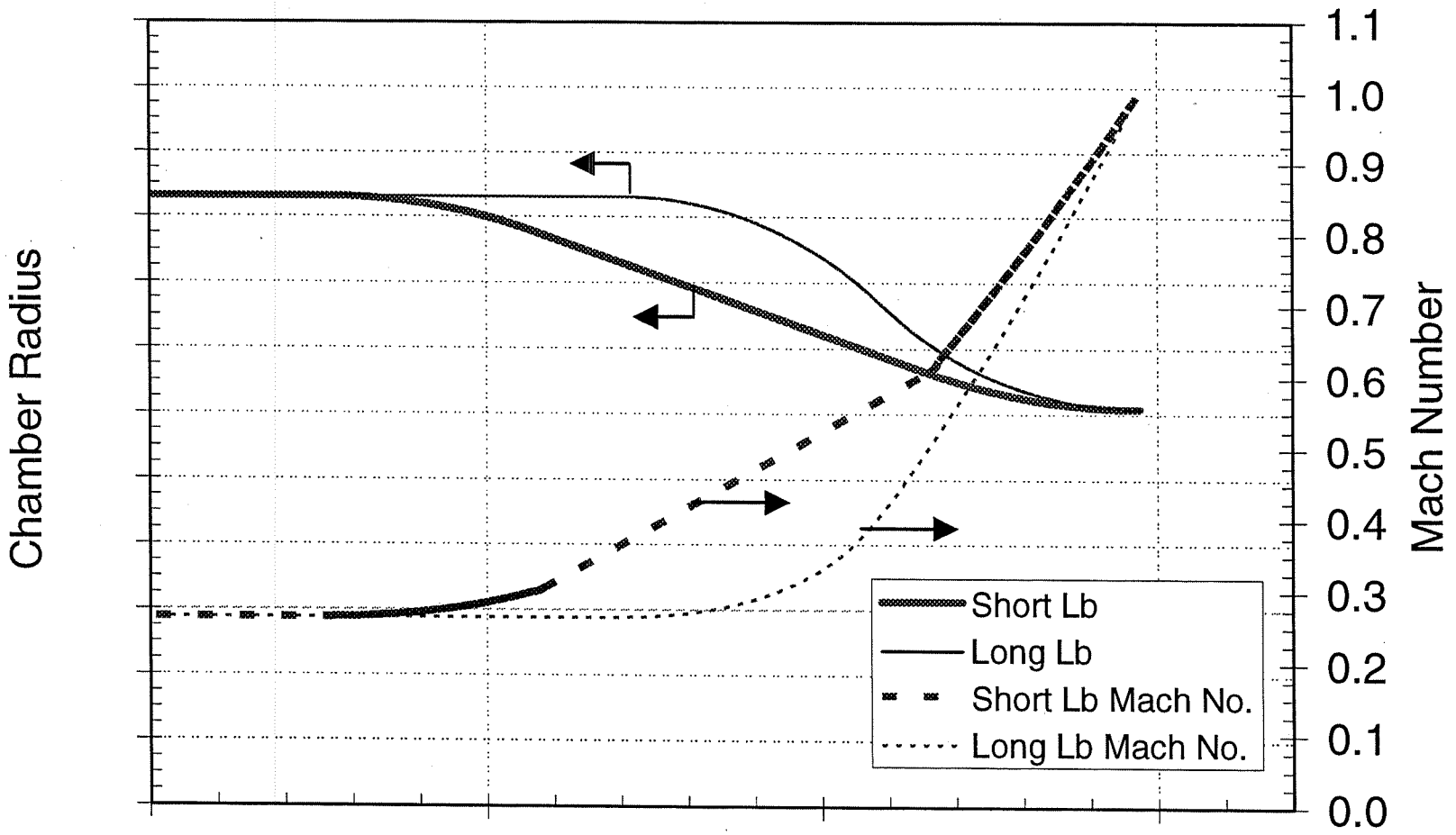

JACOBS ESTS Group

Scaling with Photoscaled Element Dimensions

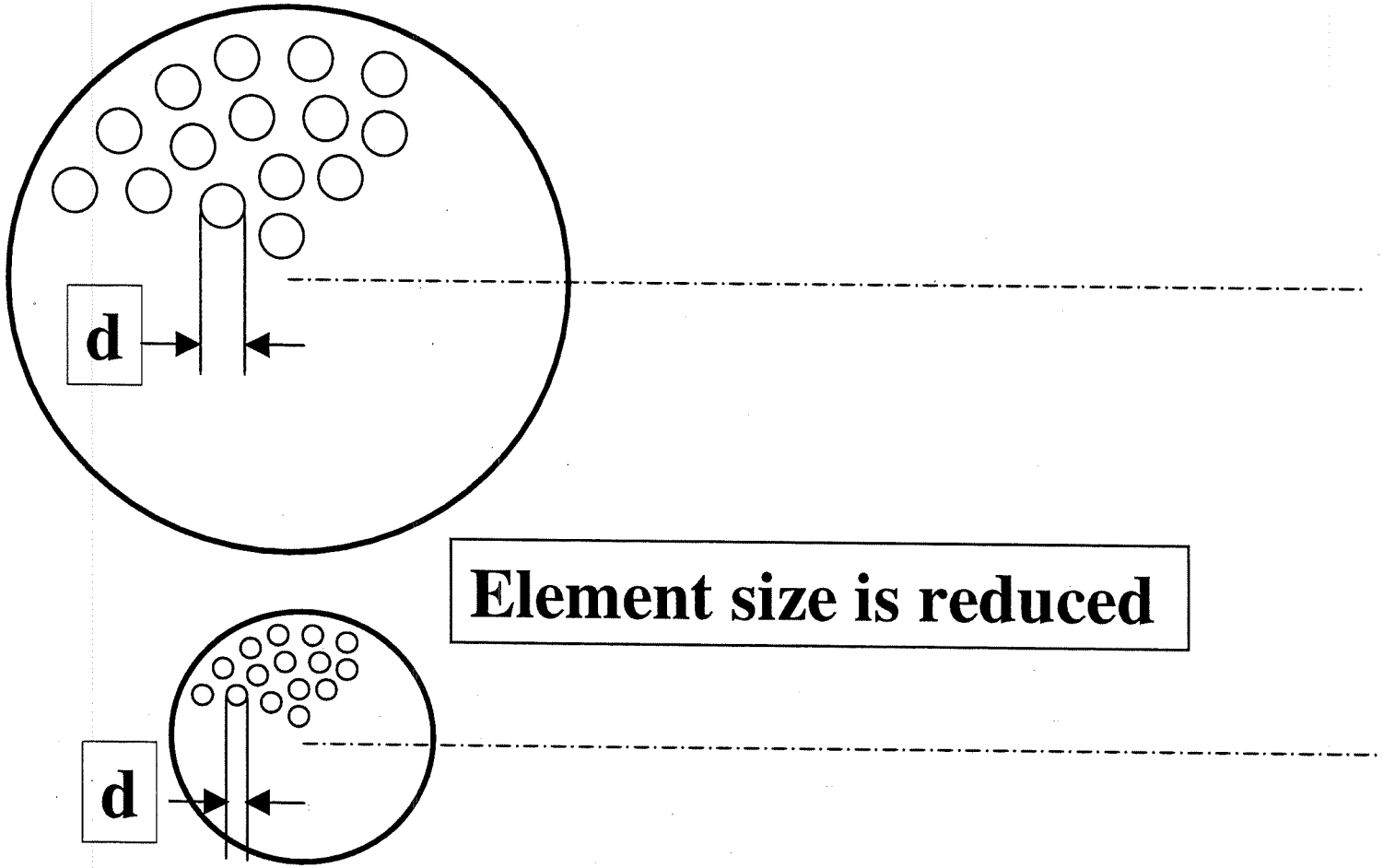

Hewitt d/V for Scaling

- Injector characteristic d/V is fixed to chamber diameter

$$\left(\frac{d_S}{d_F}\right)\left(\frac{v_F}{v_S}\right) = \left(\frac{D_{c,S}}{D_{c,F}}\right)$$

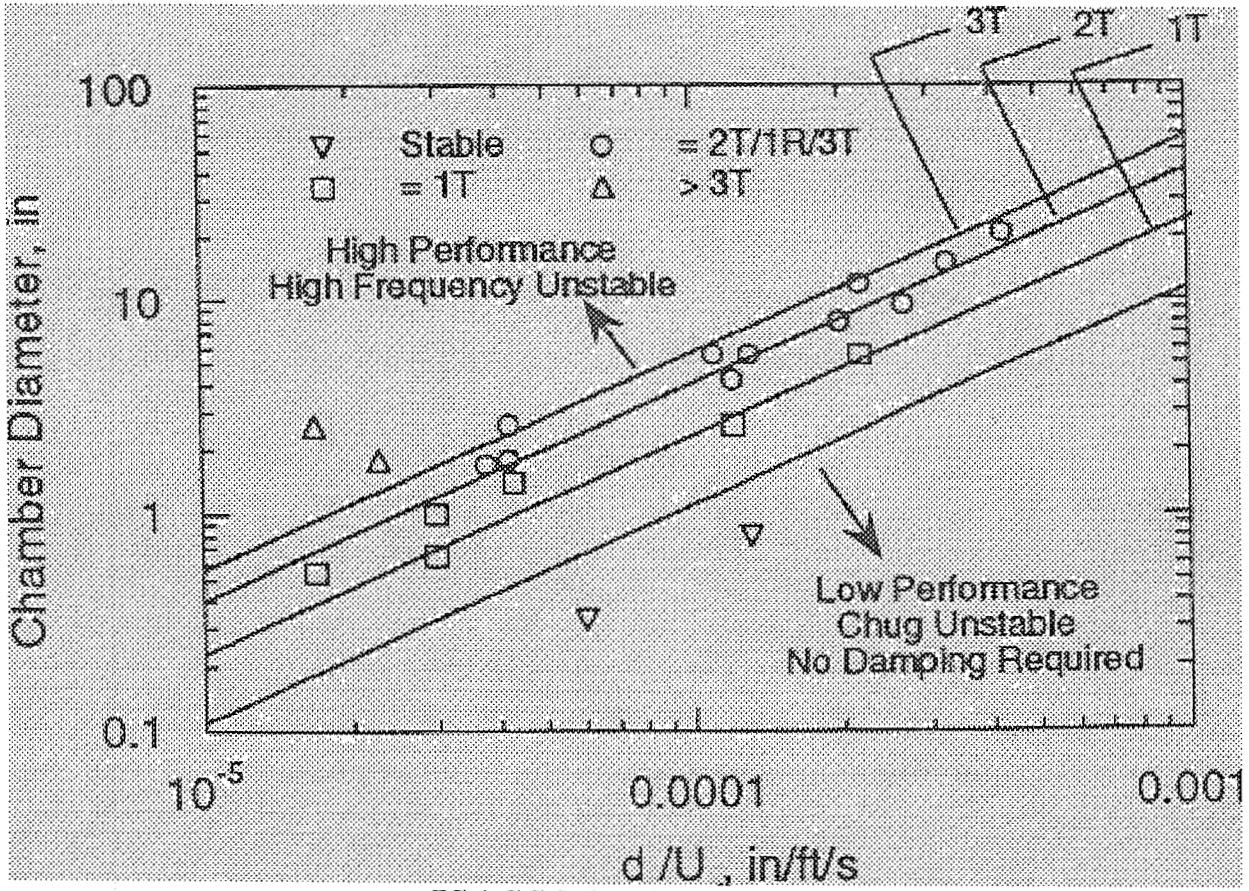

Scaling the Combustion Chamber with Geometric Photoscaling

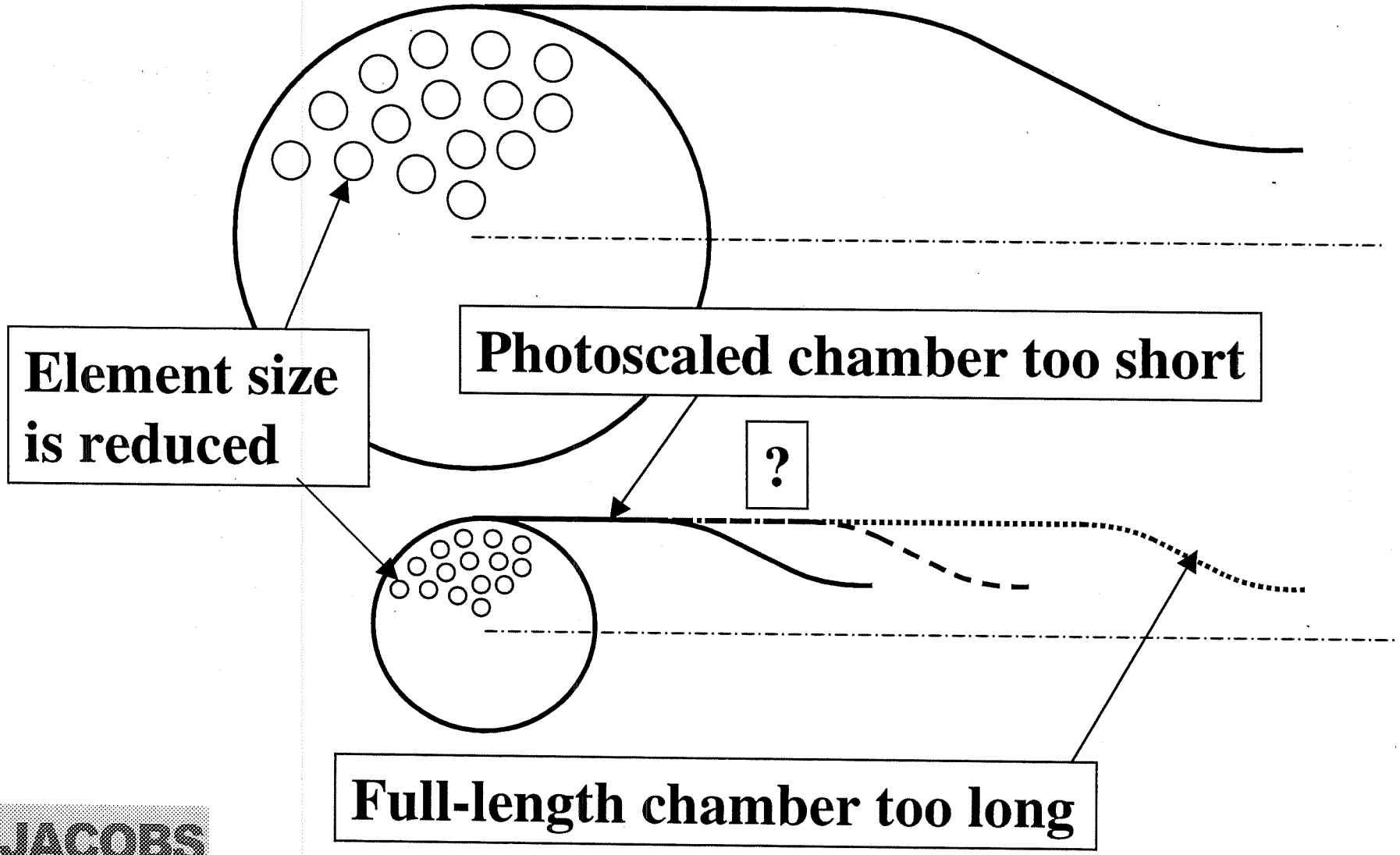

Marshall Space Flight Center

Re-evaluate the Required Similarity Groups
Example: Primary Atomization

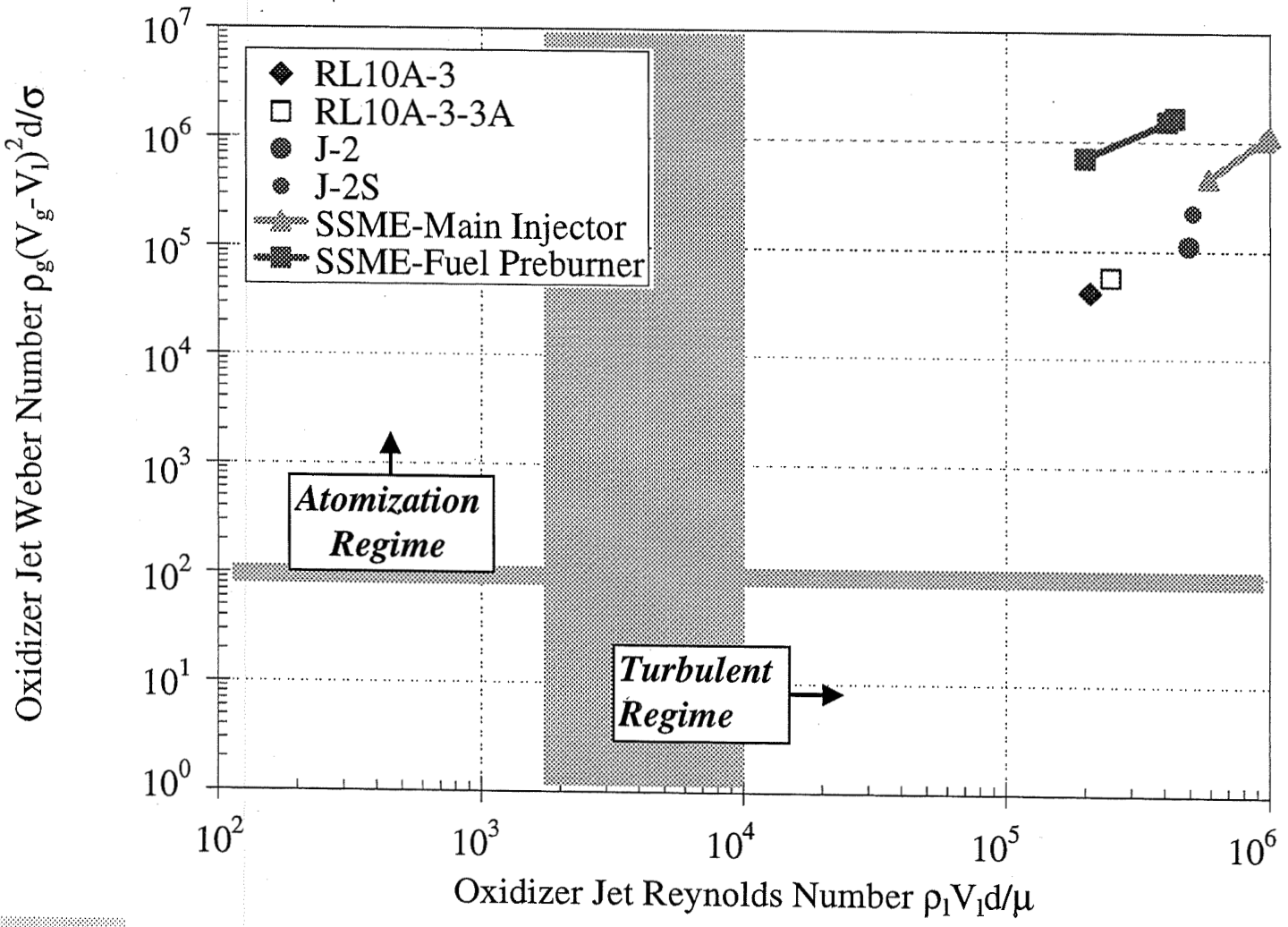

JACOBS ESTS Group

Significant Reduction of Scales Does Not Change Primary Atomization Regimes

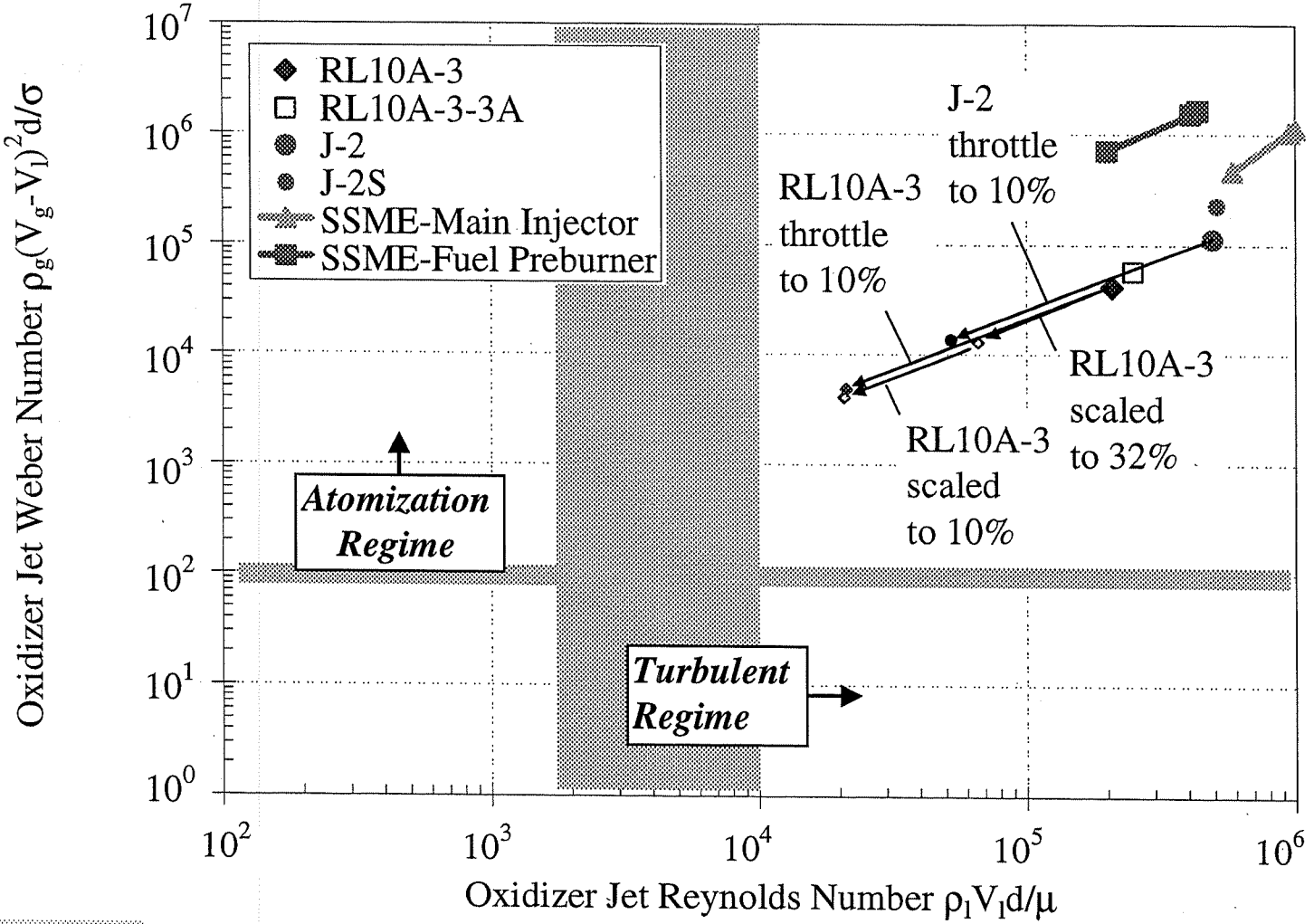

Re-evaluate the Required Similarity Groups
Example: Primary Atomization

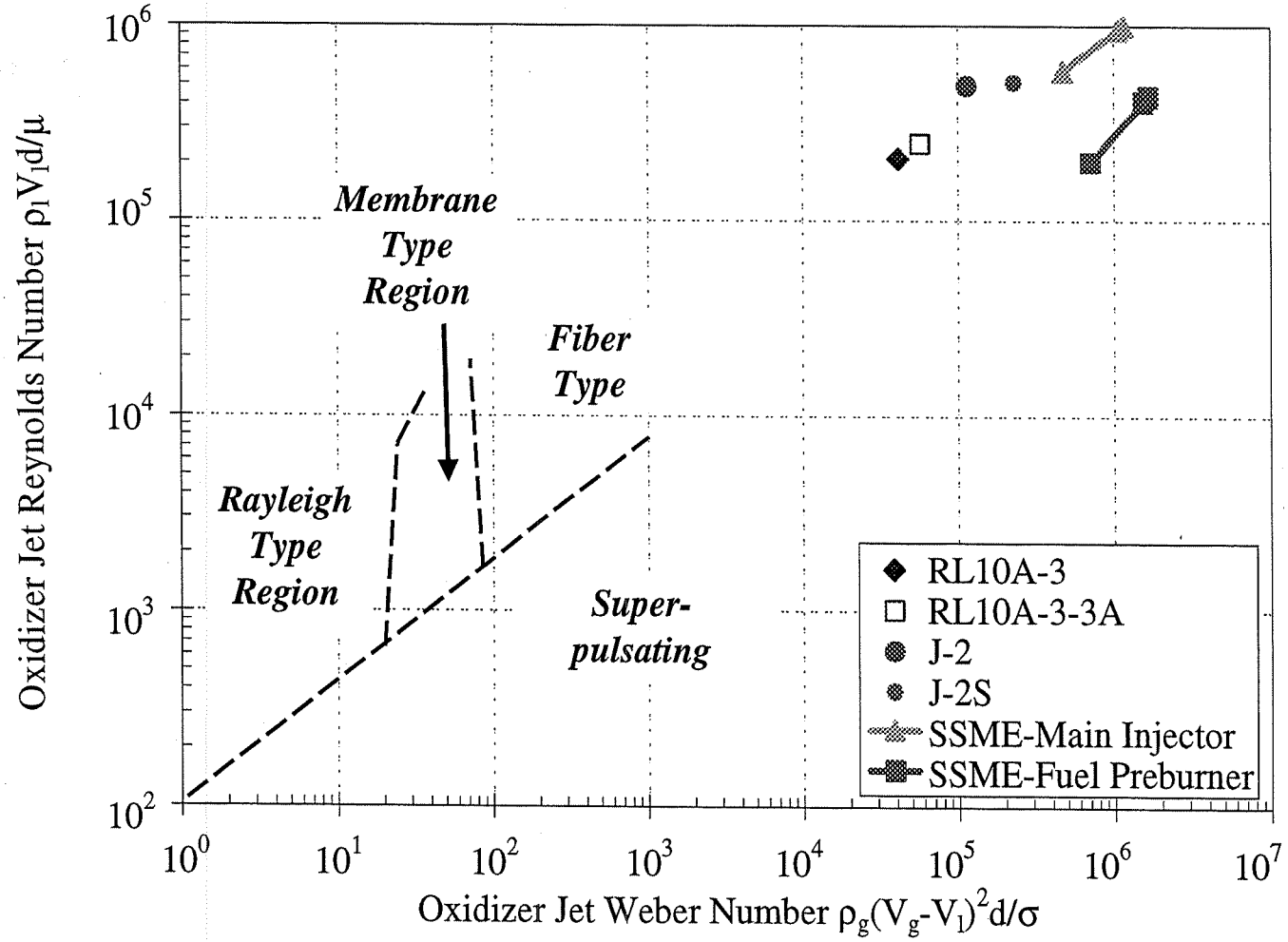

Marshall Space Flight Center

Significant Reduction of Scales Does Not Change Primary Atomization Regimes

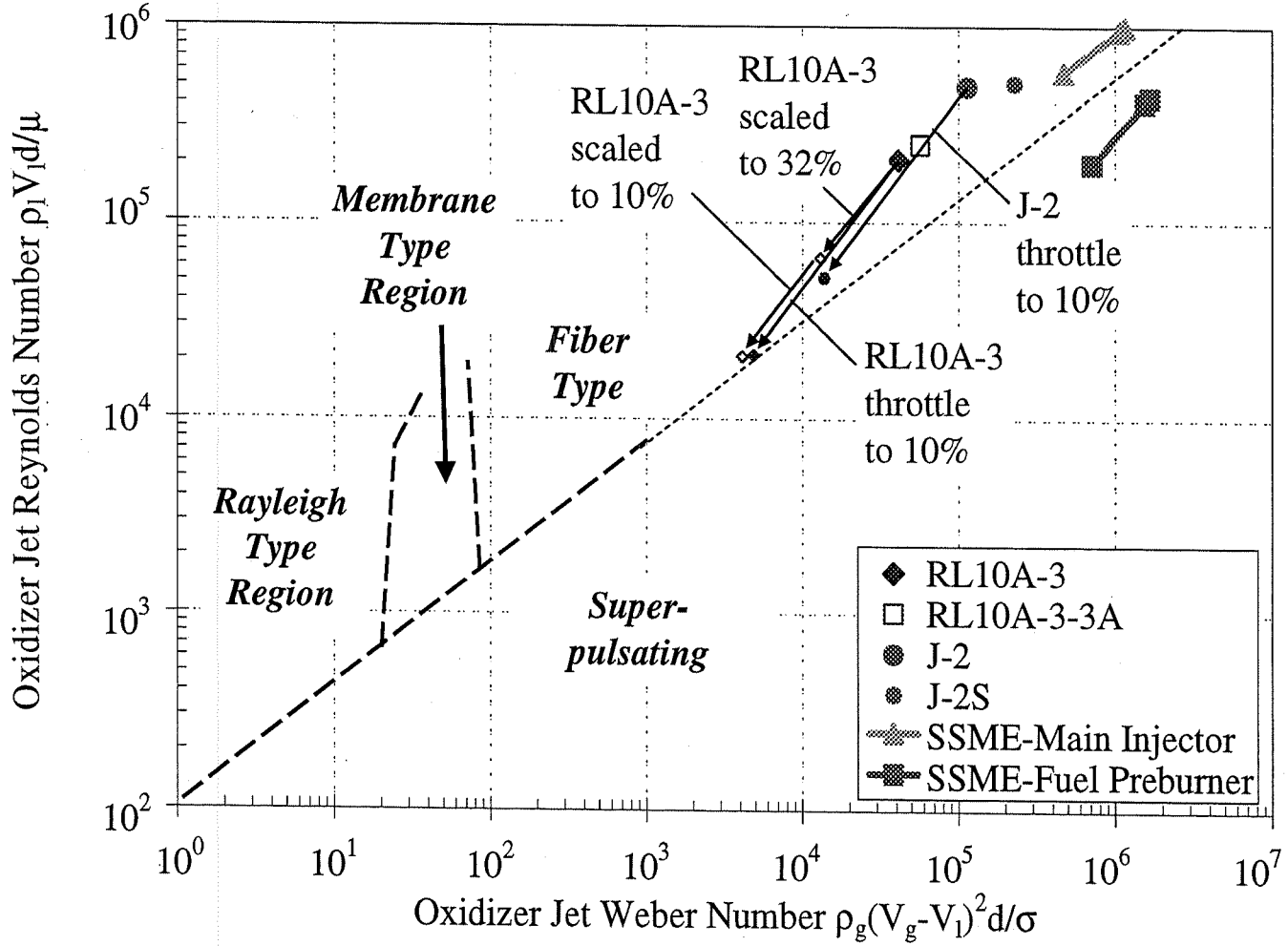

JACOBS ESTS Group

Historical Examples

- M-1
  - 1.5 Mlbf thrust
  - 100:1 ratio between fullscale and subscale thrust
- Space Shuttle Orbital Maneuvering System
  - 6000 lbf
  - 6:1 and 10:1 ratios between fullscale and subscale thrust
- NASA Lewis Research Center Thrust/Element
  - 50:1 ratio between thrust/element in constant chamber diameter

M-1 Thrust Chamber

- Thrust = 6670 kN (1,500 Klbf)
- LO_2/LH_2 Propellants
- Pc ~ 1000 psia
- Upper stage concept considered for Apollo and other missions
- Terminated in advanced component development

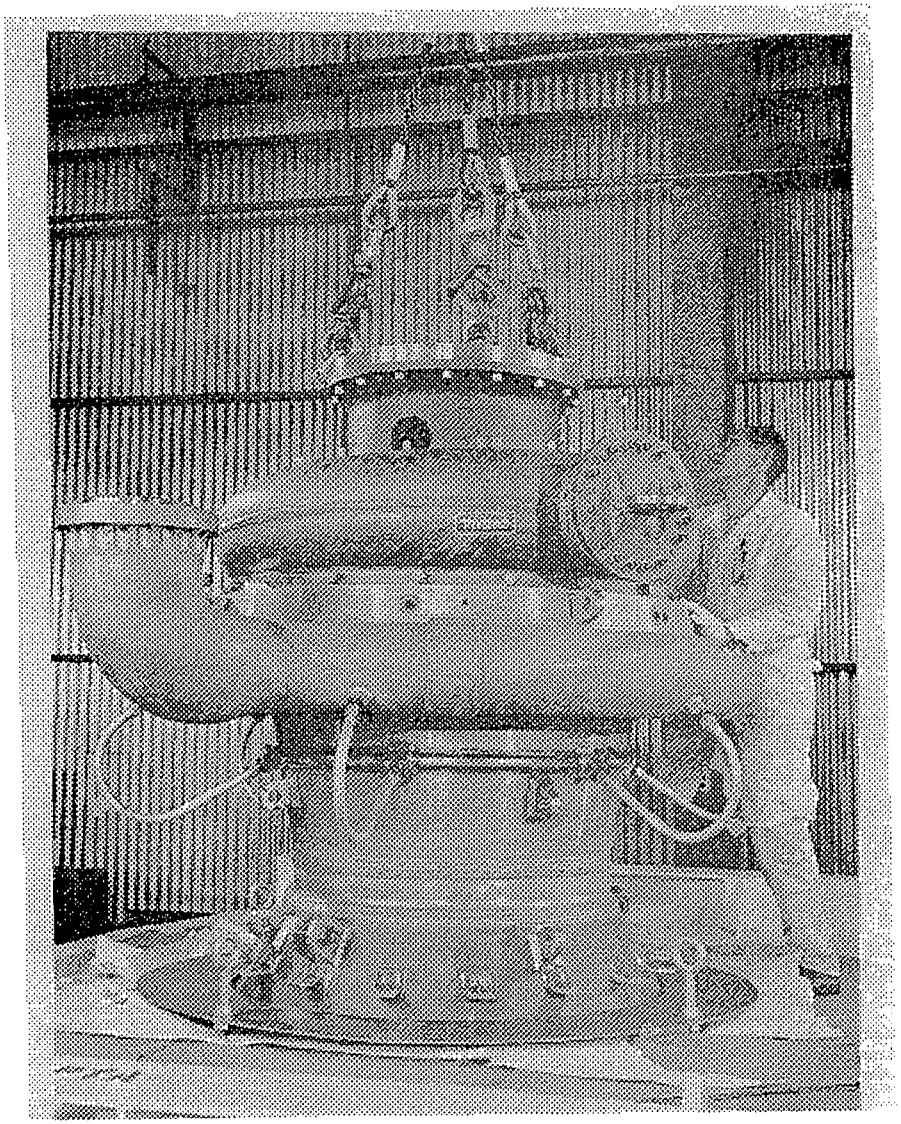

M-1 Main Injector

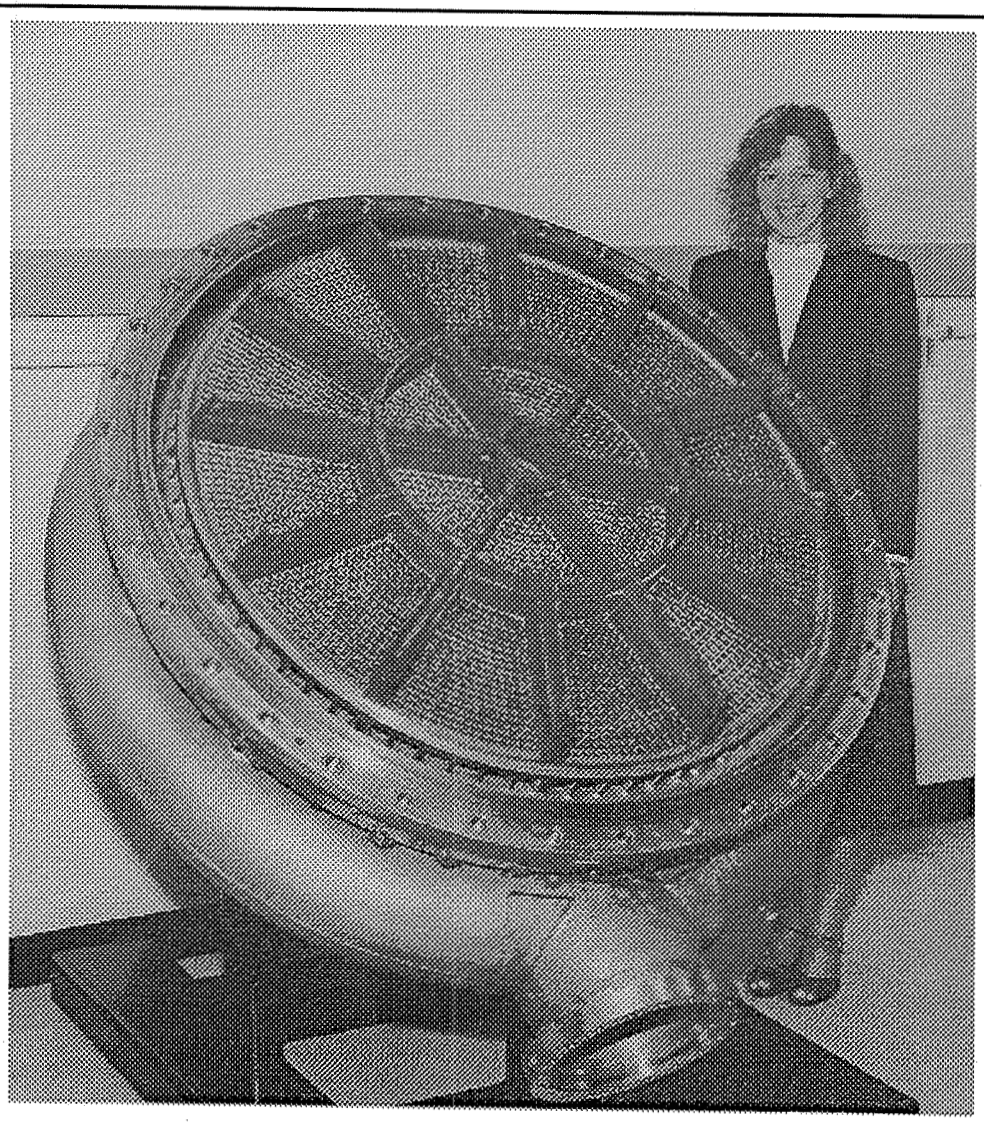

Marshall Space Flight Center

M-1 Fullscale Combustor

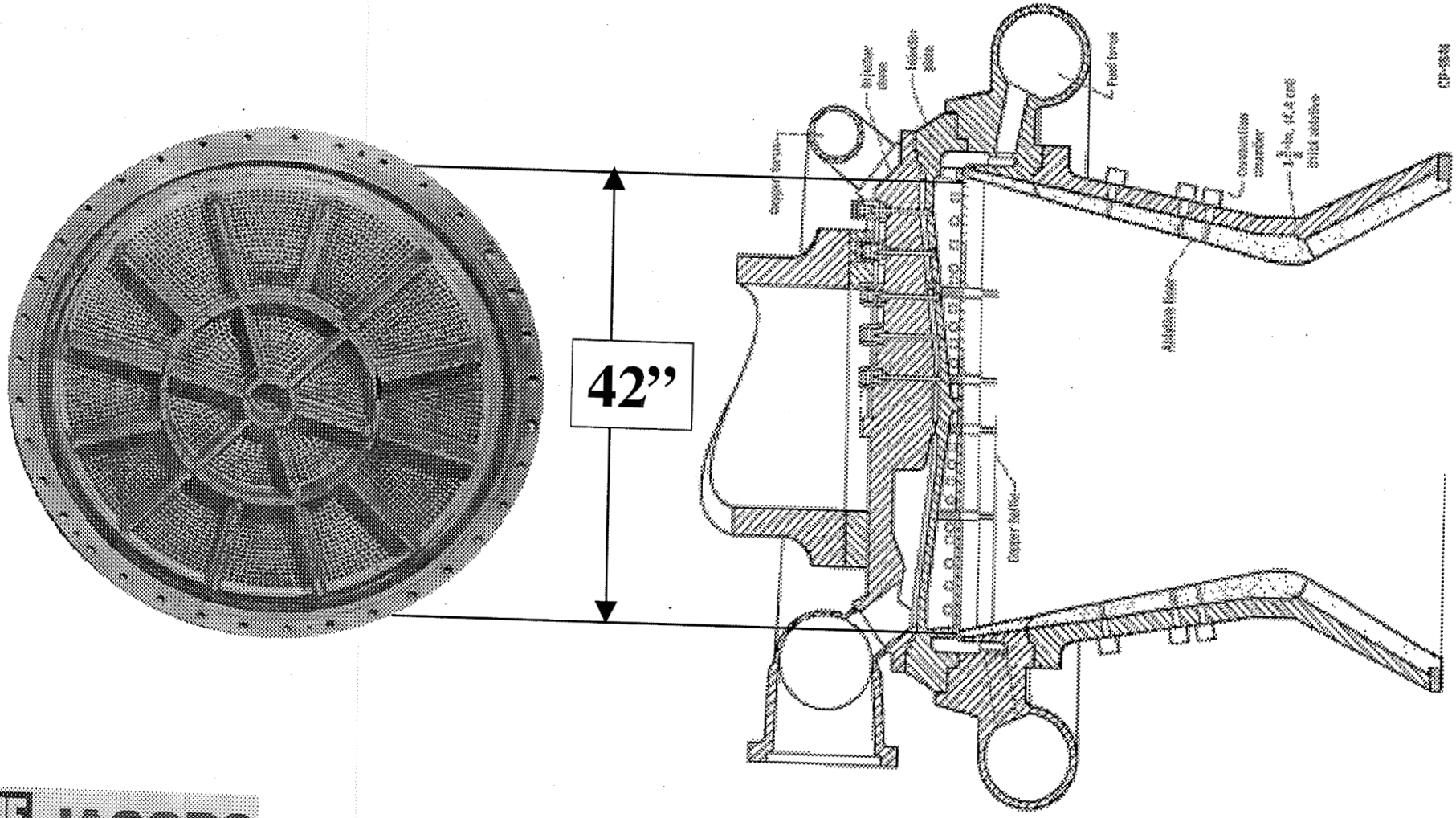

JE JACOBS ESTS Group

M-1 Subscale Combustor

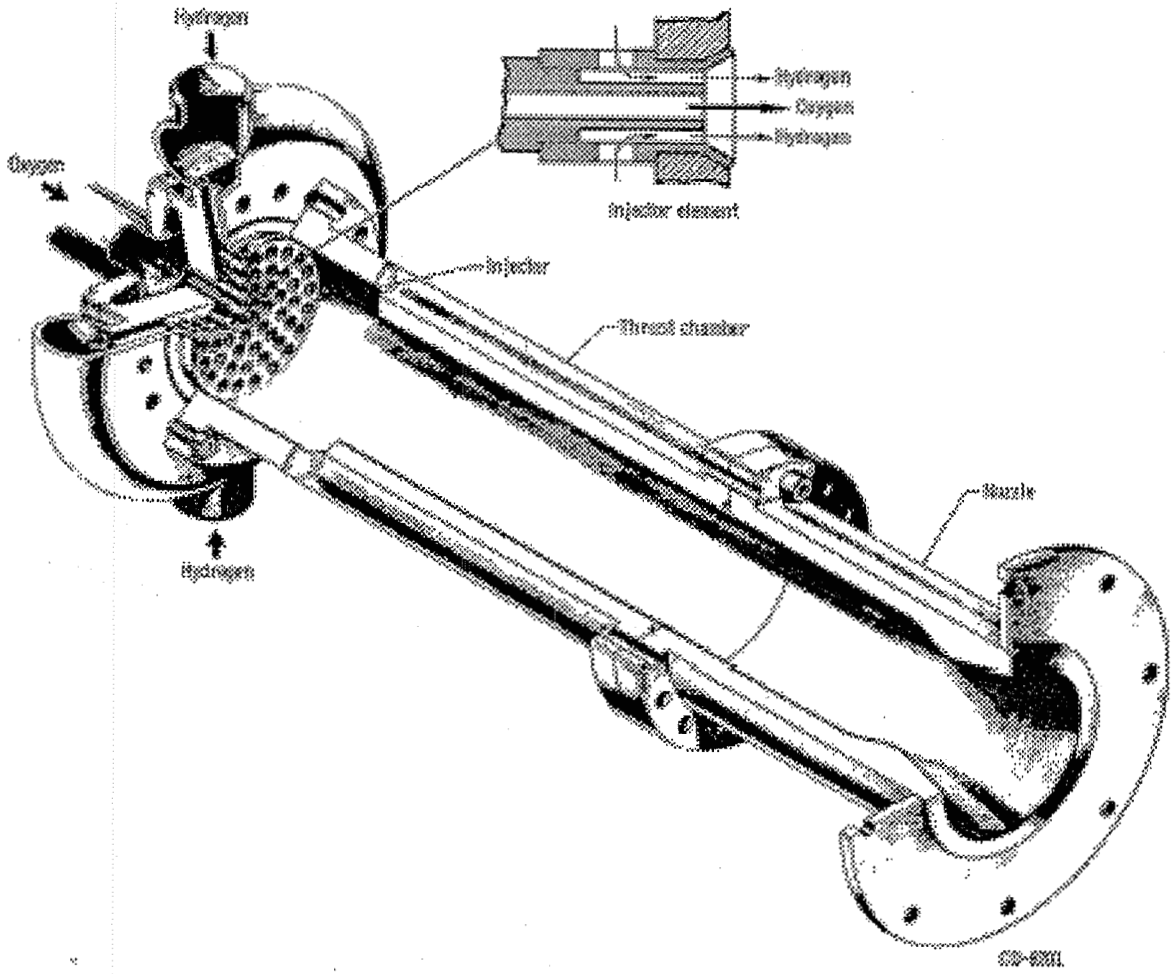

M-1 Subscale Main Injectors

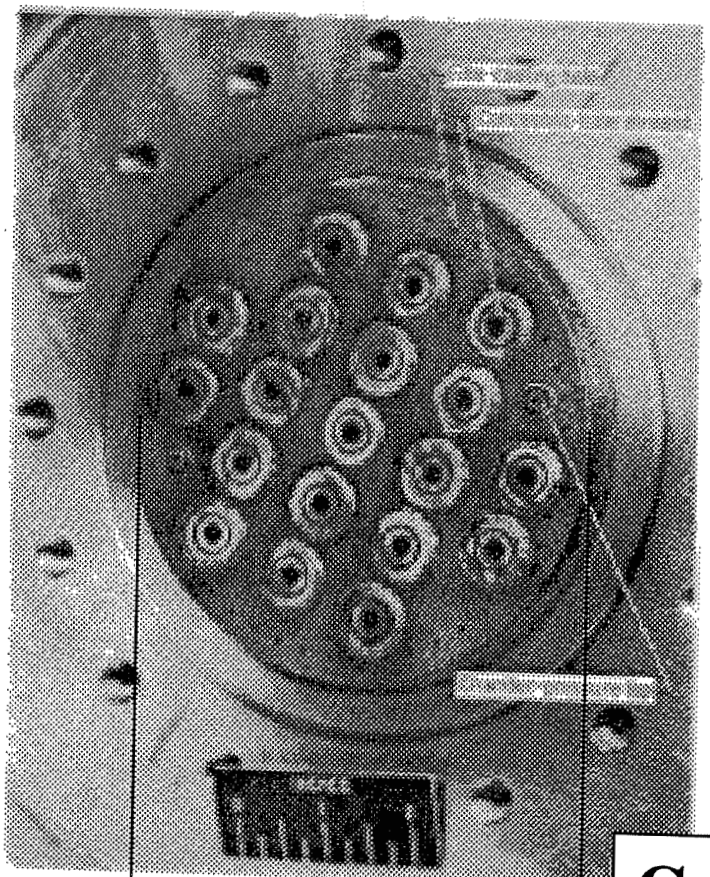

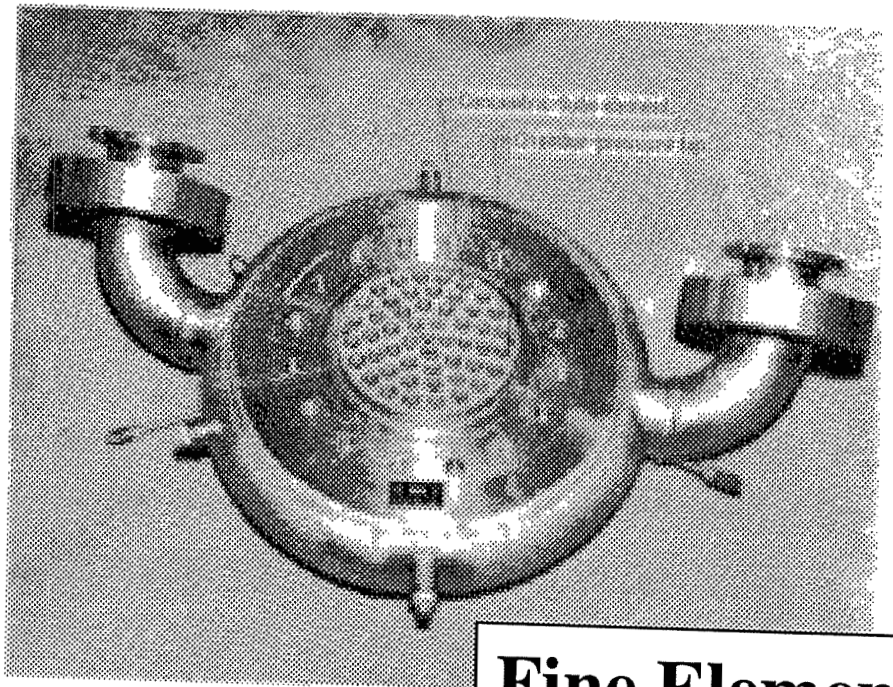

Fine Element

Coarse Element

5.39”

JE JACOBS ESTS Group

Comparison of M-1 Fullscale and Subscale Thrust Chambers

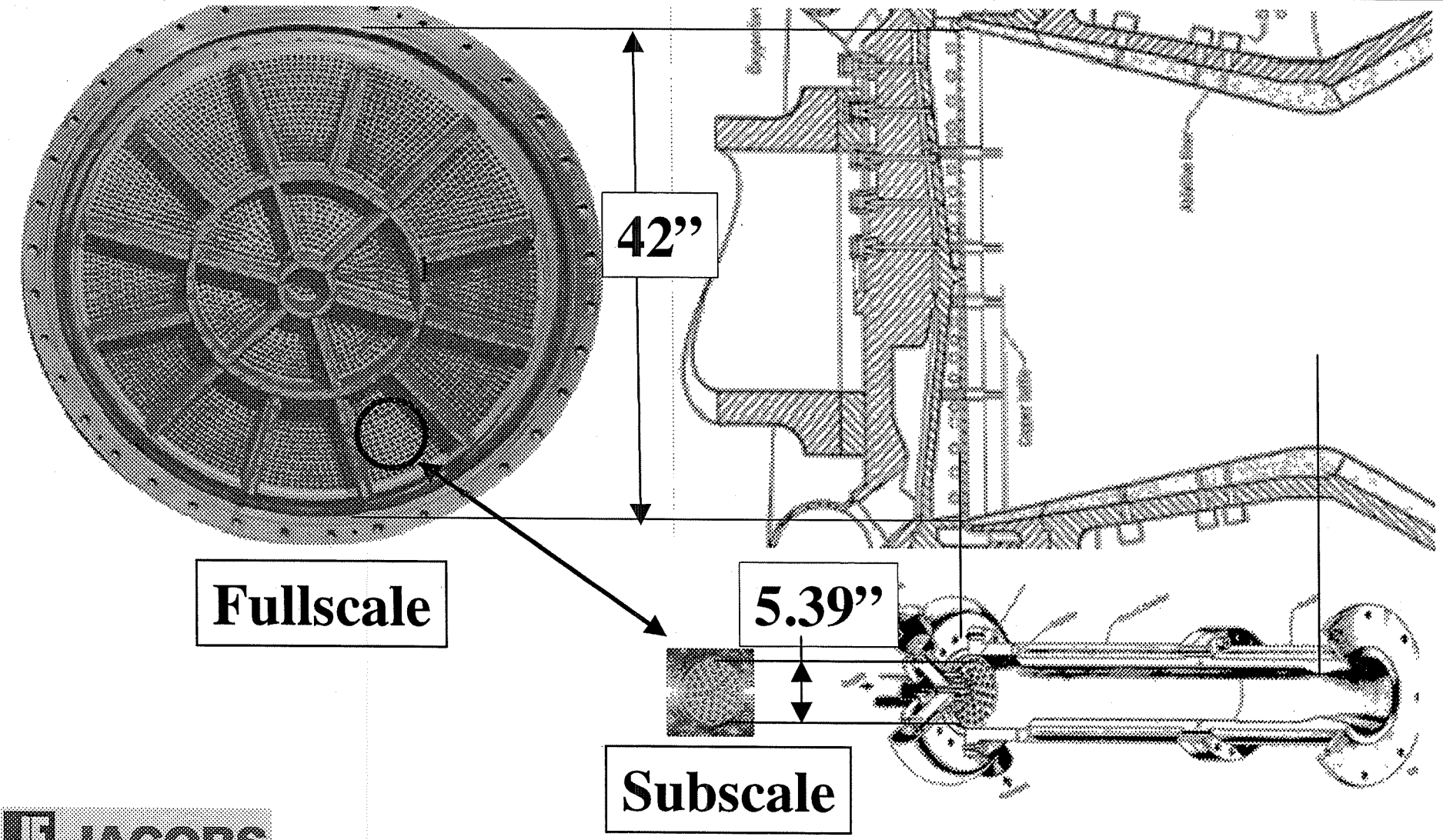

Comparison of M-1 Subscale to Fullscale Performance

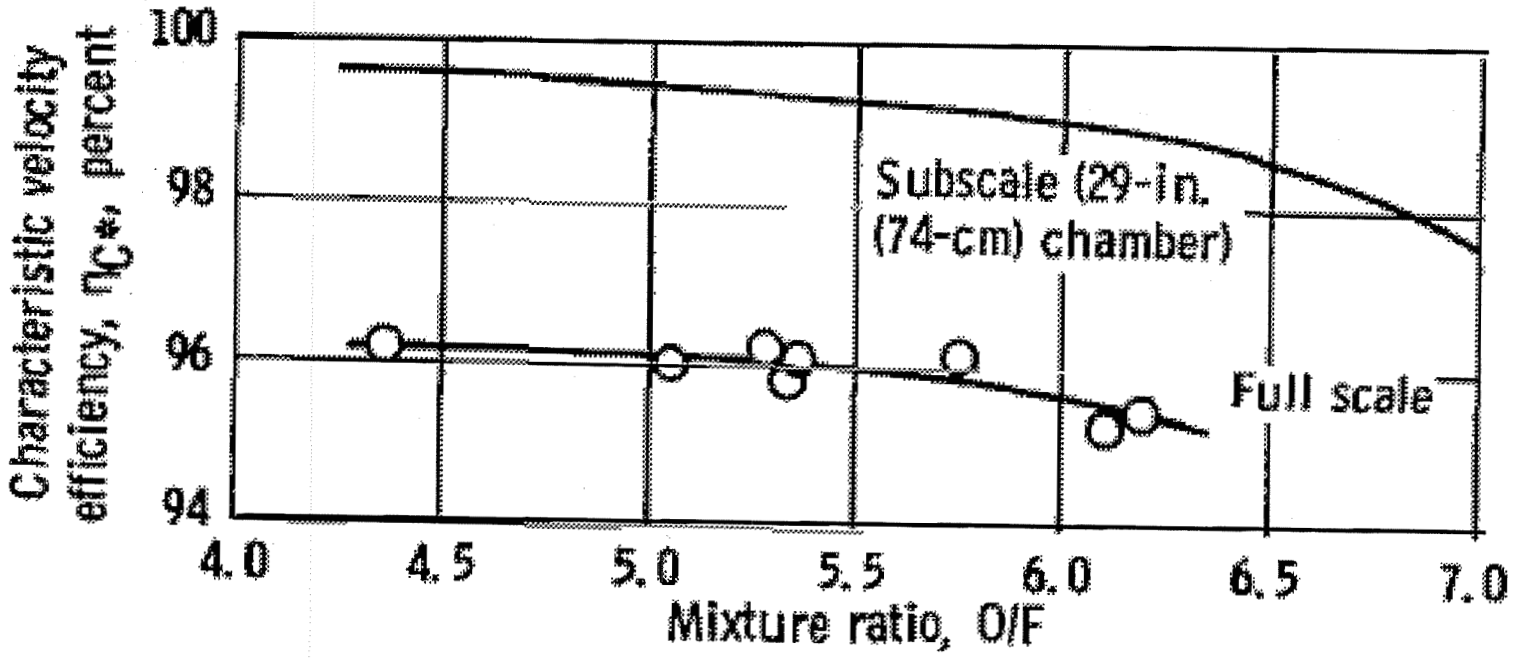

JE JACOBS ESTS Group

Marshall Space Flight Center

M-1 Performance Comparisons

- Measured total η_{C*} ~ 96.0 % (or total loss $\Delta\eta_{C*}$ ~ 4.0 %)
- Core efficiency based on subscale chamber
  - Core η_{C*} ~ 99.3 %, or $\Delta\eta_{C*}$ ~ 0.7 %
  - No barrier cooling
  - Small maldistribution losses in small hardware
  - Face coolant distribution same in subscale and fullscale
- Intentional Maldistributions
  - $\Delta\eta_{C*}$ ~ 1.7 % due to redistributing fuel for wall and baffle surface cooling
  - $\Delta\eta_{C*}$ ~ 0.6 % due to altering single element oxidizer flow for baffle surface cooling
- *M* variations between subscale and fullscale $\Delta\eta_{C*}$ ~ 0.3 %
- Total accounted $\Delta\eta_{C*}$ ~ 3.3 % out of 4.0 %
  - Not yet considered unintentional maldistributions which can be quite large for very large diameter injectors

Space Shuttle
Orbital Maneuvering Engine

- Thrust = 26.7 kN (6 Klbf)
- N_2O_4/ MMH Propellants
- Pc = 125 psia
- O/F = 1.65
- Flies today on the U.S. Space Shuttle

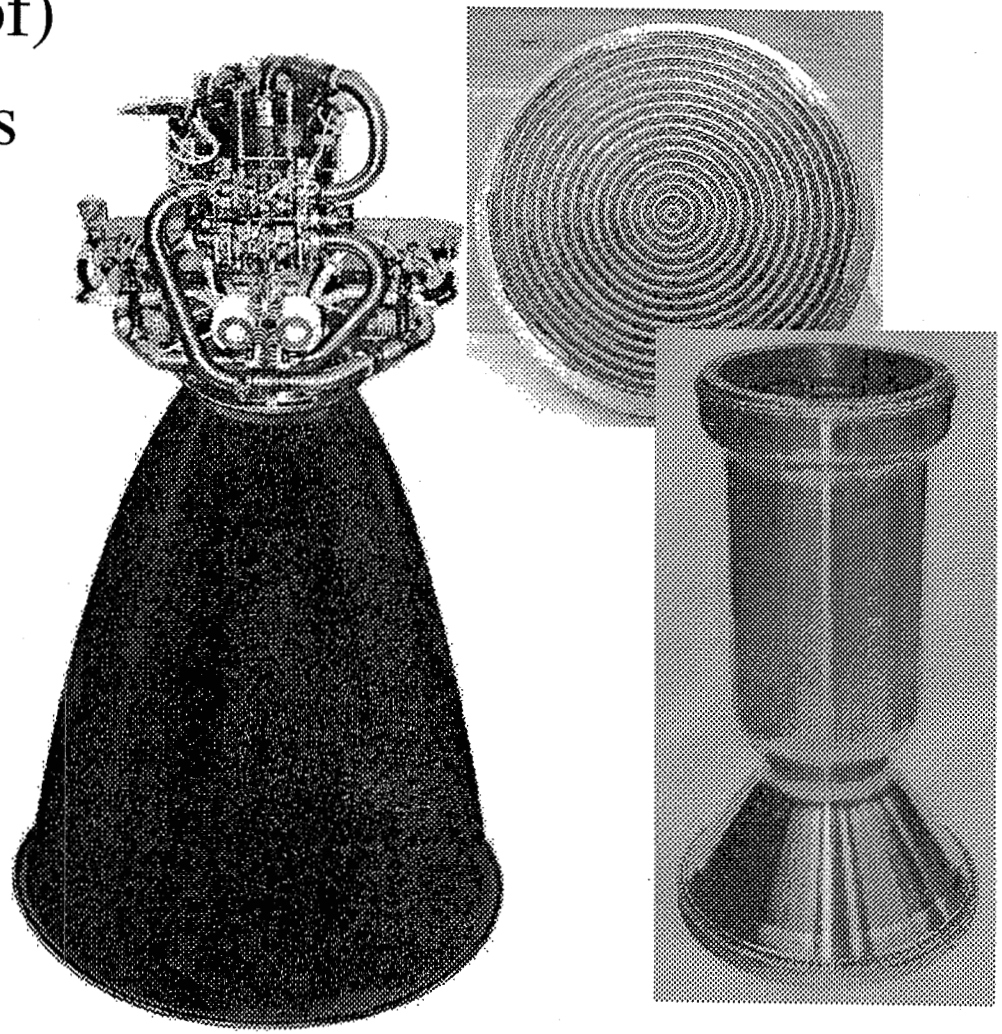

OMS UD Subscale & Fullscale Injector Comparison

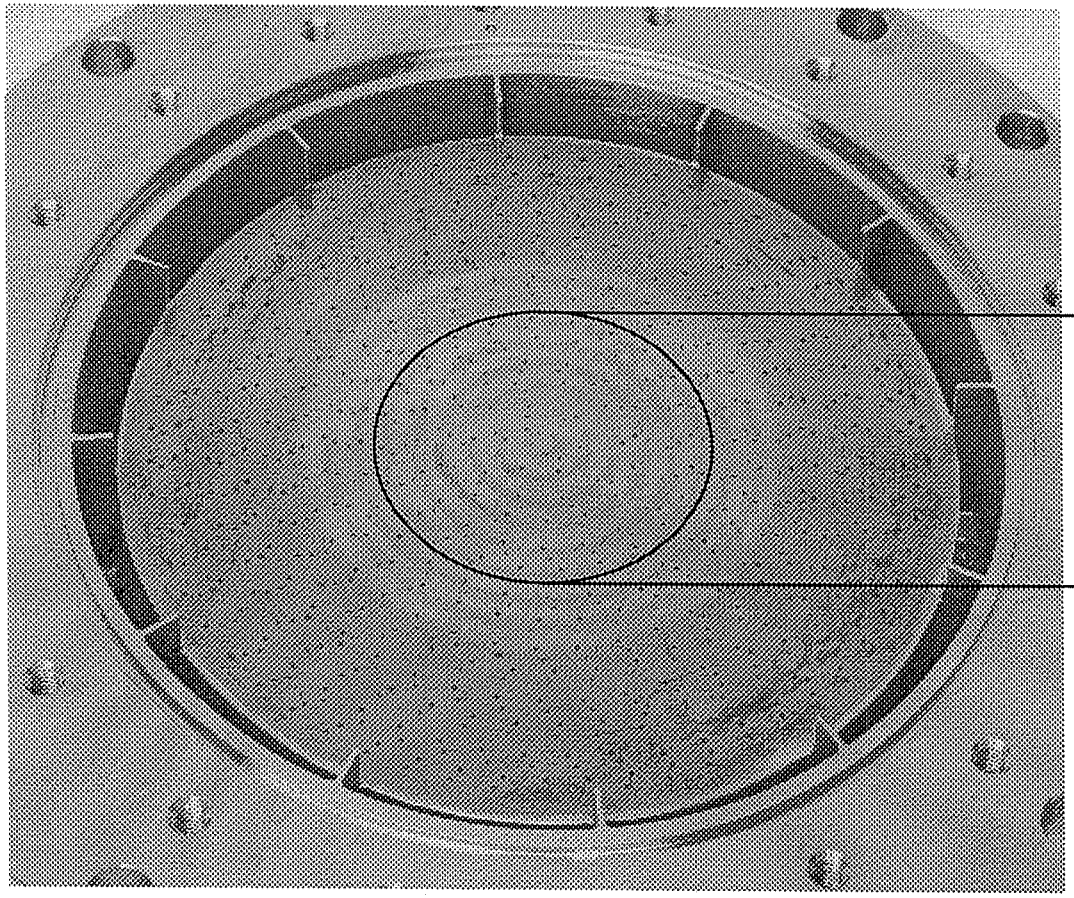

Fullscale

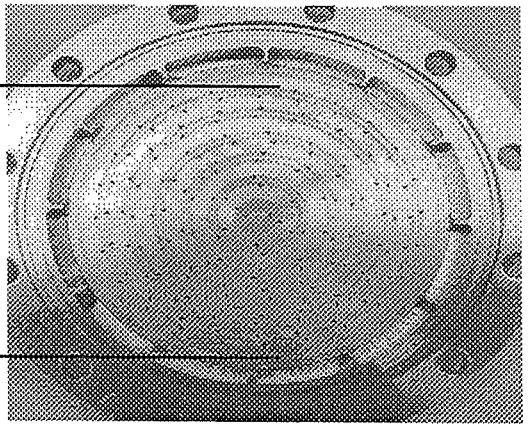

Subscale

Single Element Hot-Fire Test Results in Short Chambers (L' = 2" and 4")

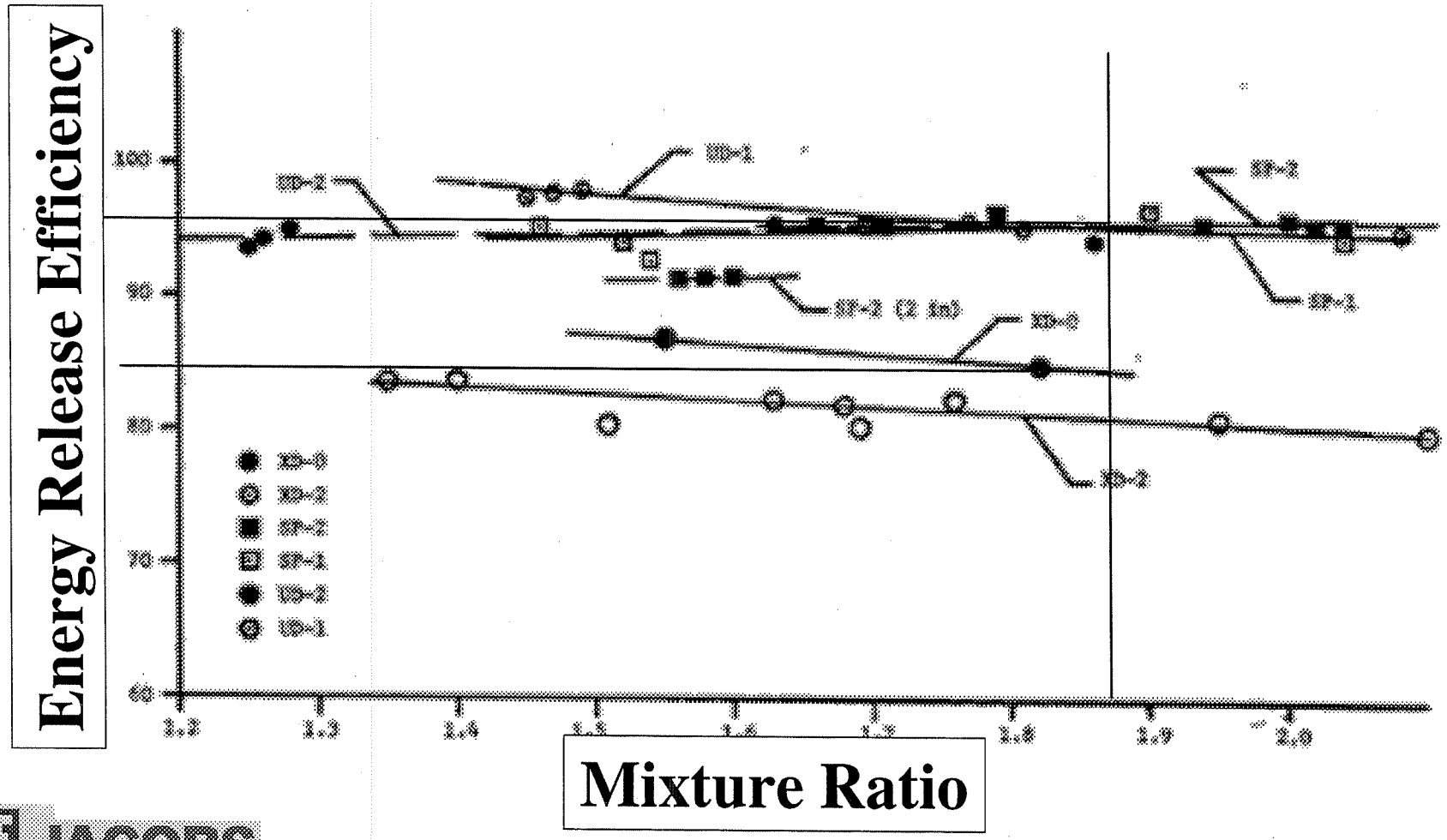

Single Element Hot-Fire Test Results in Short Chambers (L' = 4")

Marshall Space Flight Center

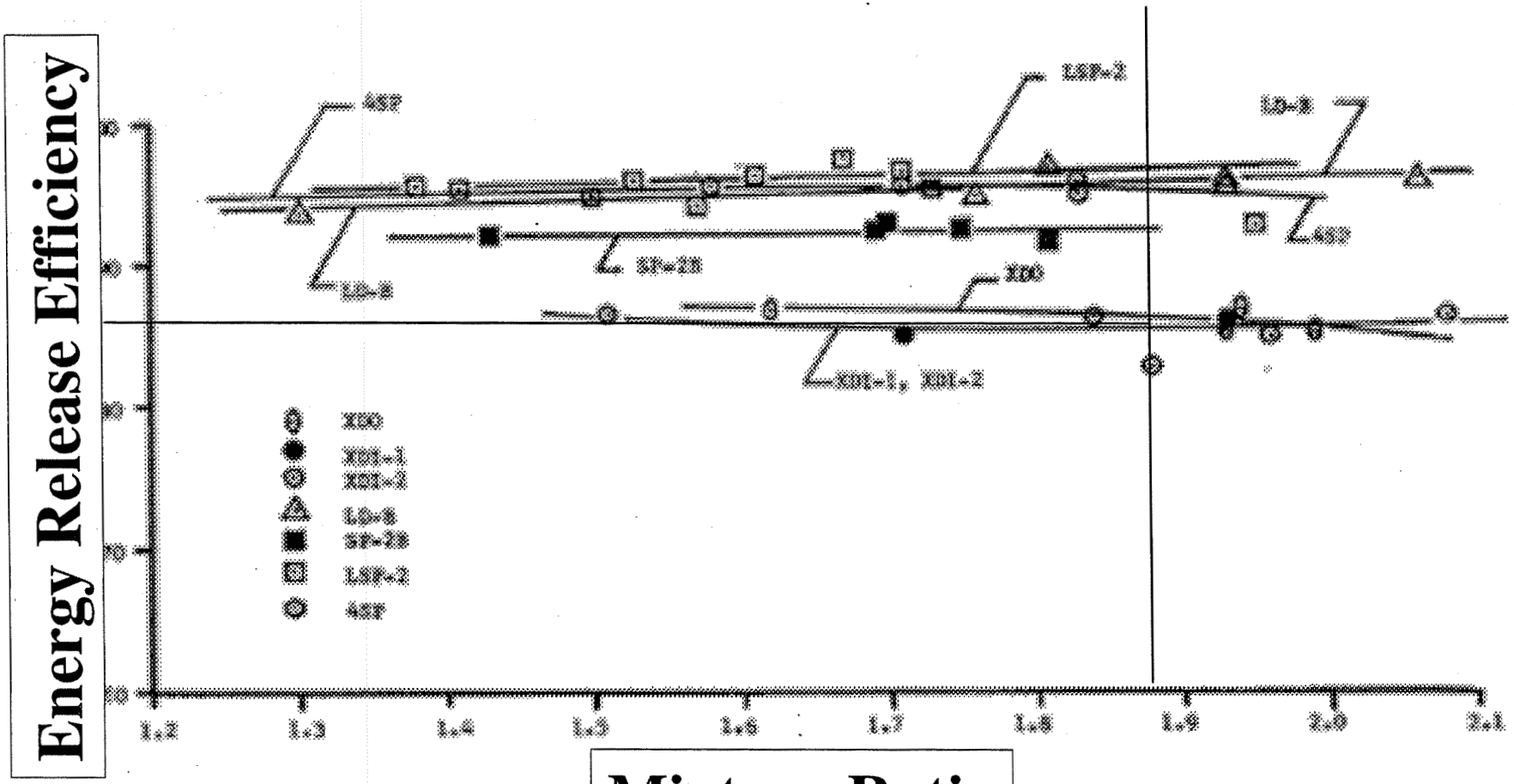

JACOBS ESTS Group

600-lbf Thrust Subscale Hot-Fire Test Results

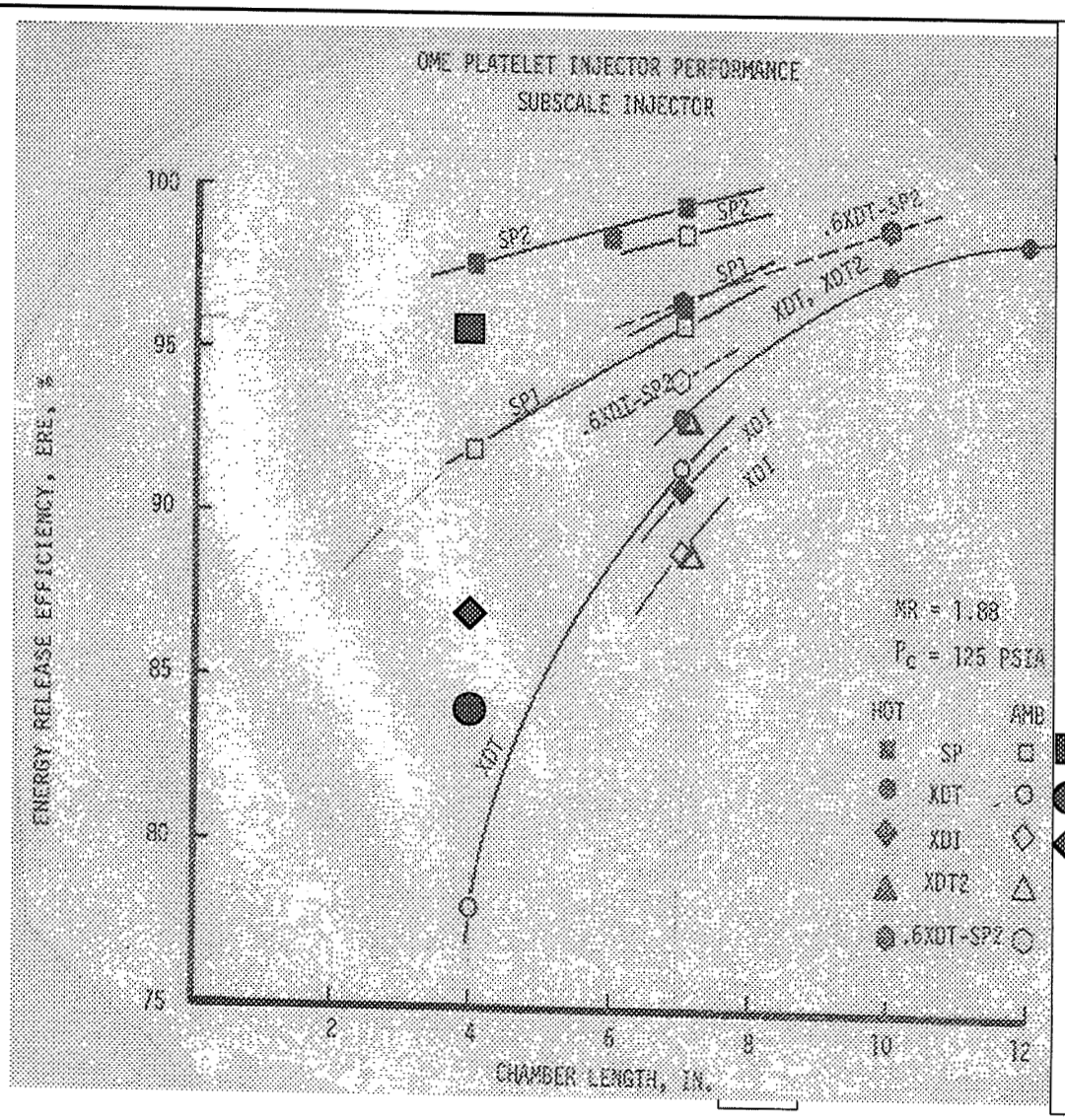

Single Element SP1, SP2

JE JACOBS ESTS Group

Marshall Space Flight Center

Fullscale OME X-Doublet Injector Faceplate (Development Element)

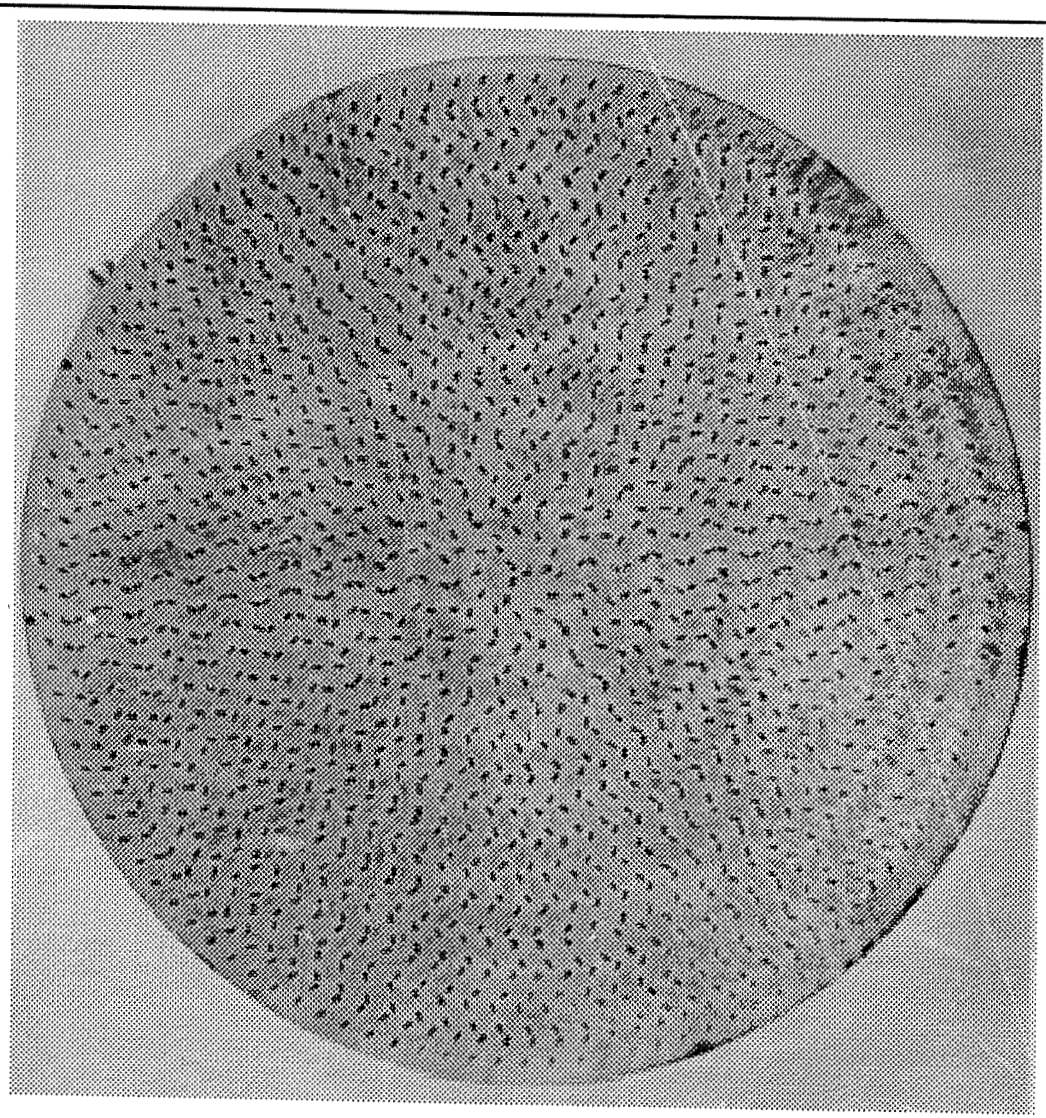

JE JACOBS ESTS Group

Fullscale OME Heat-Sink Combustion Chamber

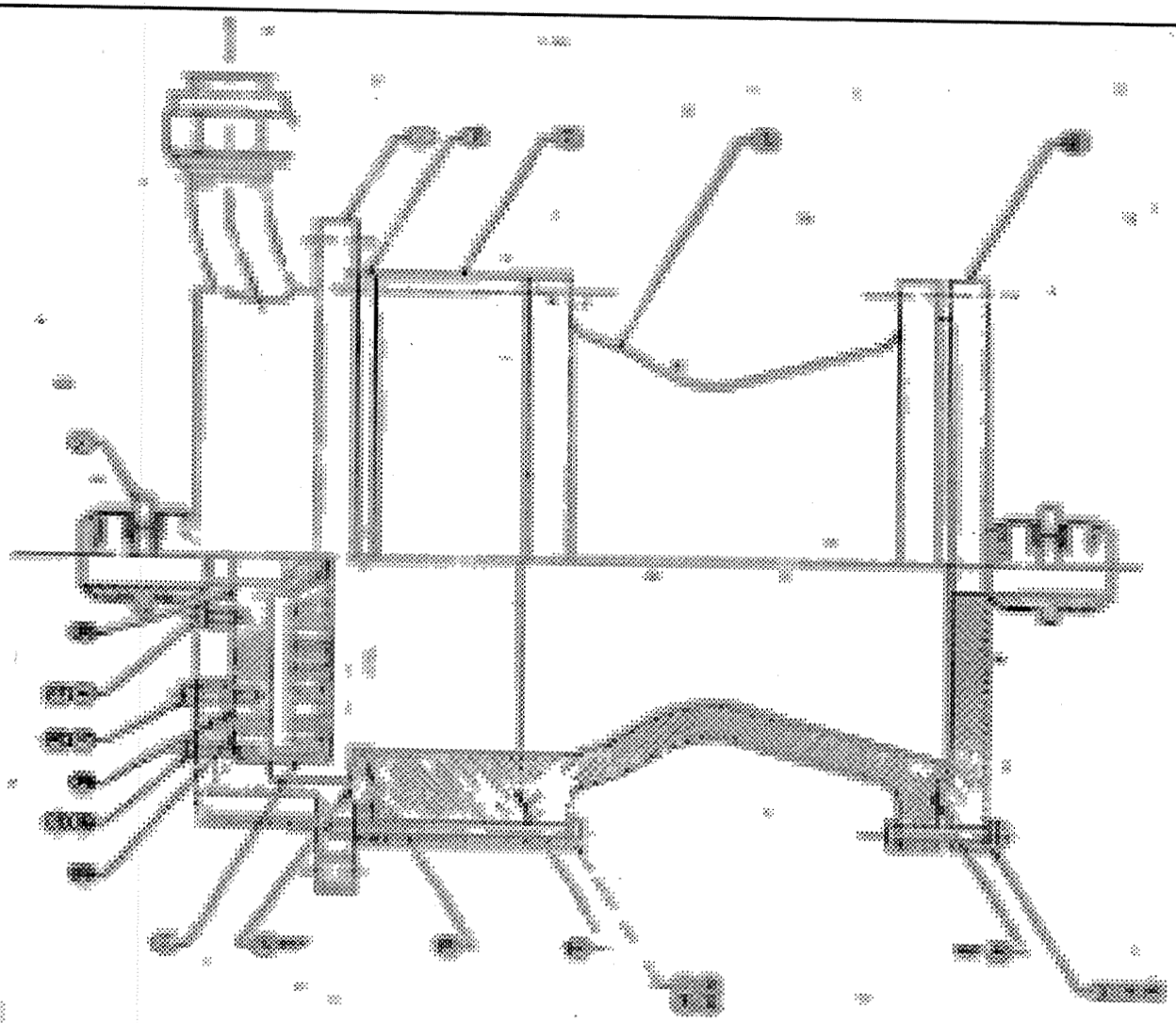

Fullscale OME XDT Performance in Heat-Sink Combustion Chamber

Marshall Space Flight Center

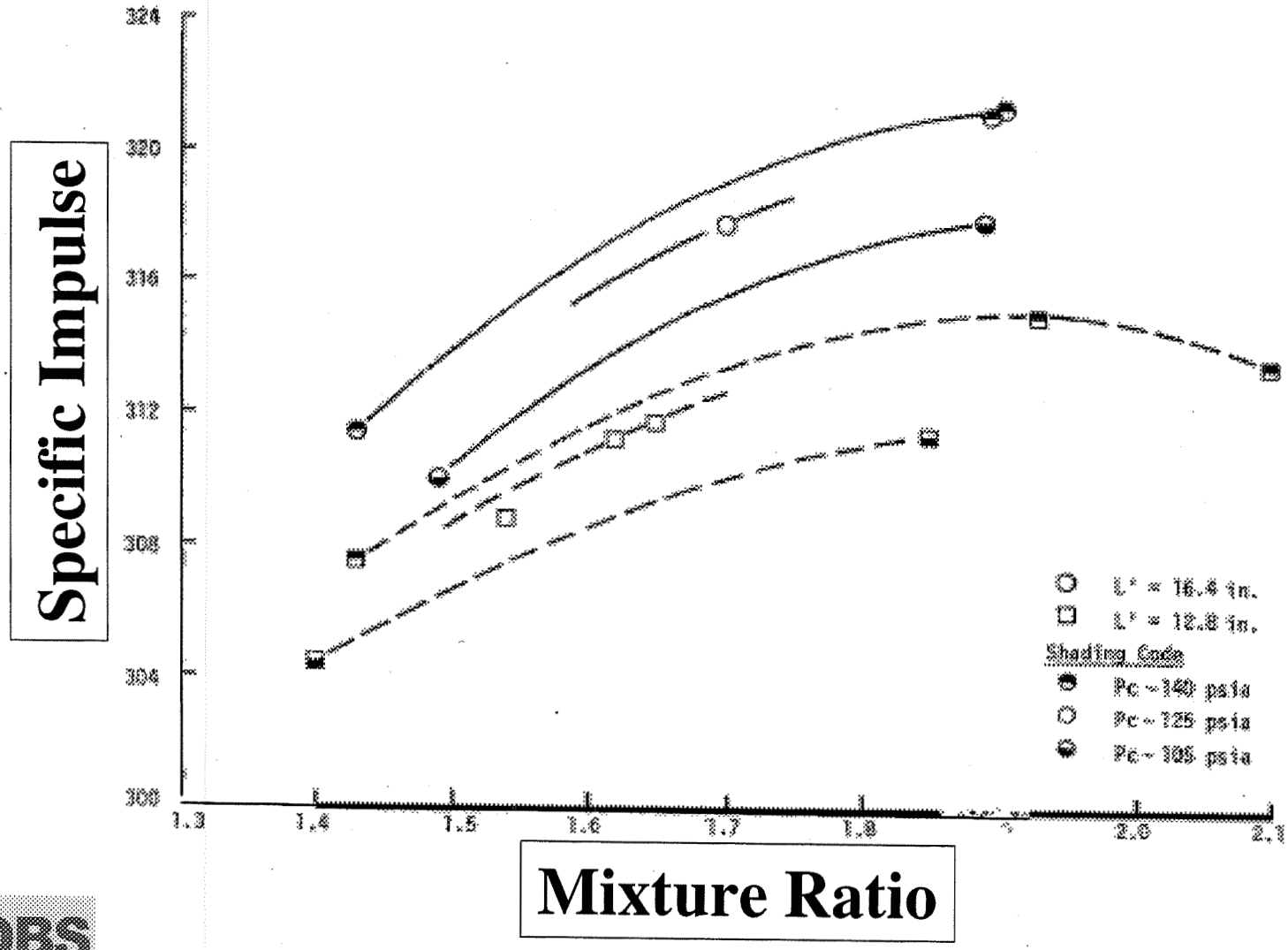

JACOBS ESTS Group

OMS Performance Comparisons

- Measured total η_{C^*} ~ 98.0 % (or total loss $\Delta\eta_{C^*}$ ~ 2.0 %)
- No barrier cooling, small maldistribution losses in small hardware
  - Intentional Maldistributions = 0
- *M* variations between subscale and fullscale $\Delta\eta_{C^*} = 0$
- Core efficiency based on subscale chamber testing largely measured the fullscale efficiency

NASA LeRC Thrust/Element Studies

- Thrust = 67 kN (15 Klbf)
- LO_2/LH_2 propellants
- Pc ~ 1000 psia
- Part of extensive injector research program in the U.S. during the 1960s

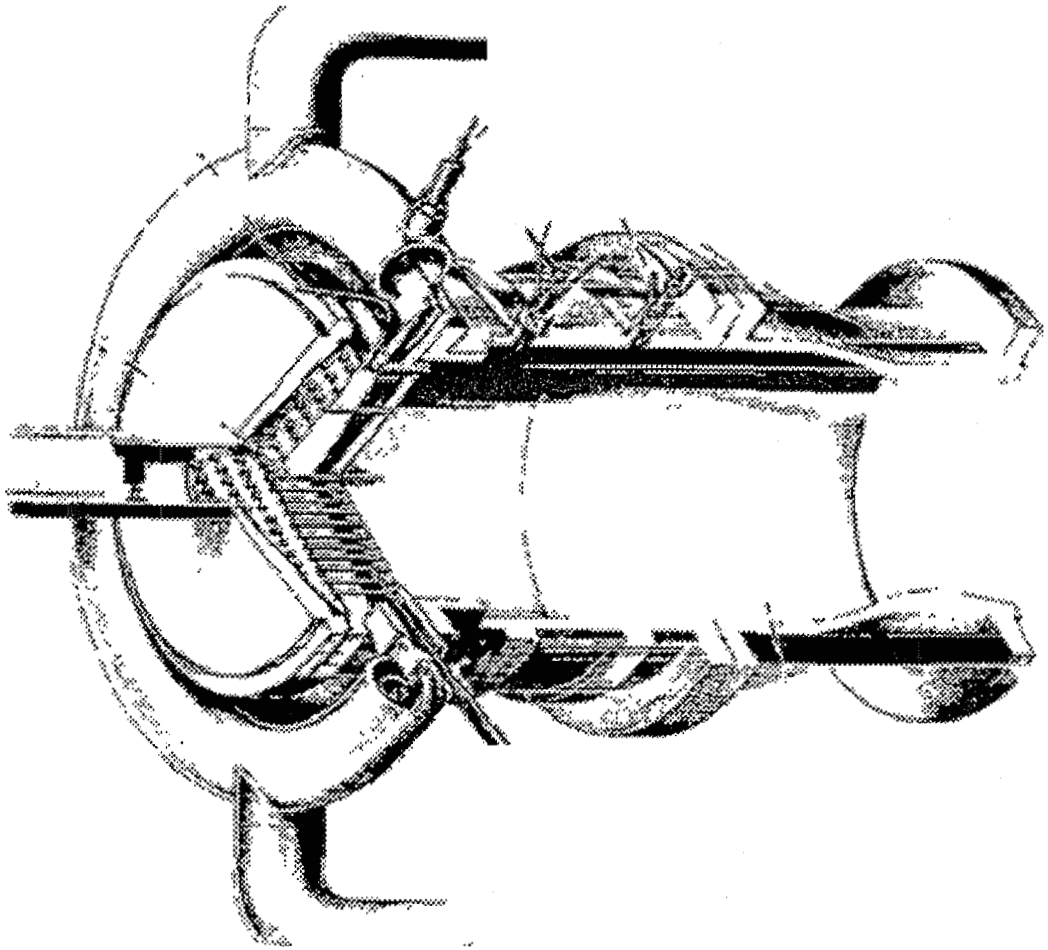

NASA LeRC Thrust/Element Studies

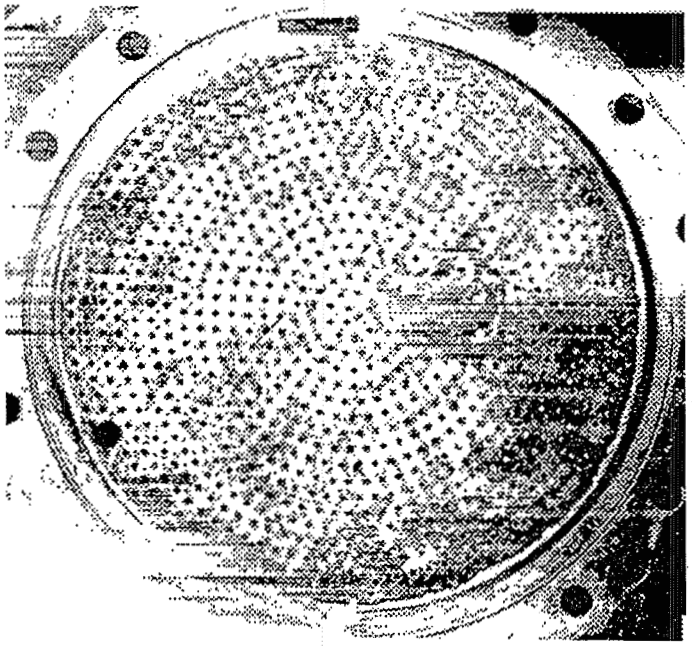

20 lbf/Element

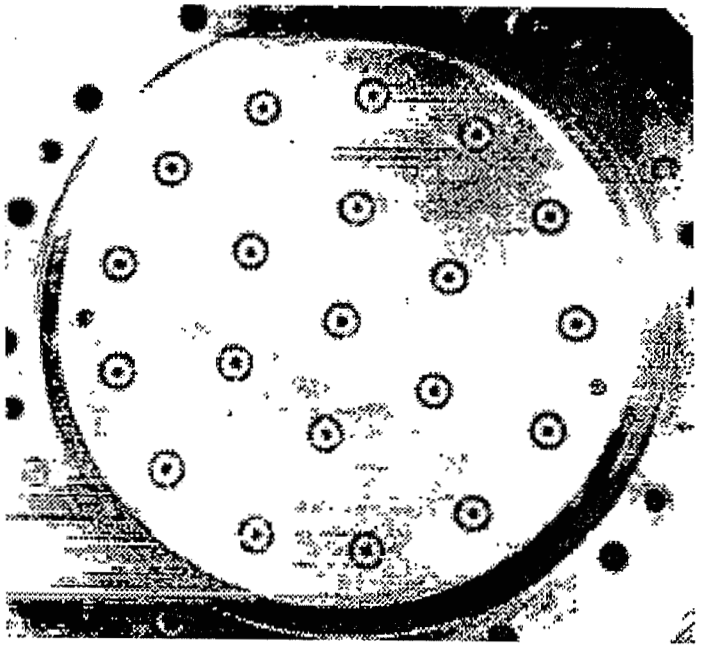

1000 lbf/Element

NASA LeRC Thrust/Element Studies

Marshall Space Flight Center

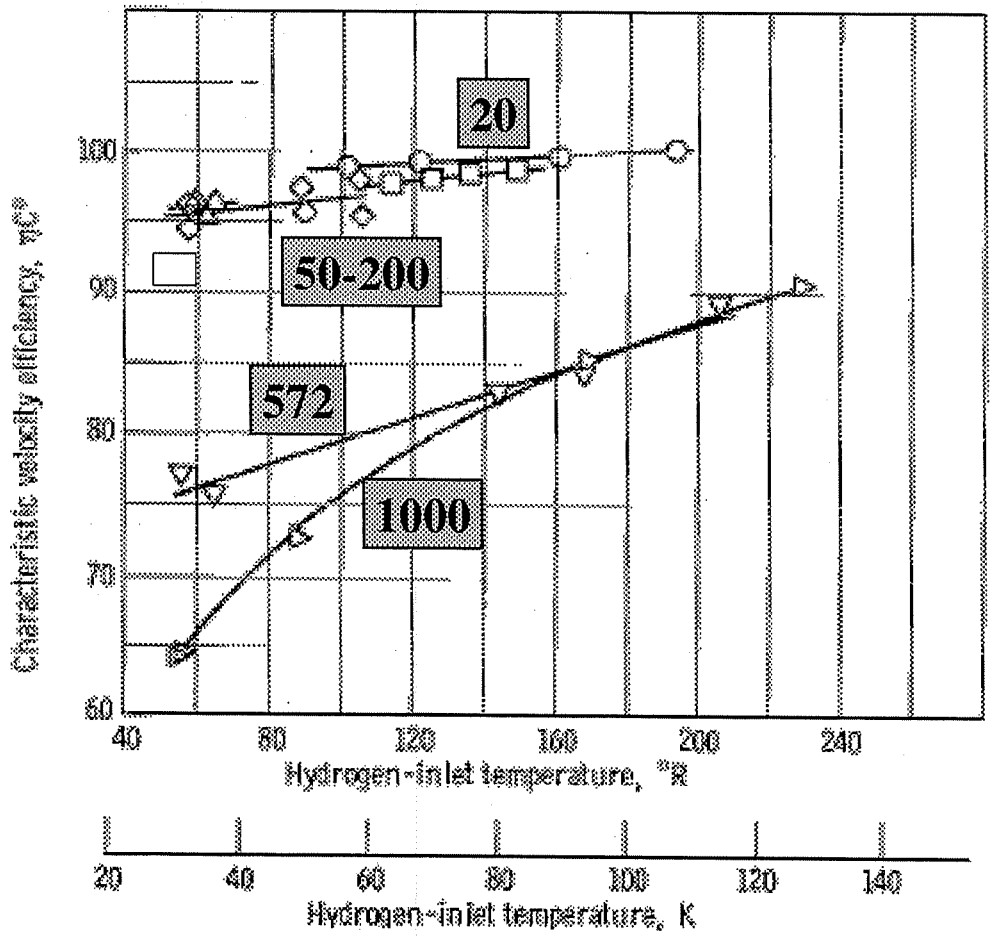

	Thrust per element, TIE, lb	(kN)	Number element E
○	20	(89)	992
□	50	(222)	397
△	100	(445)	201
◇	200	(890)	100
▽	572	(2542)	35
▷	1000	(4448)	20

L'=12"

JACOBS ESTS Group

Coarse Elements are Vaporization-limited

Marshall Space Flight Center

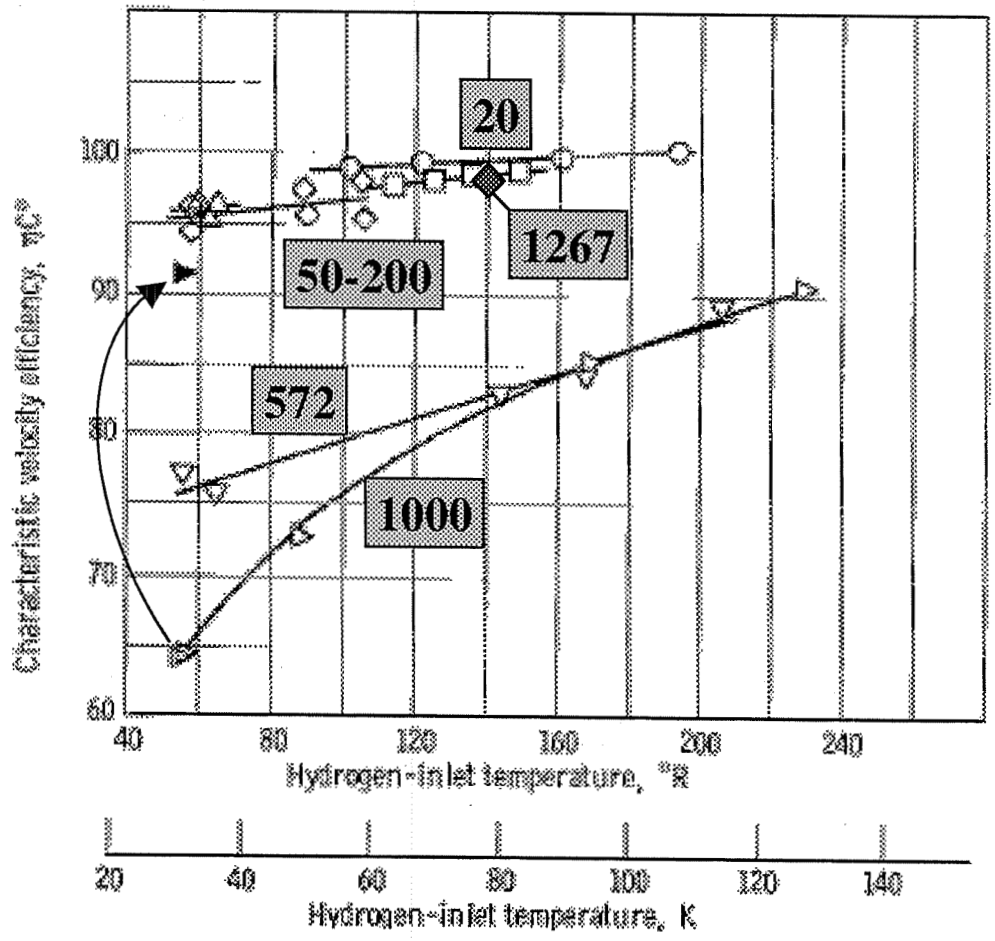

	Thrust per element, TIE, lb	(kN)	Number element E
○	20	(89)	992
□	50	(222)	397
△	100	(445)	201
◇	200	(890)	100
▽	572	(2542)	35
▷	1000	(4448)	20
▶	1000	(4448)	20

Open Symbol L'=12"
Solid Symbol L'=22"

M-1 Coarse Element, L'=29"		
◆	**1267 (5635)**	**19**

JE JACOBS ESTS Group

NASA LeRC Thrust/Element Studies

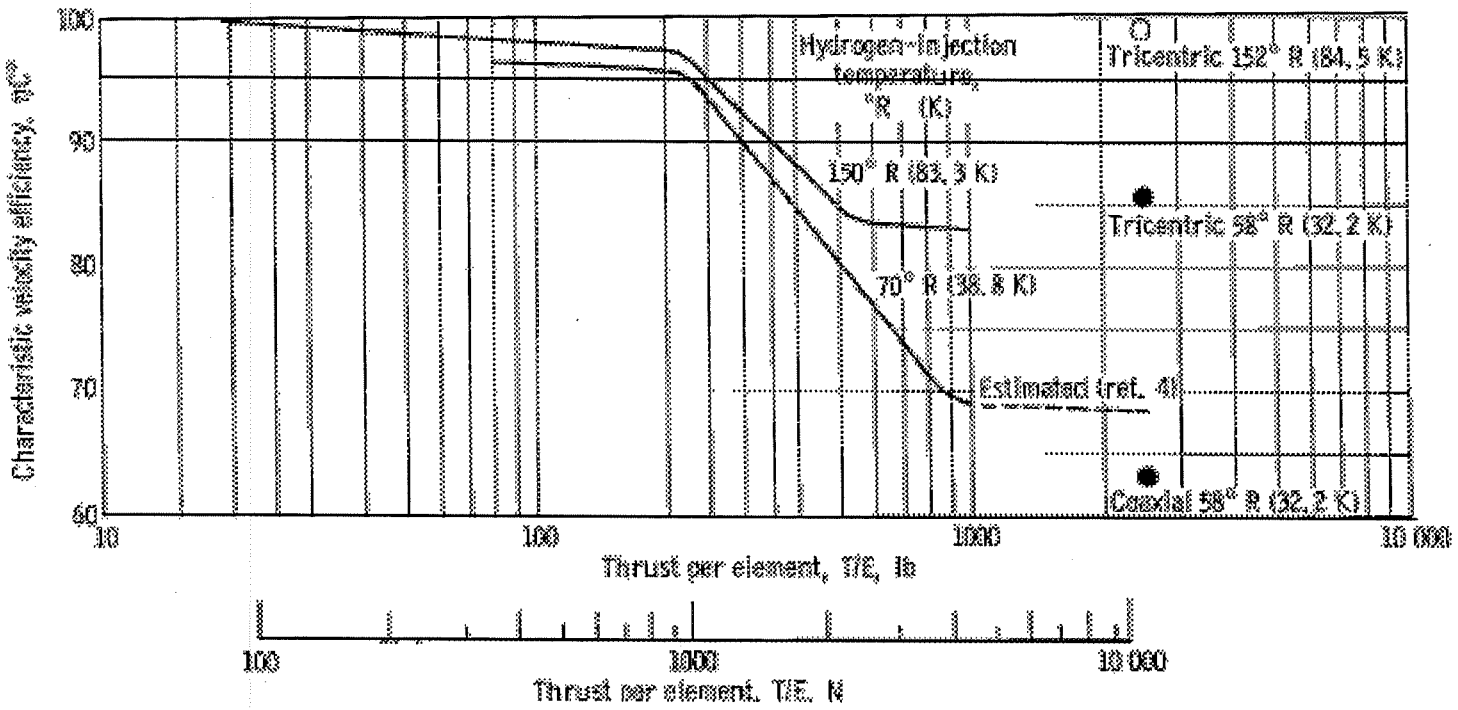

Summary of Some Historical Notions

- Use of constant element size in multiple chamber sizes…
  - "Scaling with Constant Element Dimensions"
- Chemical conversion times τ_i ~ constant
- Relationship between element dimensions and chamber dimensions is lost

Summary

- Scaling can provide invaluable guidance and validation to liquid propellant rocket engine combustor development
  - Even today !
- Reduce development costs
- Optimize hardware
  - Increase performance
  - Increase combustion stability margin
- Scaling of Combustion Performance is Practical

Summary – Scaling with Constant Element Size

- Element dimensions kept approximately constant while chamber dimensions (diameter and length scales) are changed
  - Keeps element characteristics constant while changing packaging
  - Violates all scaling rules where L ~ τ
    - Injector retains ~ constant τ's
  - Performance can scale well
    - Chamber configuration should maintain constant Mach No.
    - or, ensure reaction completed in barrel
  - Heat transfer not scaled well
    - Chamber wall surface area and outer row element coverage not scaled
  - Combustion stability not scaled well
    - Elements subjected to higher frequency resonances

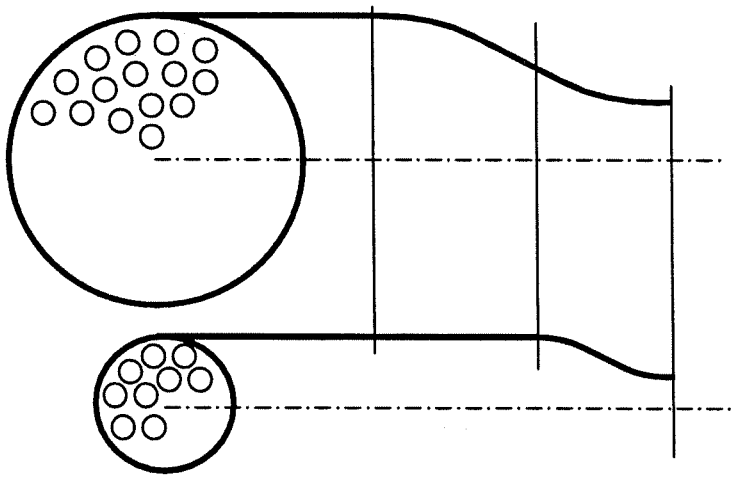

Summary – Scaling with Geometric Photoscaling

- Element dimensions change proportionally with all chamber dimensions (diameter and length scales)
  - Relationships between geometry and element are retained
  - Violates scaling rules where element *Re* = constant
  - Performance scaling uncertain
  - Heat transfer should scale well
    - Chamber wall surface area and outer row element coverage scaled proportionally
  - Combustion stability can scale well
    - Hewitt d/V characteristic is maintained

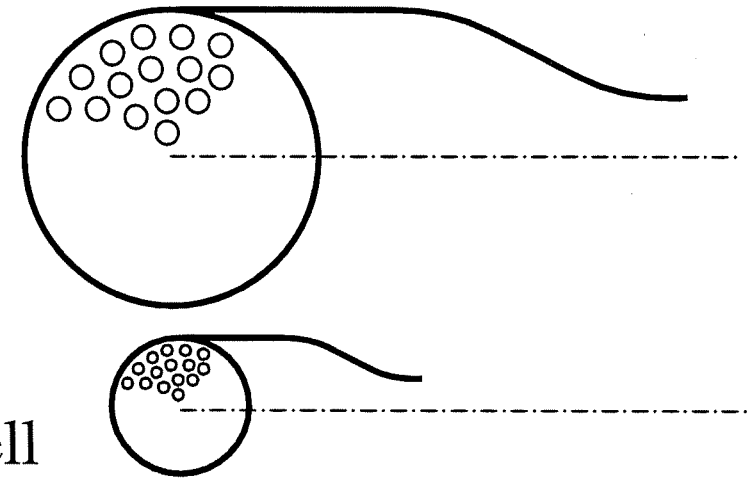

Understanding Scaling in the Future ?

- Continue to "mine" the historical data base to help define the scaling relationships
  - History provides a wealth of scaling information – thousands of thousands of tests with thousands of combustors !
  - Don't let this expensive progress go to waste
- Establish scaling relationships for all important individual processes in LPRE
  - Research activities in injection, primary atomization, secondary atomization, vaporization, reaction, mixing, reaction
  - Include scaling studies in your physics-based activities
- Use combustion Computational Fluid Dynamics (CFD) analyses to perform scaling "numerical experiments"

Backup Slides

H-1 Baffle Compartment is Smaller than F-1 Baffle Compartment

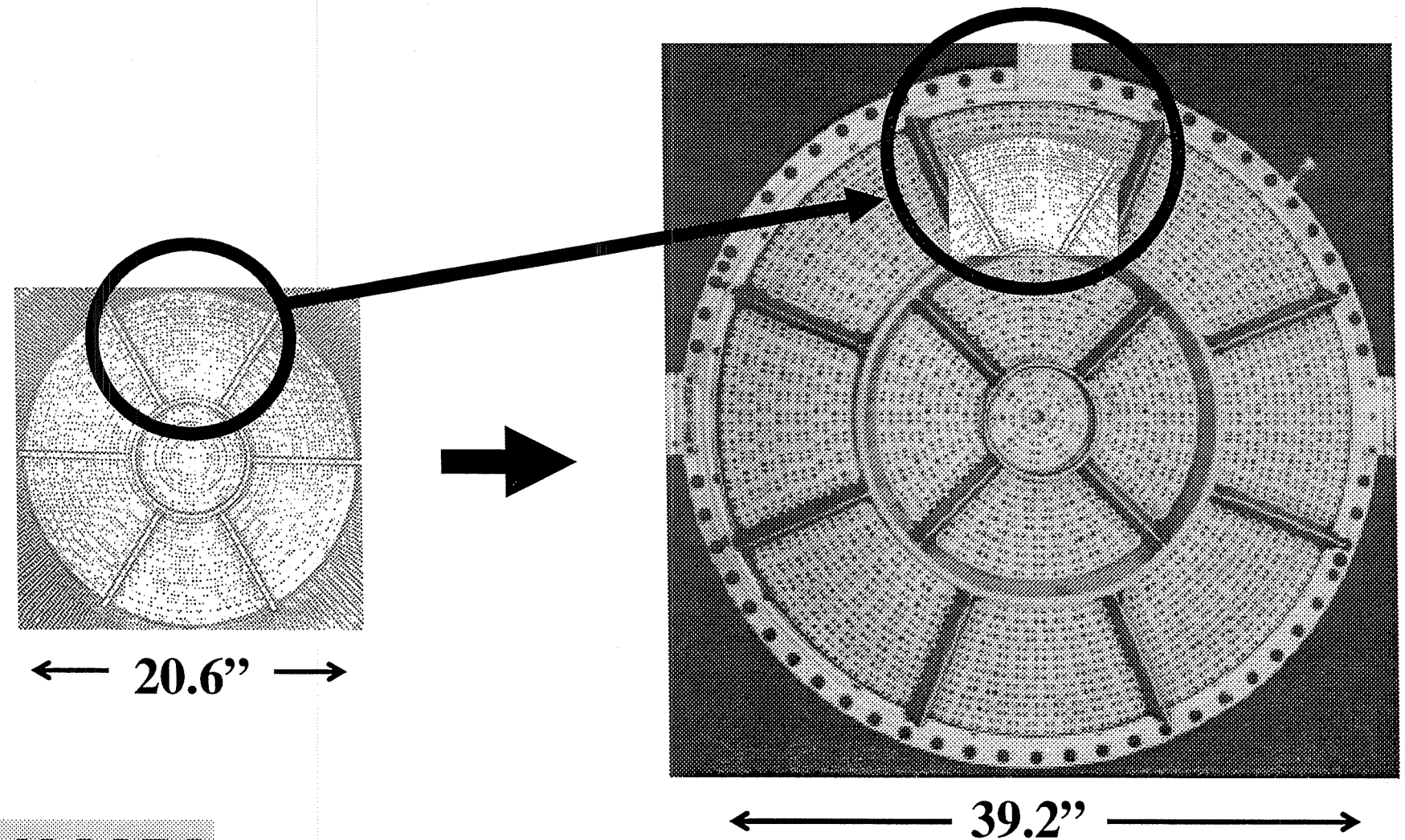

The Meaning of $\left(\frac{\tau_{i,S}}{\tau_{i,F}}\right) = \left(\frac{L_S}{L_F}\right)^{2n/(n+1)}$

- For n = 1/3 (i.e., $\tau \sim 1/p^{1/3}$, from Reardon SP-194)

  then $\left(\frac{\tau_{i,S}}{\tau_{i,F}}\right) = \left(\frac{L_S}{L_F}\right)^{1/2}$

  – As the length scales are reduced, the chemical conversion times must be reduced as the *square root*

  – For example, as $L_S = \frac{1}{2} L_F$ (half geometric scale)

  then $\tau_{i,S} = \sqrt{\frac{1}{2}}\, \tau_{i,F} = 0.707\ \tau_{i,F}$

  – The chamber pressure is increased even more,

  since $(p_S / p_F)^n = (\tau_{i,F} / \tau_{i,S})$,

  or $p_S = 2.8\ p_F$

The Meaning of $\left(\frac{\tau_{i,S}}{\tau_{i,F}}\right) = \left(\frac{L_S}{L_F}\right)^{2n/(n+1)}$

- For n=1/3, and $d_S = ½\, d_F$
  - then $A_S = ¼\, A_F$, $v_S = 1.4 v_F$, $p_S = 2.8 p_F$ (or, $\rho_S = 2.8 \rho_F$)
  - Element flow continuity $m_S = (2.8\rho_F)(¼\, A_F)(1.4 v_F) = m_F$
    - Note that through half-size element, $m_S = ¼\, m_F$ normally
  - Element pressure drop $\Delta P_S \sim \rho_S v_S^2 \sim 2.8\rho_F 2 v_F^2 \sim 5.5\, \Delta P_F$
- Therefore, through a half-sized element, have to *~triple* the density while increasing flowrate
  - Note that *Re* are still matched
- When this happens, does $\tau_{i,S} = 0.707\, \tau_{i,F}$ as required ?

The Meaning of $\left(\frac{\tau_{i,S}}{\tau_{i,F}}\right) = \left(\frac{L_S}{L_F}\right)^{2n/(n+1)}$

- For n = $\sqrt{2}$ (i.e., $\tau \sim 1/p^{1.4}$)

  then $\left(\frac{\tau_{i,S}}{\tau_{i,F}}\right) = \left(\frac{L_S}{L_F}\right)^{1.17}$

  - As the length scales are reduced, the chemical conversion times must be increased slightly
  - For example, as $L_S = ½\, L_F$ (half geometric scale)

    then $\tau_{i,S} = 0.44\ \tau_{i,F}$
  - The chamber pressure is increased even more,

    since $(p_S / p_F)^n = (\tau_{i,F} / \tau_{i,S})$,

    or $p_S = 1.8\ p_F$

The Meaning of $\left(\frac{\tau_{i,S}}{\tau_{i,F}}\right) = \left(\frac{L_S}{L_F}\right)^{2n/(n+1)}$

- For n=$\sqrt{2}$, and $d_S = ½\, d_F$
  - then $A_S = ¼\, A_F$, $v_S = 1.1 v_F$, $p_S = 1.8 p_F$ (or, $\rho_S = 1.8 \rho_F$)
  - Element flow continuity $m_S = (1.8\rho_F)(¼\, A_F)(1.1 v_F) = ½\, m_F$
    - Note that through half-size element, $m_S = ¼\, m_F$ normally
  - Element pressure drop $\Delta P_S \sim \rho_S v_S^2 \sim 1.8\rho_F 1.2 v_F^2 \sim 2.2\, \Delta P_F$
- Therefore, through a half-sized element, have to *increase* the density and flowrate
  - Note that *Re* are still matched
- When this happens, does $\tau_{i,S} = 0.707\, \tau_{i,F}$ as required ?

The Meaning of $\left(\frac{\tau_{i,S}}{\tau_{i,F}}\right) = \left(\frac{L_S}{L_F}\right)^2$

- Suppose we break τ_i into 4 processes
  - atomization, vaporization, mixing, and reaction
- Suppose all 4 processes are reduced proportionally
  - Are timescales of all these processes reduced as the square of the length scale reduction ?
- What are typical timescales for atomization, vaporization, mixing, and reaction ?

The Meaning of $\left(\frac{\tau_{i,S}}{\tau_{i,F}}\right) = \left(\frac{L_S}{L_F}\right)^2$

- Typical timescales
  - Atomization
    - Initial breakup length $\tau \sim L/v \sim L^2$
      since for constant *Re*, $L \sim 1/v$
    - Droplet size $d \sim v/L$
    - Secondary breakup $\tau \sim d/v \sim 1/L$
  - Vaporization
    - Droplet lifetime $\tau \sim d^2 \sim v^2/L^2 \sim 1/L^4$
  - Mixing
    - Gas phase mixing $\tau \sim d^2 \sim v^2/L^2 \sim 1/L^4$
  - Reaction kinetics

Typical Timescales from SP-194

COMPARISON OF CHARACTERISTIC TIMES

TIME LAG CORRELATION: $\tau \sim D_L^m / M_L^{\frac{1}{2}} P_L^{\frac{1}{2}}$

$m \approx \frac{1}{2}$ (IMPINGING JETS)

$m = 0$ (COAXIAL)

DYKEMA ANALYSIS: $\frac{1}{f} \sim \frac{D_L R_L}{V_L}$

STRAHLE ANALYSIS: $t_{CH} = \frac{\rho C_p R_L^2}{\lambda} \sim P_L R_L^2$

HEIDMANN-WIEBER ANALYSIS: $\tau \sim R_L^{3/4} / M_L^{\frac{1}{2}} P_L^{\frac{1}{3}}$

DROP SIZE (INGEBO): $R_L \sim D_L^k / V_L^{0.8}$ (APPROX.)

$0.1 < k < 0.5$

Scaling with Constant Element Dimensions – Maintain Constant *M* Even for Single Element

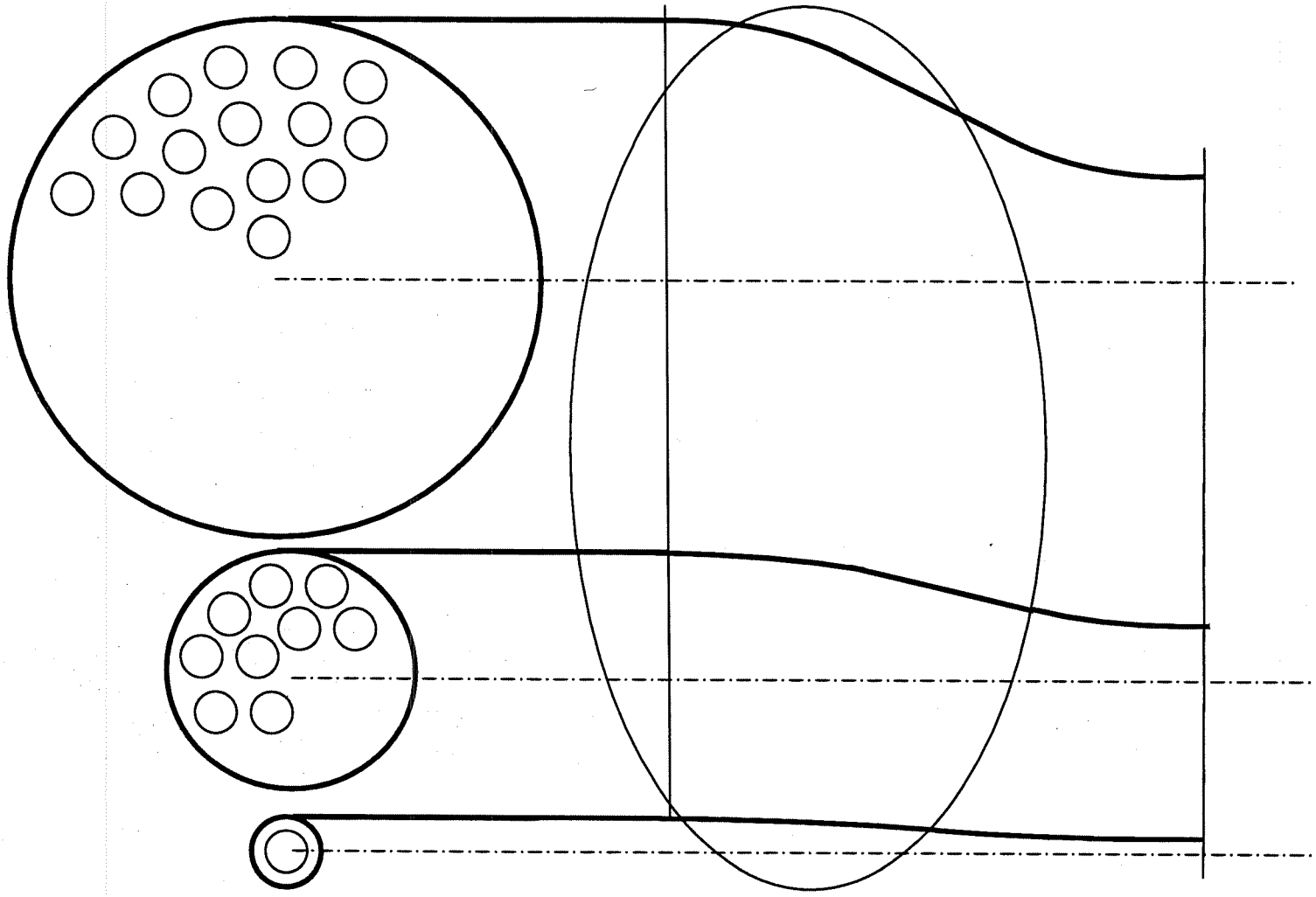

Geometric Photoscaling

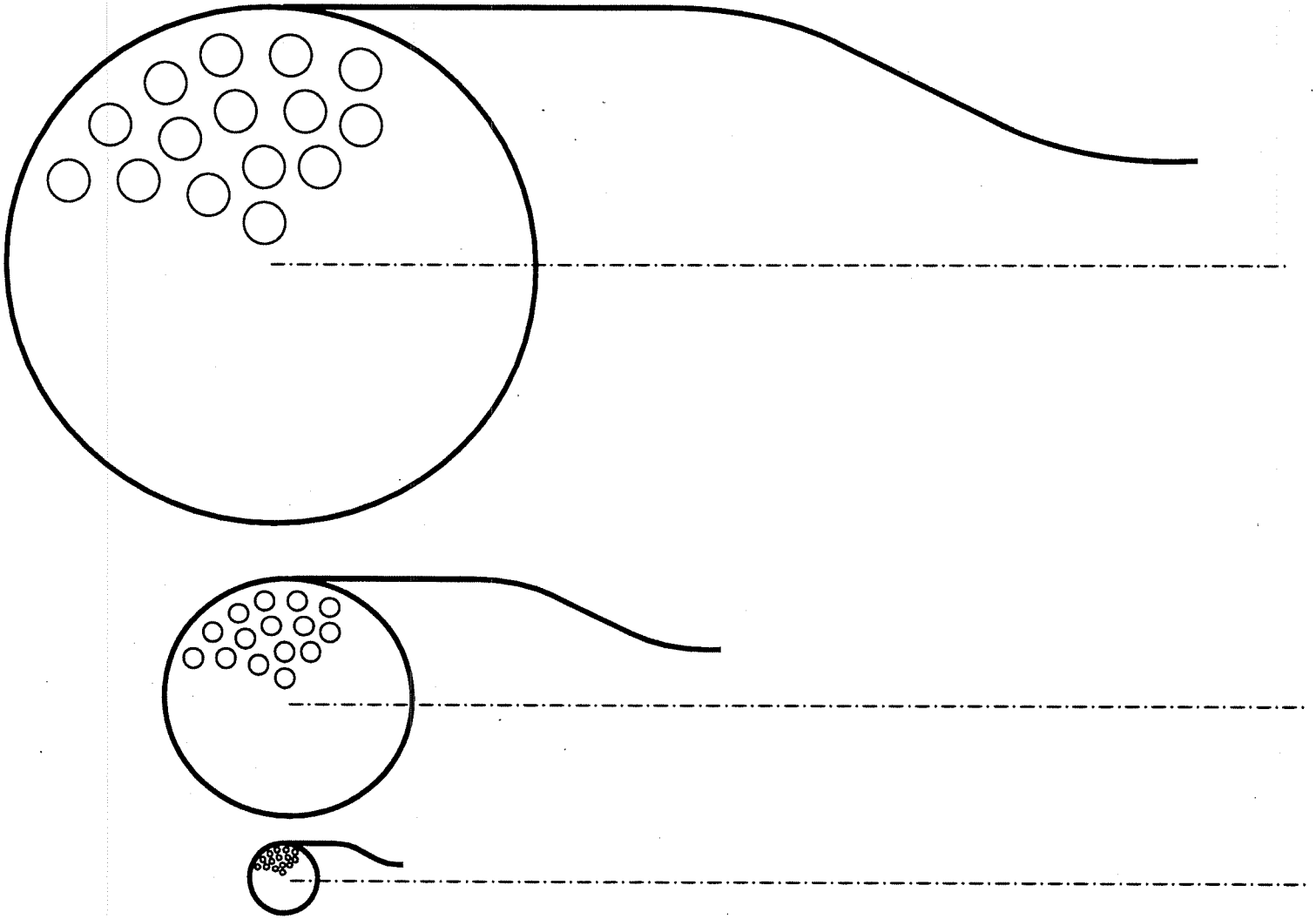

Hewitt d/V for Scaling

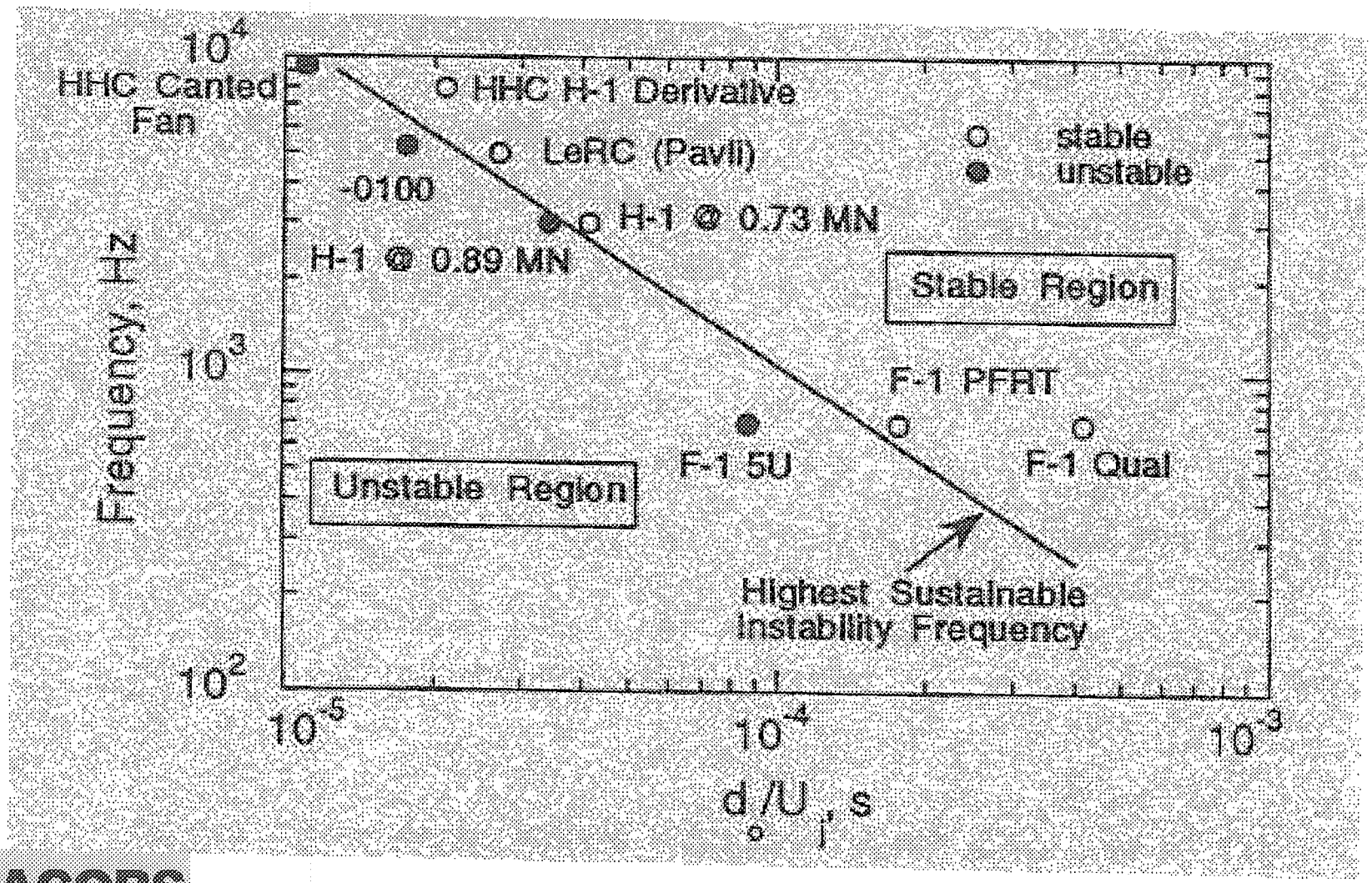

M-1 Main Injector Face

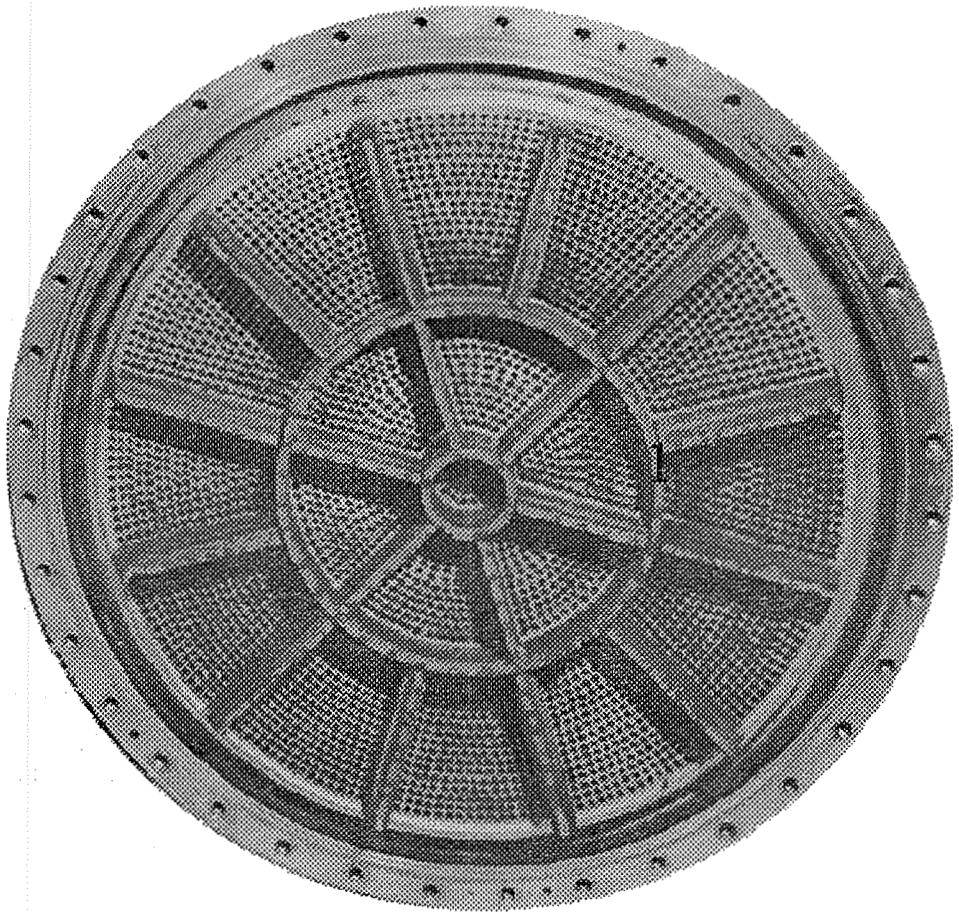

M-1 Unielement Combustor

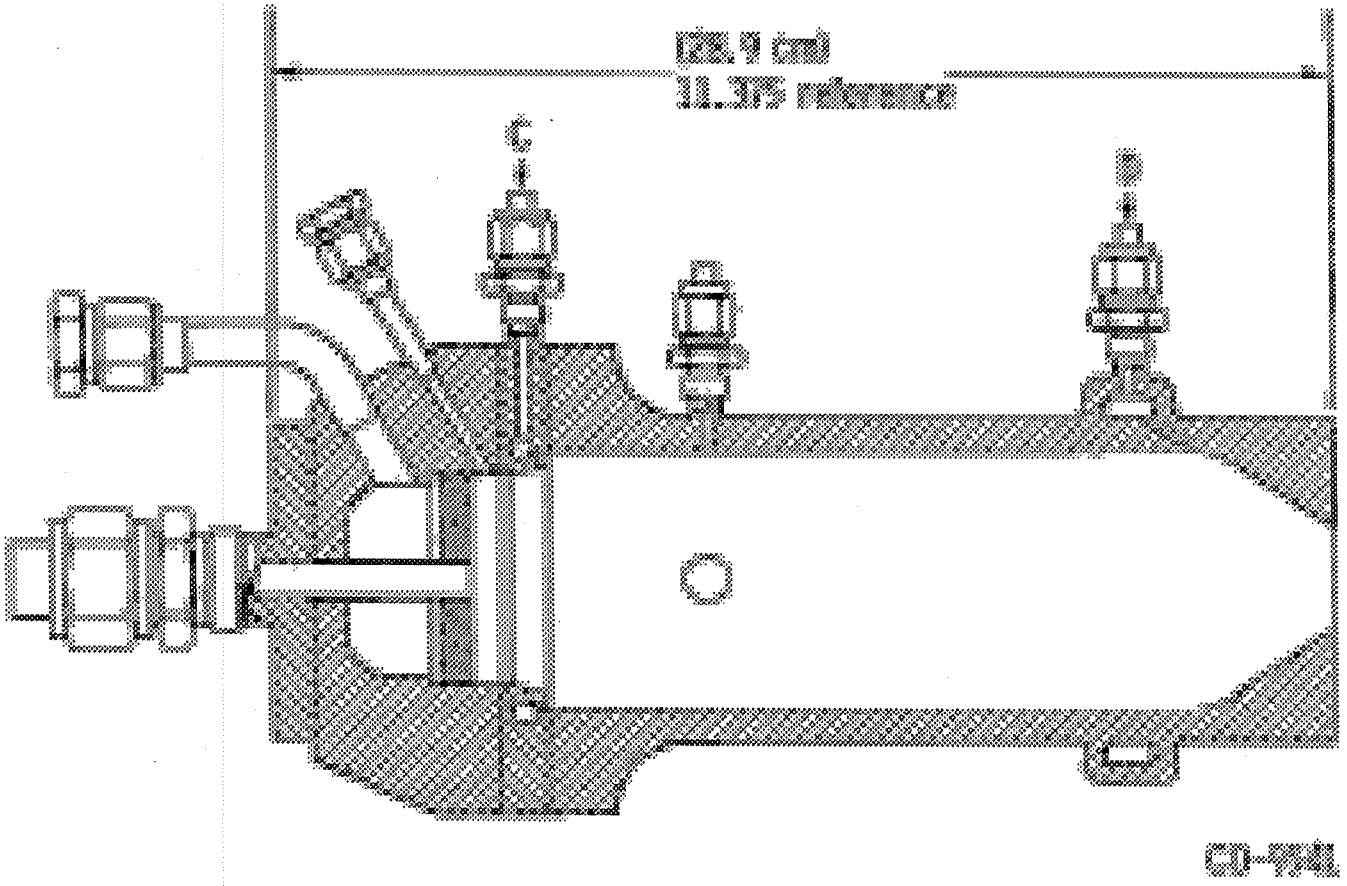

600-lbf Thrust Subscale Hot-Fire Test Results

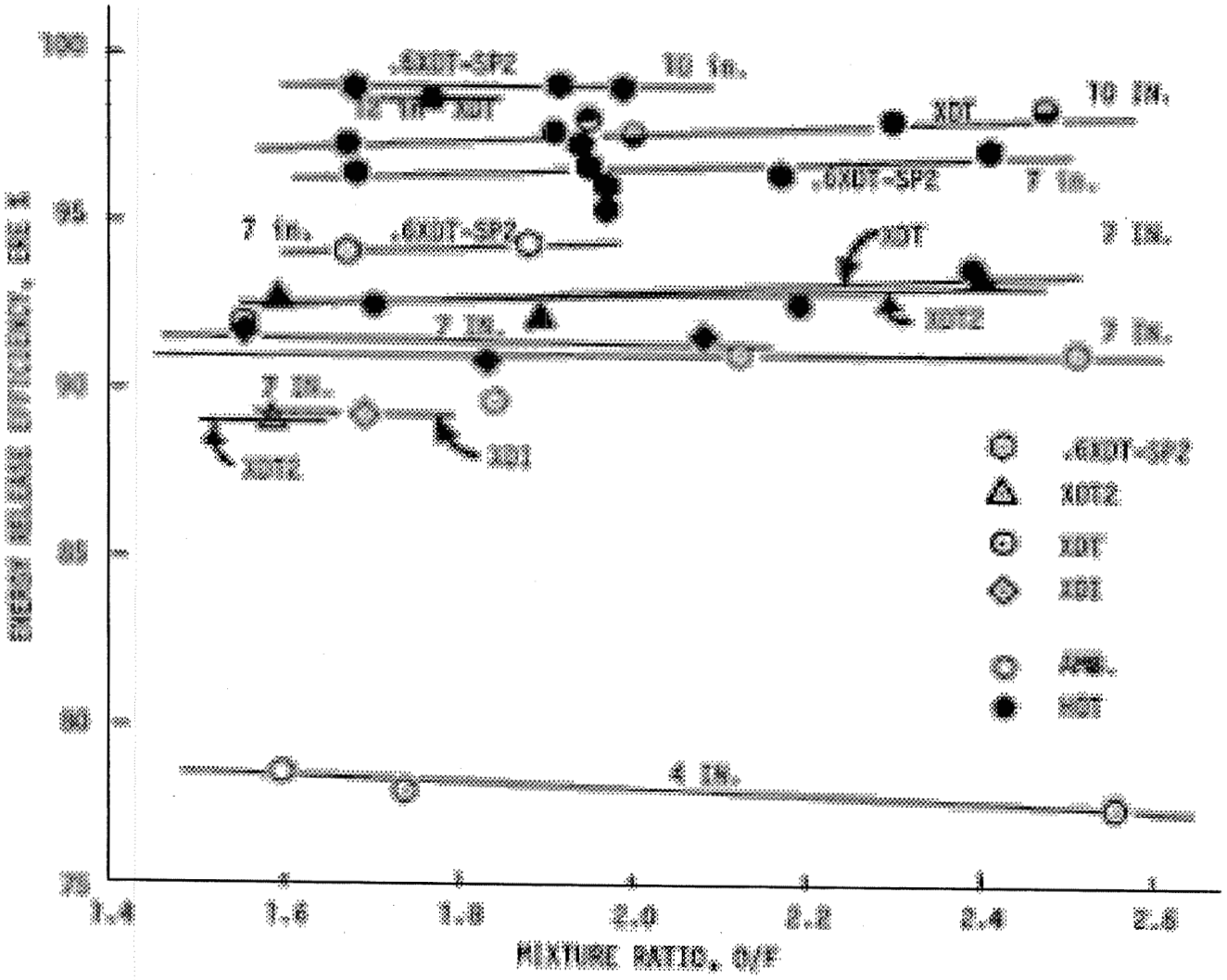

Fullscale OME XDT Performance in Heat-Sink Combustion Chamber

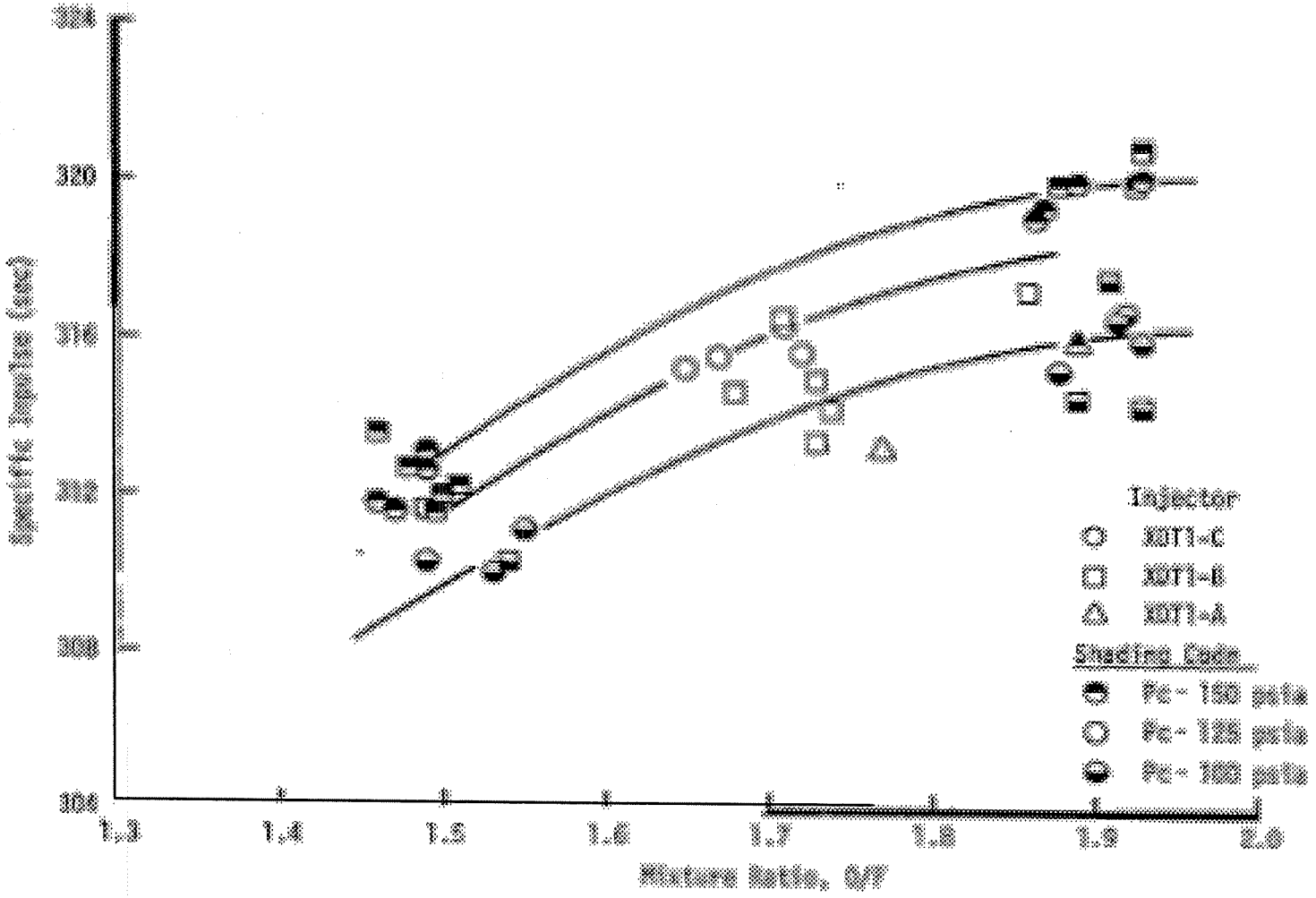

NASA LeRC Thrust/Element Studies

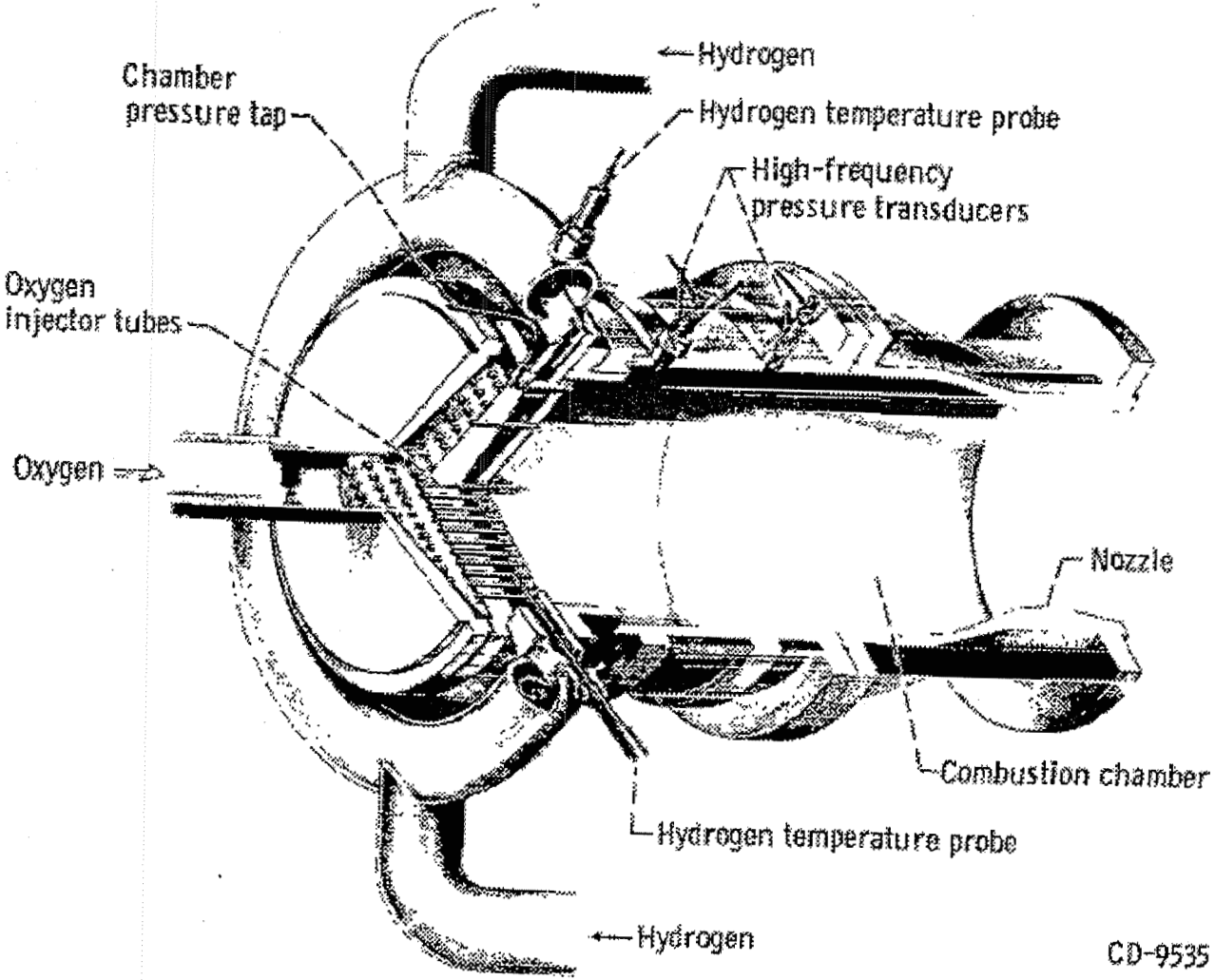

NASA LeRC Thrust/Element Studies

Marshall Space Flight Center

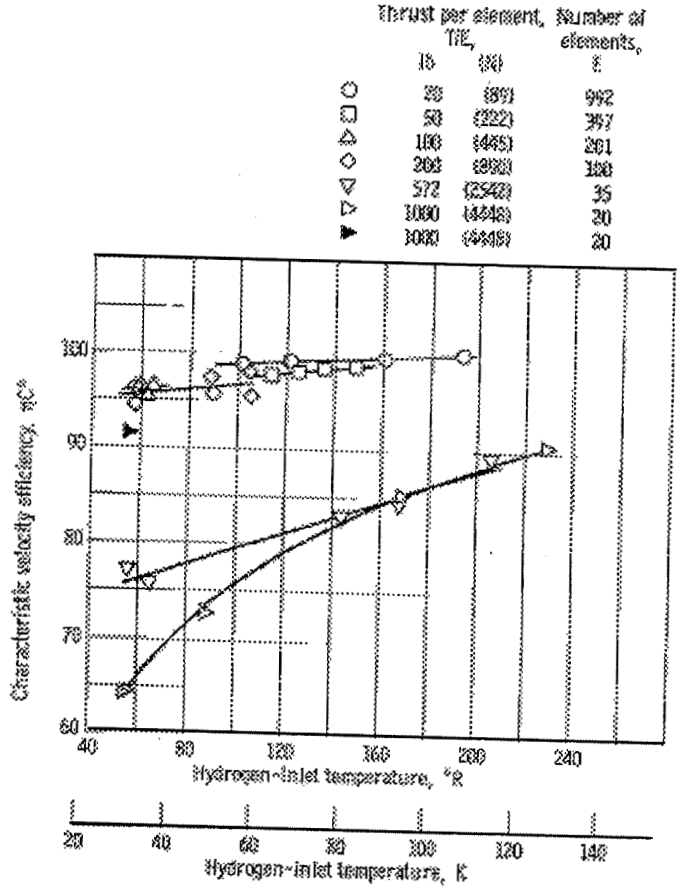

Figure 33. - Effect of hydrogen temperature on combustion efficiency as indicated by characteristic velocity efficiency. Combustion chamber length, 12 inches (0.305 m) except for solid symbol where length equals 22 inches (0.559 m).

JE JACOBS ESTS Group

ITIP Combustion Chamber Comparison

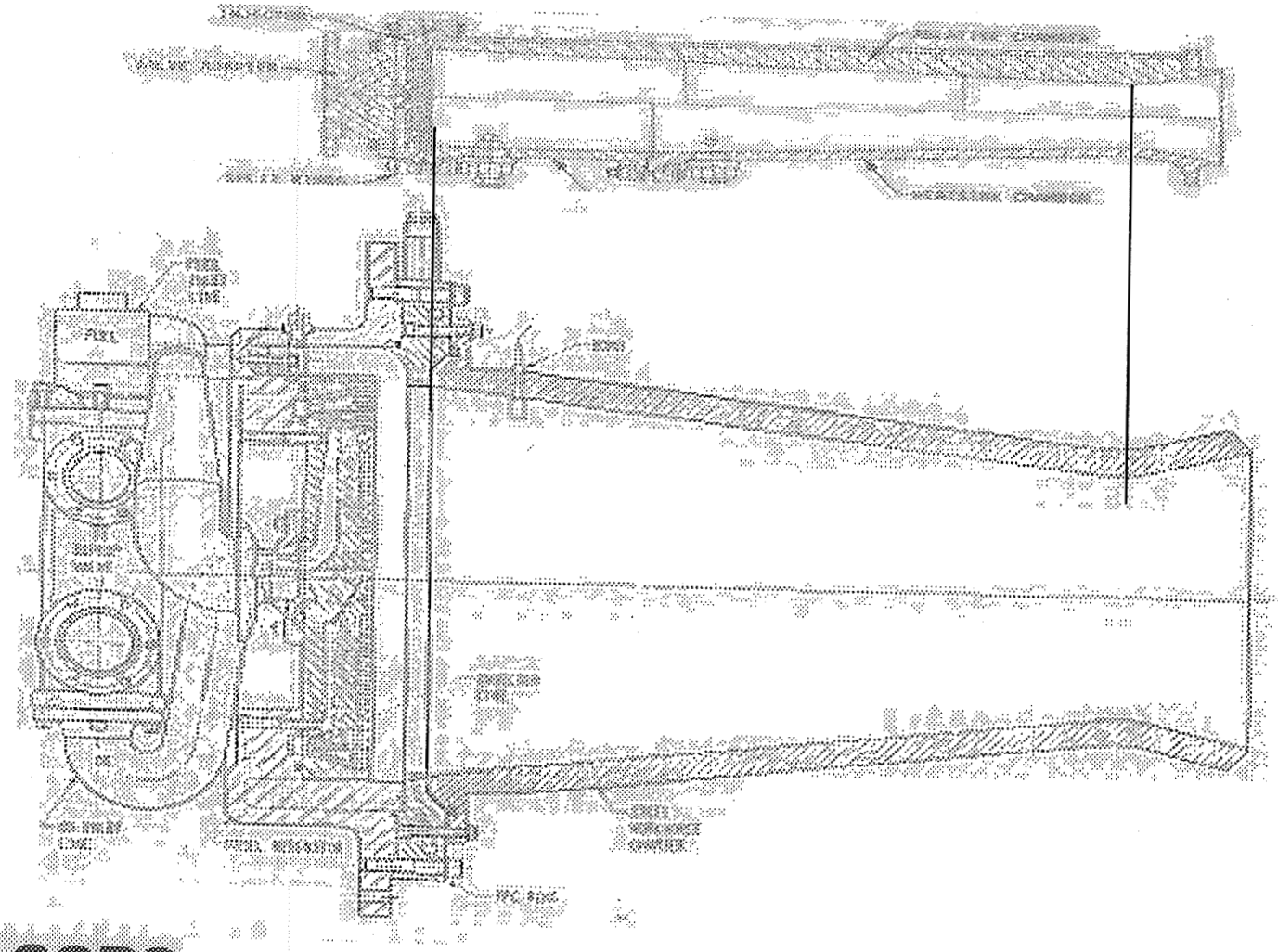

1000 lbf

6000 lbf

JE JACOBS ESTS Group